HYDROMAGNETIC WAVE DAMPING IN THE MAGNETOSPHERE

by

ALFREDO RENÉ NAVATO y ROSARIO

B.S.M.E., University of the Philippines (1951)

B.S.E.E., Manuel L. Quezon University (1956)

A.B., Berchmans College (1962)

SUBMITTED IN PARTIAL FULFILLMENT

OF THE REQUIREMENTS FOR THE

DEGREE OF DOCTOR OF

PHILOSOPHY

at the

MASSACHUSETTS INSTITUTE OF TECHNOLOGY

September 21, 1973

in February 1974

Signature of Author.....

Department of Earth and Planetary

Sciences, September 21, 1973

Certified by.....

Thesis Supervisor

Accepted by.....

Chairman, Departmental Committee on

Graduate Students

DEDICATION

To my mother, Adelina, and to the memory of my father, Alfredo.

ABSTRACT

It is found that collisionless damping of unguided Alfven waves is strong enough in the inner magnetosphere to be of significance for ground-based diagnostics of the magnetosphere and for the understanding of some magnetospheric processes. The statistical approach to the study of a homogeneous Vlasov plasma in a strong, uniform magnetic field is used to derive a lowest order approximation (in the ratio of the gyroradius to a characteristic length of inhomogeneities) to the dispersion equations for hydromagnetic waves propagating at arbitrary angles to the ambient magnetic field. This approximation is equivalent to the "guiding center approximation," and the corresponding physical mechanism for wave-particle interaction is the magnetic moment-magnetic field gradient interaction. For a magnetospheric plasma model made up of a superposition of bi-maxwellian components, numerical solutions of the dispersion equations show negligible damping close to the earth. However, in the vicinity of the equatorial plane, in a region extending a few earth radii inside the plasmapause, hot protons strongly damp unguided Alfven waves. Typically, a wave of frequency f cps would be reduced to $\exp(-33.3f)$ of its power after traversing this region. Damping estimates from the shapes of observed power spectra of magnetic and electric field fluctuations are in reasonable agreement with the calculated damping rates. Occasionally, much more severe damping is inferred from the observed spectra. Applications of this study to some magnetospheric phenomena are pointed out.

Thesis Supervisor: Theodore R. Madden

Title: Professor of Geophysics

TABLE OF CONTENTS

CHAPTER 1: INTRODUCTION

Hydromagnetic waves (i.e., waves in a magnetized plasma with frequencies much below the ion cyclotron frequency) and their surface manifestations (micropulsations and telluric currents) are growing in importance as diagnostic probes of the magnetosphere. Extensive reviews on this subject have been written by Jacobs (1970), Aubry (1970), Orr (1973), Campbell (1973), and others. Most studies focused on wave propagation characteristics in the magnetospheric plasma with the assumption of negligible effects of both wave-particle interactions and the shape of plasma particle velocity distribution functions. However, there are many phenomena which, if they are to be understood quantitatively, require that the effects of wave-particle interactions be distinguished from other effects, e.g., boundary effects. Among those investigations which take wave-particle interactions into account are Robert's (1966) study of the "bounce-resonance" interaction, Kennel and Wong's (1967) study of the cyclotron interaction for waves propagating at any angle relative to the ambient magnetic field, and Hasegawa's (1969) study of the drift mirror instability. Finally, we come to studies of Landau damping types of wave-particle interactions for hydromagnetic waves.

1.1 Brief history

Cornwall, Coroniti, and Thorne (1971) applied Kennel and Wong's theory to the study of Landau damping of ion cyclotron waves just inside the plasmapause. In a brief comment, Parker (1968) directed attention to Barnes' (1966) solution of the dispersion relation for a two-component, strongly magnetized, collisionless plasma, which suggested that hydromagnetic waves in the magnetosphere might be heavily damped by the electromagnetic wave analogue of Landau damping, also called "transit time damping" (Stix, 1962) and "magnetic moment-magnetic field gradient interaction" (Barnes, 1967). Generalizing Barnes' (1966) solution to a multi-component plasma, Navato (1970, 1971) verified Parker's suggestion that hydromagnetic waves propagating at large angles (but not perpendicular) to the magnetic field would be damped in a few wavelengths. Following Kutsenko and Stepanov's (1960) different approach to the solution of the hydromagnetic wave dispersion relation for a magnetized, collisionless plasma, Hasegawa (1970) arrived at damping estimates in the magnetosphere similar to those of Navato. However, Kutsenko and Stepanov's treatment is valid only for cases where the ion thermal speed is less than the wave speed. Consequently, it is limited to cases of small damping rates. The present study, which is free of this limitation, attempts to explore the significance of damping of hydromagnetic waves in the inner magnetosphere by the "magnetic moment-magnetic field gradient" (MMMFG) interaction.

1.2 Scope of the investigation

We will review briefly the evidence for high rates of damping of hydromagnetic waves from the M.I.T. mid-latitude telluric station in New Hampshire. Then we will derive the linearized equations of motion for a collisionless (Vlasov) plasma in a strong magnetic field following the "statistical" theory of Chandrasekhar, Kaufman, and Watson (1957, 1958a, 1958b) which will be designated as the CKW plasma theory. This theory is equivalent to the "guiding center approximation" in "orbit" theories in plasma kinetic theory. Next we will derive the dispersion equations for hydromagnetic waves in a homogeneous, uniformly magnetized Vlasov plasma made up of a superposition of bi-maxwellian particle populations. A simple model of the magnetospheric plasma typical of the geomagnetic equatorial regions in the midnight meridian will be constructed from the results of satellite measurements. We will present numerical solutions of the dispersion equations for the magnetospheric plasma, valid for damping rates greater than the limits of validity of previous studies. We will discuss the physics of the MMMFG interaction and point out the significance of the results for magnetospheric physics and micropulsation studies. The wave mode of special interest in this study is the unguided Alfven mode since much of the wave energy received by the M.I.T. telluric station is probably due to waves in this mode.

1.3 Plasma models and wave modes

The large number of plasma models and wave modes in plasma physics can lead to confusion. For the sake of clarity, the

model and wave modes suitable to the study of hot plasma damping of hydromagnetic waves will be compared to other more commonly discussed models and wave modes.

First of all, to study hot plasma damping from first principles, we need a microscopic model. The principal parameters which govern the choice of a plasma model and the characteristics of the wave modes that the plasma can support are the wave frequency, the plasma density, and the strength of the magnetic field in which the plasma is immersed. The Clemmow-Mullaly-Allis diagram (e.g., Allis, Buchbaum, and Bers, 1963, p. 80, for a macroscopic plasma model) is a helpful way of representing the principal parameter regimes relative to wave propagation.

For high frequencies, a fairly simple plasma model consisting of free electrons and a stationary, neutralizing background of ions is used. In this theory, called the magnetoionic theory, Lorentz's (1909) theory of electrons is applied to motions of free electrons in a static magnetic field and an alternating electric field. The equations of motion are of the linearized, hydrodynamic type. Two different modes of electromagnetic waves can propagate. When the direction of propagation is parallel to the static magnetic field, both modes become circularly polarized, one left-hand circularly polarized, the other right-hand circularly polarized.

For moderate frequencies, the ion motion in now taken into consideration. Two compression waves are introduced. One mode is the plasma-ion wave, which is the acoustic branch of the compression wave. In this mode, ions and

electrons move together in the same direction, like sound waves. The other mode is the plasma-electron oscillation at the plasma frequency. This is the optical branch of the compression wave in which ions and electrons move in opposition, thereby increasing the restoring force and increasing the frequency of oscillation.

For low frequencies, if we take an incompressible, infinitely conducting fluid (a macroscopic model) in which the Lorentz force $\vec{J} \times \vec{B}$ acts, we get a guided Alfven wave. This wave is a member of the electromagnetic family but one with the displacement current negligible compared to the real current.

If we relax the incompressibility assumption we get three magnetohydrodynamic (MHD) modes. Four modes arise in a two-component fluid model plasma. In the low frequency limit there are only three modes because the inertial effect of the electrons becomes negligible.

In contrast, it is shown at the end of Chapter 3 that our microscopic plasma model can support an infinite number of separate wave modes. Tajiri (1967) states that the first three least damped modes, in order of increasing damping, are the guided Alfven mode, the unguided Alfven (fast magnetosonic) mode, and the acoustic (slow magnetosonic) mode.

1.4 Evidence for strong damping of hydromagnetic waves

Santirocco and Parker (1963) obtained a series of micropulsation spectra in Bermuda. If peaks are disregarded in the spectra, it becomes possible to fit the curves between .005 and 0.1 cps by a function that is a product of a power-law factor and an exponential factor. If

P = power density, $(mv/km)^2/cps$
f = frequency, cps
n = power-law index
δ = attenuation factor
C = a constant of proportionality

the spectra may be approximated by the expression

$$P = Cf^n e^{-\delta f} \qquad (1.1)$$

The basic parameters of the spectra would be n and δ. The attenuation factor is proportional to the damping rate. When waves with one angle of propagation relative to the earth's magnetic field predominate, then δ is independent of frequency. It seems possible to fit constant δ curves to the observed spectra. The index n, which may be positive or negative, depends on several factors. It depends on the normalization used for the spectra, i.e., whether power density is given in power / cps or in power / octave. Over the limited frequency range of interest in this study it is hoped that the wave source spectrum can be adequately modeled by a power-law type spectrum, which would then affect the value of n. The index n furthermore depends on whether magnetic, $d\vec{B}/dt$, or electric measurements are being made. For electric field fluctuations, the value of n also depends partly on the relationship between the electric and magnetic fields. This relationship depends in turn on the conductivity structure of the earth in the region in which the telluric station is located.

Figure 1.1 plots values of n and δ estimated for the series of Bermuda micropulsation spectra with power density expressed in terms of power/cps. The average value of the power-law index n was -2.13, and the average attenuation factor δ

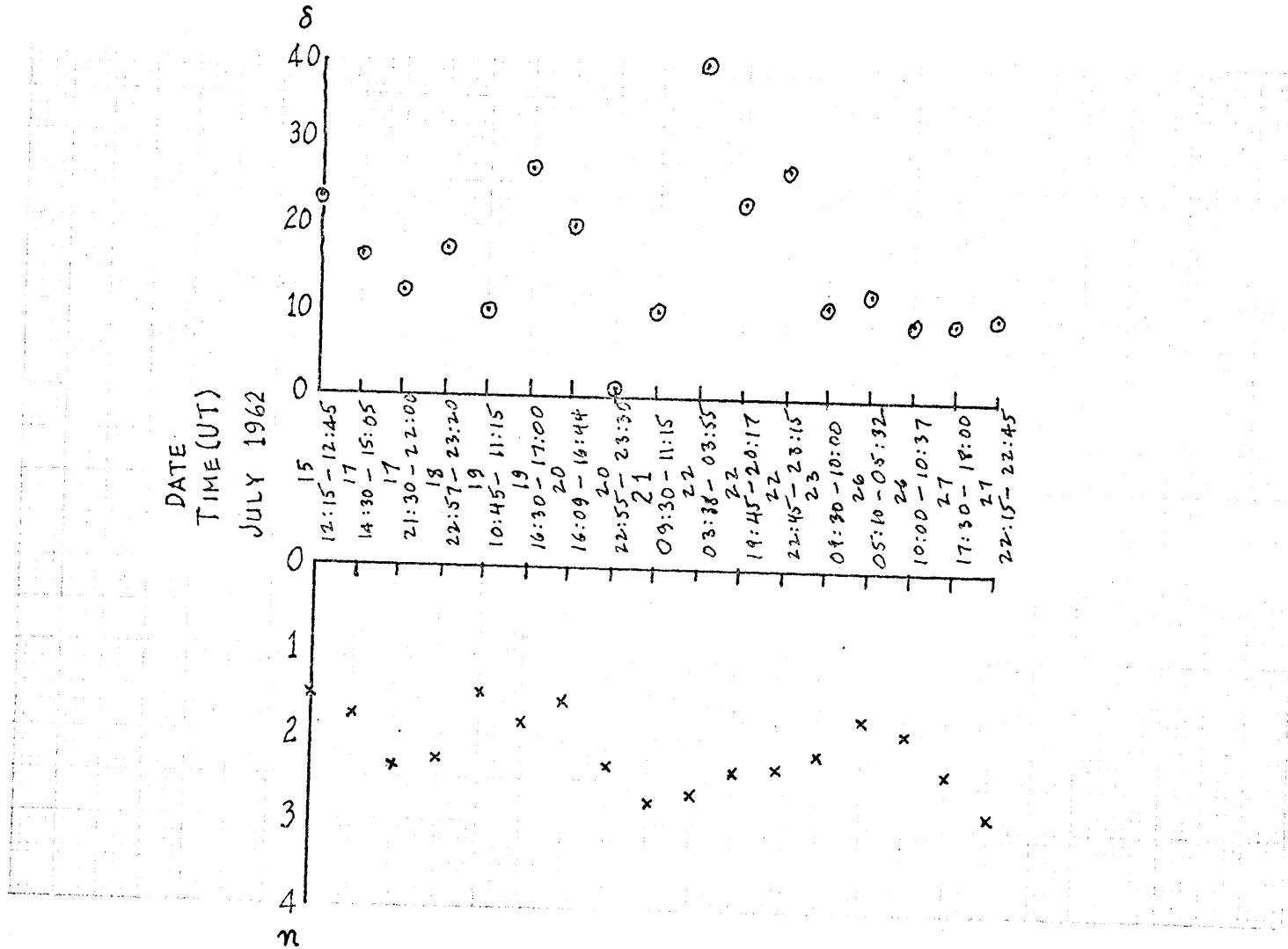

Figure 1.1 Estimates of power-law index n and attenuation factor δ for Bermuda magnetic field fluctuations

is 16.4 which is high enough to indicate considerable damping.

In this study, we consider damping to be strong when a wave, with wavelength equal to the height of the damping region in the plasmasphere, is reduced to $1/e$ of its power while traversing the damping region. We estimate that a value of the attenuation factor of 50 or greater implies strong damping.

Figure 1.2 shows telluric fluctuations observed at the M.I.T. telluric station in New Hampshire. The geomagnetic coordinates of the midpoint of the 75 km interval between the lead plate electrodes of the station are 54.9° N and 357.2° E (43.5° N geographic latitude, 288° E geographic longitude). The midpoint lies on a field line with McIlwain's magnetic shell parameter $L = 3$. The frequency range is from DC to 2 cps. The top strip shows amplitude levels in the Pc1, or "pearl", band, while the second strip shows amplitude levels in the frequency bands of most interest in this study, the Pc2 and Pc3 bands. In the top strip there occurs a sudden enhancement of amplitude at about 16:45 EST lasting for an hour. A simultaneous drop in amplitude to less than a fourth of its former level occurs in the Pc2 and 3 bands, and lasts as long as the Pc1 enhancement. This simultaneous enhancement and drop in levels of the "pearl" band and Pc2 and 3 bands are not unusual.

The "pearl" event is generally believed to be caused by hot protons (tens of kev) in the vicinity of the plasmapause (e.g., Liemohn, 1967). Figures 1.3 and 1.4 show schematic diagrams of the structure of the magnetosphere to help identify structures referred to in this study. Figure 1.3 shows a cross-section along the noon-midnight meridian plane. Figure 1.4 shows a cross-

Figure 1.2

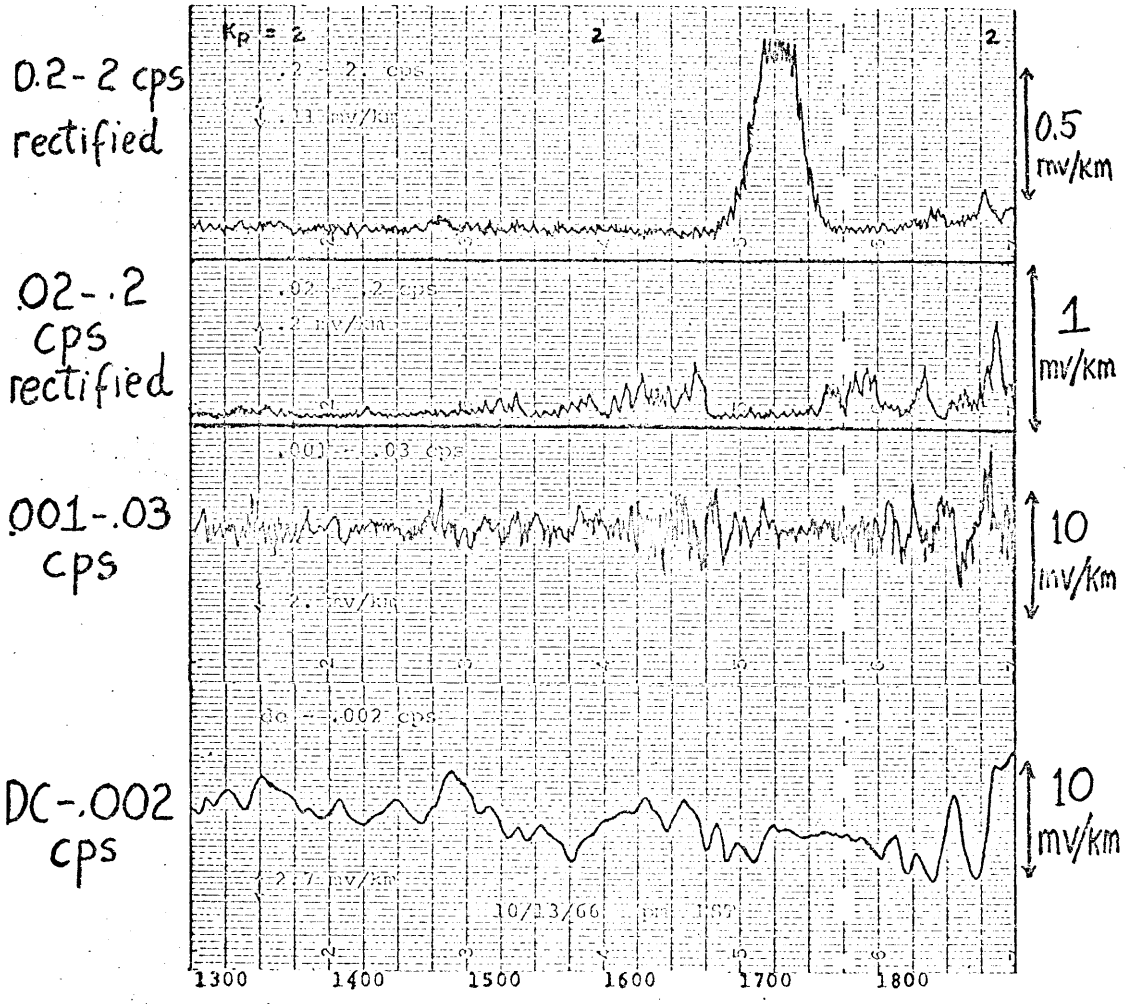

TELLURIC FLUCTUATIONS
NEW ENGLAND 10/13/66

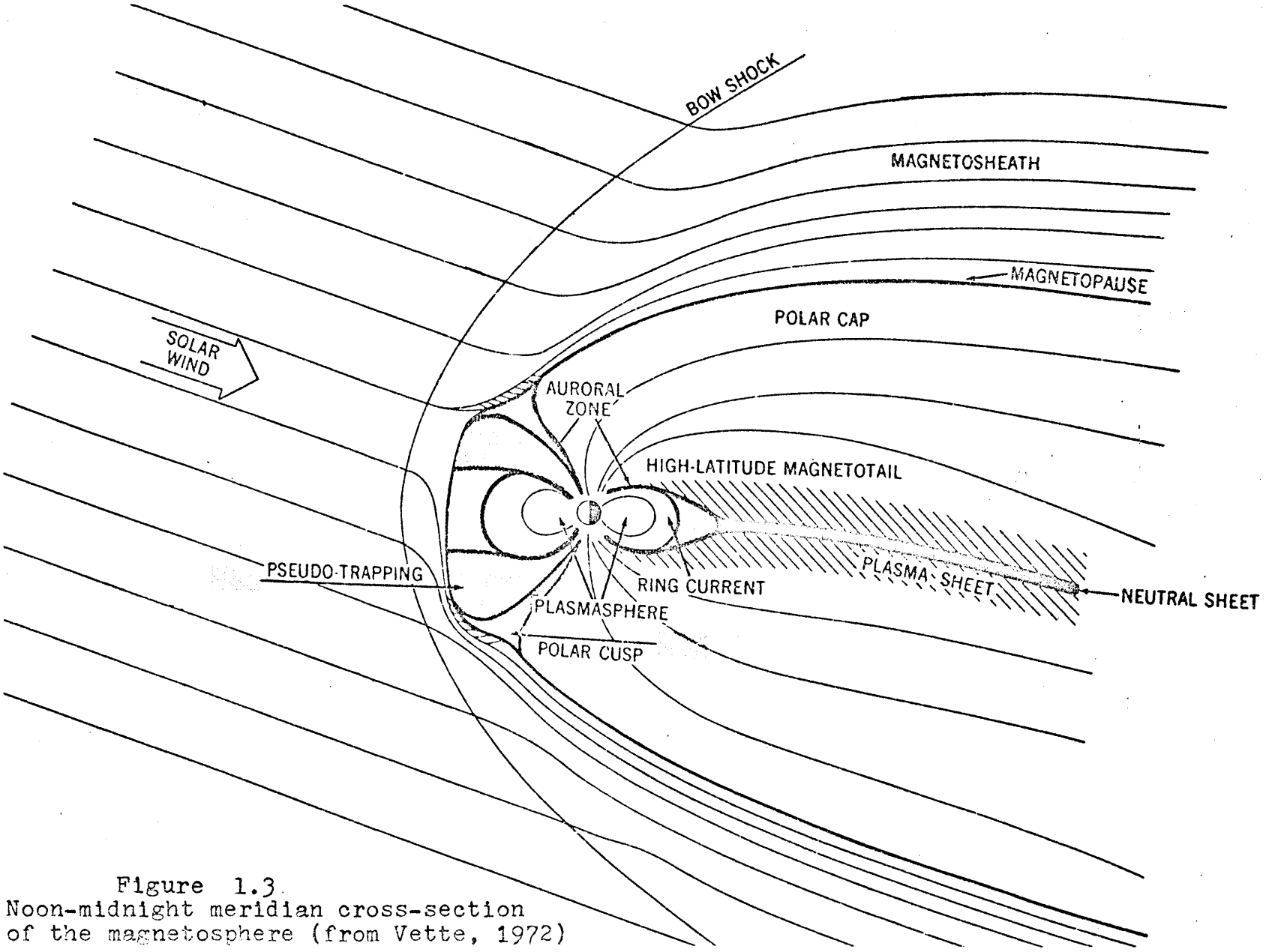

Figure 1.3
Noon-midnight meridian cross-section
of the magnetosphere (from Vette, 1972)

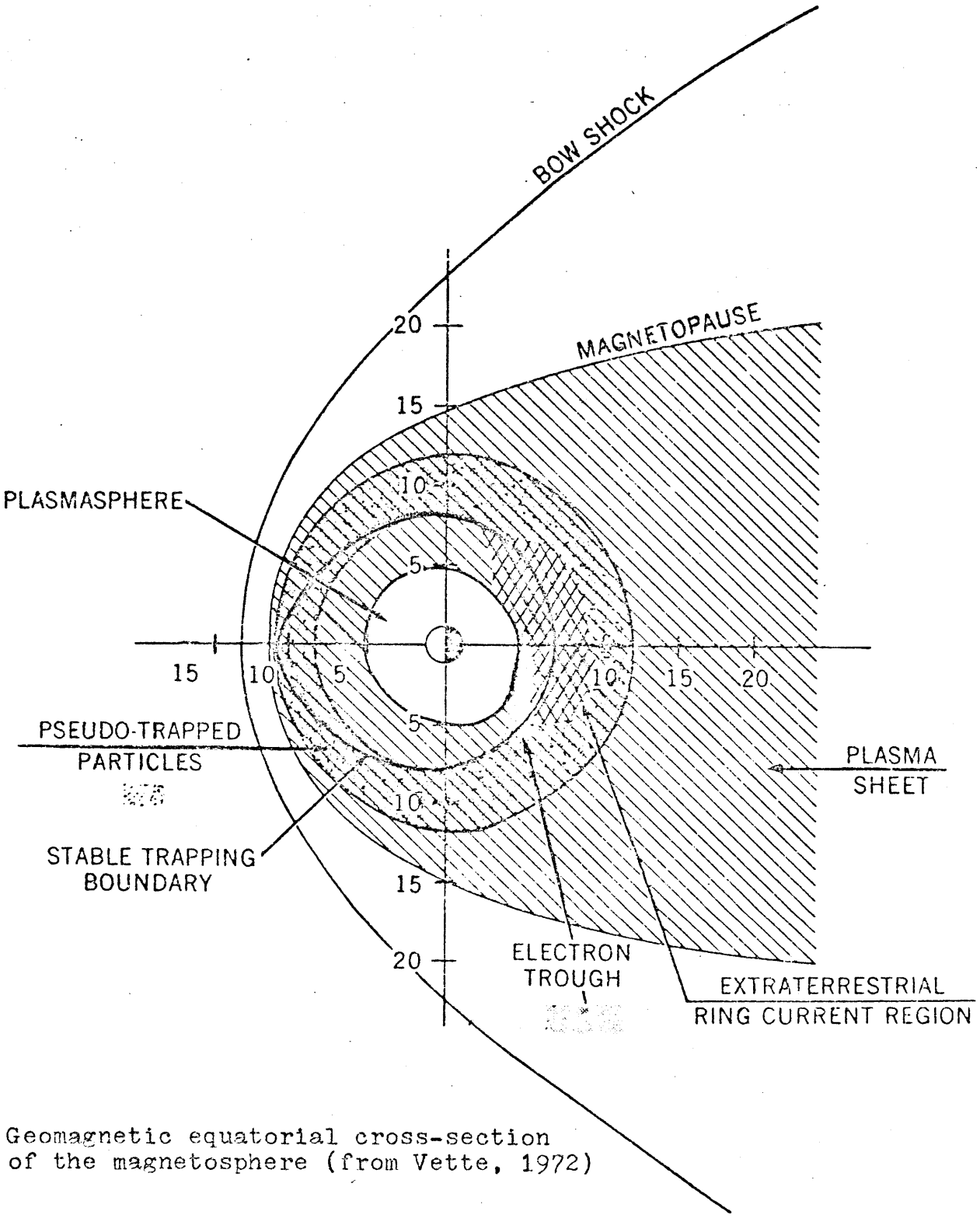

Geomagnetic equatorial cross-section
of the magnetosphere (from Vette, 1972)

Figure 1.4

section along the geomagnetic equatorial plane.

It is reasonable to think that the drop in amplitude in the second strip, the unguided Alfven wave band, was due to the same hot proton population, or another (but similar) hot proton population from the same plasma cloud, which caused the simultaneous "pearl" event on the top strip. In Chapter 4, we will see how one and the same hot proton population can simultaneously enhance the "pearl" band (generally thought to be the ion cyclotron mode, which is a guided Alfven wave) and damp the unguided Alfven mode in the Pc2 and 3 bands.

Indirect evidence of damping within the plasmasphere cavity with a quality factor Q independent of frequency comes from studies of plasmasphere resonances by Madden (1968).

Micropulsations and telluric fluctuations often exhibit spectral peaks at periods of 7 to 15 minutes, 60 to 100 seconds, and 20 to 30 seconds (Madden, 1968; Saito, 1962). Madden investigated the interpretation that the two highest frequency peaks (see Figure 1.5) are the first (i.e., fundamental) and second harmonic resonance oscillations of unguided Alfven waves trapped inside the resonance cavity formed between regions of strong gradients of Alfven speed within the plasmapause. Figure 1.5 is a histogram of peaks in the dynamic spectra of telluric fluctuations observed at the M.I.T. telluric station. Figure 1.6 shows Madden's model of the strong Alfven speed gradients forming a toroidal cavity around the earth, inside which wave energy may be trapped. Madden used a spherical model of the plasmasphere. The peak frequencies observed from the M.I.T. telluric station in New Hampshire agree with the

Figure 1.5

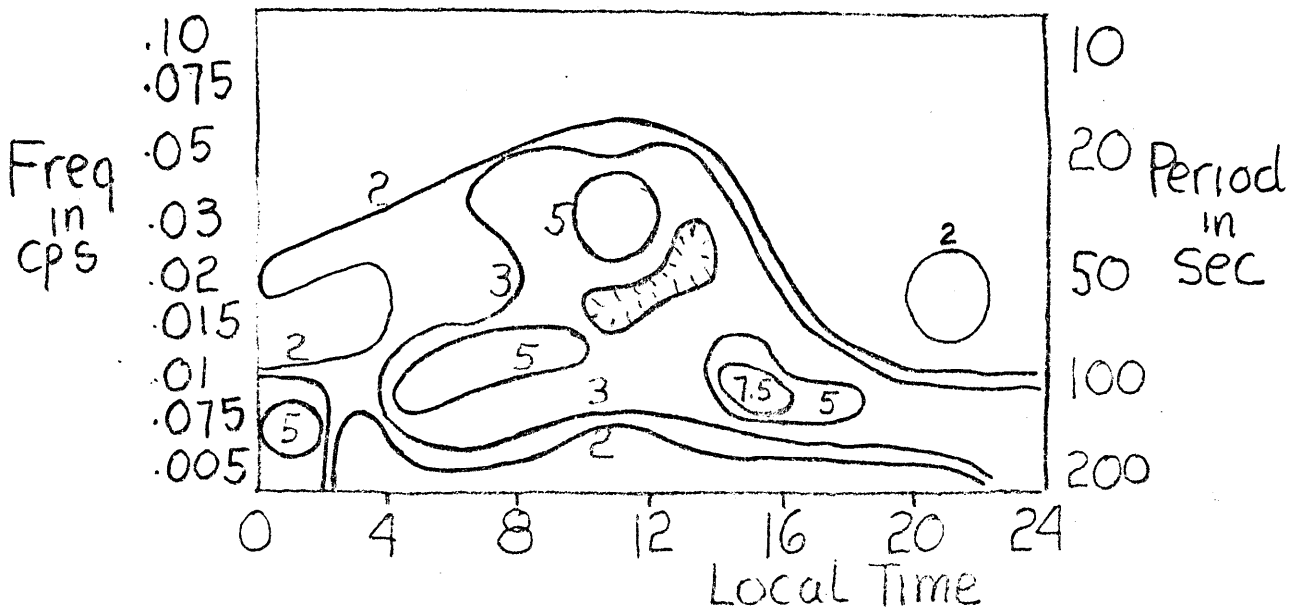

PC 2,3,4 Spectral Activity
New England Feb & June 1966

Figure 1.6

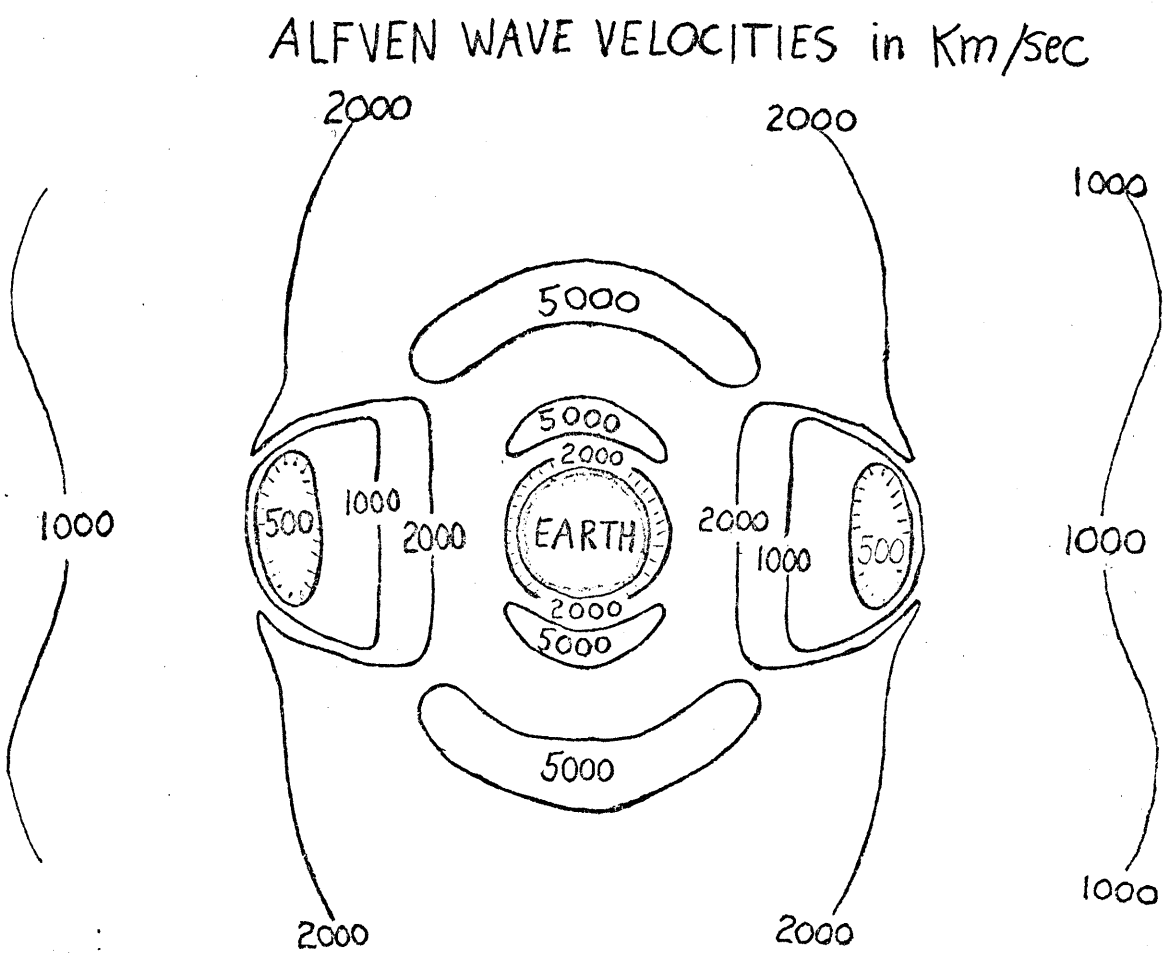

EFFECT of PLASMA PAUSE
on ALFVEN WAVE VELOCITIES

predicted frequencies, and their diurnal variations correlate well with the variations in the plasmapause geometry. If only leakage of energy due to imperfect reflection at the cavity boundaries and collision damping are allowed in the model, Madden found that the higher harmonics should become increasingly sharp and prominent in the spectrum (see Figure 1.7). Such higher harmonics are not seen in the observed spectra.

When the Q is independent of frequency, higher frequency waves with their shorter wavelengths go through more cycles and suffer greater attenuation than lower frequency waves in traversing a given distance in the magnetosphere. Assuming this time a damping distance of one wavelength in the cavity, Madden showed that on a simple model of the cavity the third harmonic just ceases to be recognizable (see Figures 1.7 and 1.8). In the plasmasphere cavity, the calculated spectrum would be affected by damping in the manner shown in Figure 1.7. The peaks corresponding to higher harmonics, instead of becoming sharper and more prominent, become smoothed out and reduced. The absence of higher harmonics from the observed spectra may indicate strong damping of hydromagnetic waves in the plasmasphere.

Figure 1.7

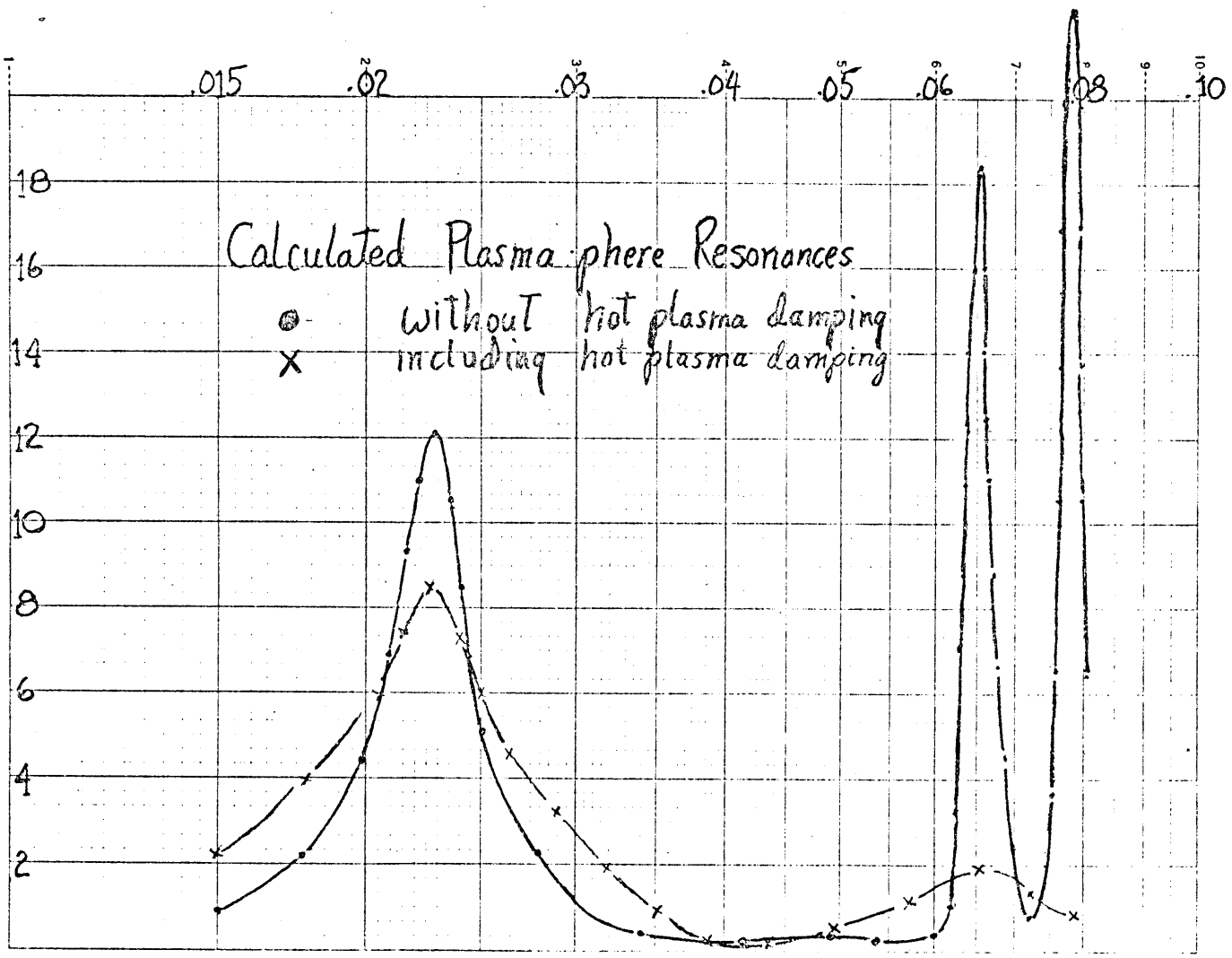
.015
.02
.03
.04
.05
.06
.08
.10
18
16
14
12
10
8
6
4
2
Calculated Plasma sphere Resonances
without hot plasma damping
including hot plasma damping

Figure 1.8

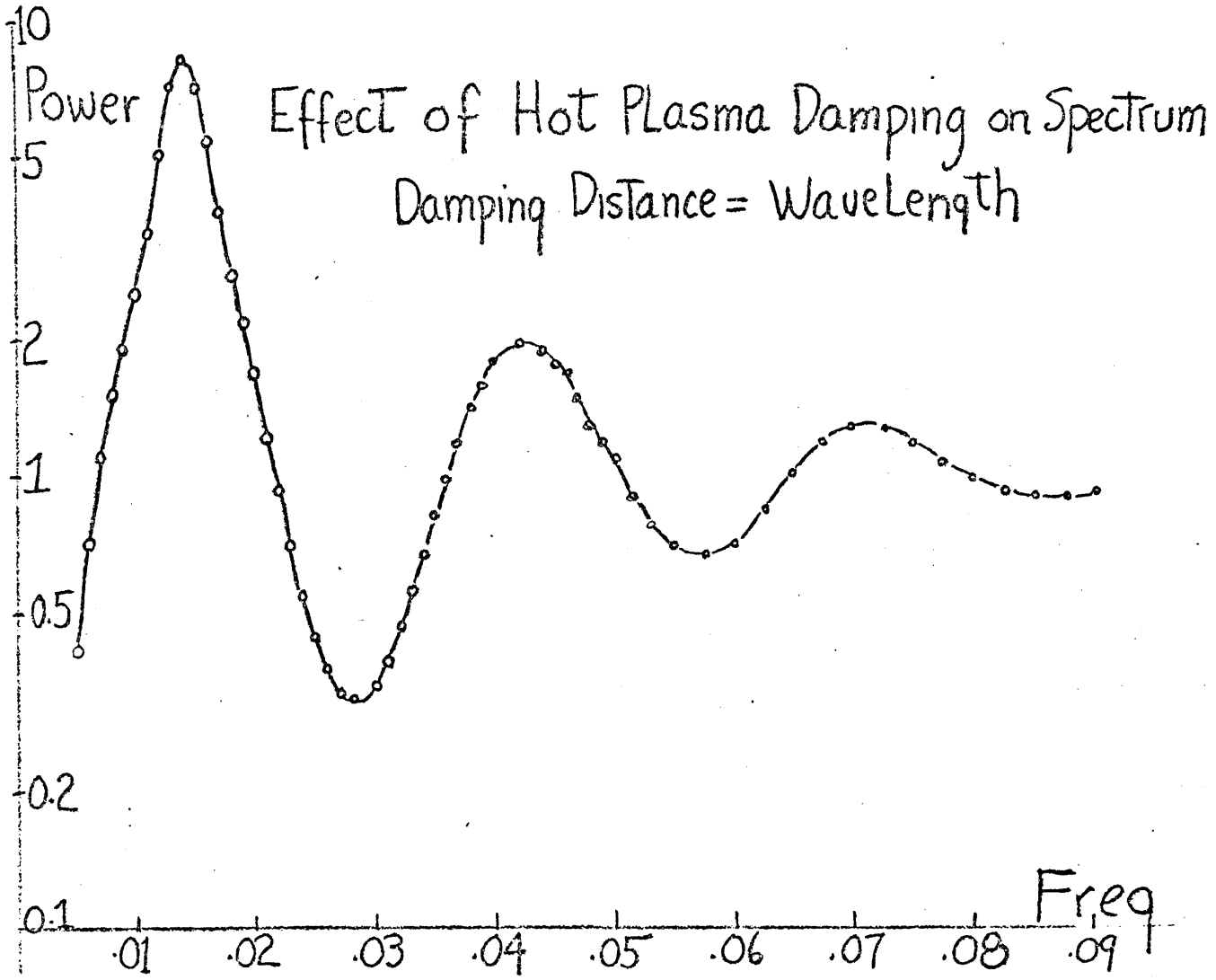
Effect of Hot Plasma Damping on Spectrum
Damping Distance = WaveLength
Power
10
5
2
1
0.5
0.2
0.1
Freq
.01
.02
.03
.04
.05
.06
.07
.08
.09

CHAPTER 2

EQUATIONS OF MOTION FOR A VLASOV PLASMA IN A STRONG MAGNETIC FIELD

The solution of the Boltzmann equation for a collisionless plasma in a strong magnetic field will be derived in this chapter following the theory of Chandrasekhar, Kaufman, and Watson (1957, 1958a, 1958b). The theory is presented here to make it more accessible (it appeared in a series of papers), to correct mistakes and to supply omissions in the original papers. Asterisks mark new and unpublished equations.

2.1 Collisionless Boltzmann's equation in terms of hydrodynamic-like quantities

The equation to be solved is the collisionless Boltzmann's equation

$$\frac{\partial \bar{f}}{\partial t} + v_j \frac{\partial \bar{f}}{\partial x_j} + A_j \frac{\partial \bar{f}}{\partial v_j} + \frac{e}{m} \epsilon_{ijk} \frac{\partial \bar{f}}{\partial v_i} v_j B_k = 0 \qquad (1)$$

where A_j is the particle acceleration due to an external body force. Let

$$\bar{f}(x_i, v_i, t) = \bar{f}^o(x_i, v_i) + \bar{f}'(x_i, v_i, t) \qquad (2)$$

= distribution function in phase space.

Let us find the equations which $\bar{f}^o$ and $\bar{f}$ must satisfy. The equation that must be satisfied by $\bar{f}^o$ is

$$v_j \frac{\partial \bar{f}^o}{\partial x_j} + A_j \frac{\partial \bar{f}^o}{\partial v_j} + \frac{e}{m} B^o \lambda \epsilon_{ijk} \frac{\partial \bar{f}^o}{\partial v_i} v_j n_k = 0 \qquad (3)$$

where $\vec{B}^o \equiv B^o \lambda (x_i) \vec{n}$ (4)

= ambient magnetic field

$\vec{n}$ = a unit vector in the direction of $\vec{B}^o$, with $n_1 = n_2 = 0$, $n_3 = 1$.

We want solutions in terms of hydrodynamic-like parameters of each particle species of the plasma. We will need to take moments of equation (2).

Particle number density, $N = \int \bar{f} \, d^3v$ (5)

Local mean velocity, $V_i = \frac{1}{N} \int \bar{f} v_i \, d^3v$ (6)

Pressure tensor, $p_{ij} = m \int \bar{f} (v_i - V_i)(v_j - V_j) \, d^3v$ (7)

Let $B_i = B_i^{\,o} + B_i'$ (8)

$A_i = A_i^{\,o} + A_i'$ (9)

$N = N^o + N'$ (10)

$v_i = V_i^o + v_i'$ (11)

$p_{ij} = p_{ij}^o + p_{ij}'$, etc. (12)

where variables with superscript "o" refer to time-dependent components, and primed variables refer to time-dependent components.

For convenience in deriving the moments of equation (1),

we will rewrite equation (1) in terms of the distribution function f of the peculiar velocity v_i rather than of the velocity v_i.

$$v_i = v_i - V_i^\circ \tag{13}$$

In terms of v_i, equation (3) becomes

$$(v_j + V_j^\circ)\frac{\partial f^\circ}{\partial x_j} + \left(\frac{e}{m}\epsilon_{ijk} v_j B_k^\circ + \frac{1}{mN^\circ}\frac{\partial p_{ij}^\circ}{\partial x_j} - v_j \frac{\partial V_i^\circ}{\partial x_j}\right)\frac{\partial f^\circ}{\partial v_i} = 0 \tag{14}$$

The time-independent component of the acceleration A_i° due to external body forces is hidden in the pressure divergence term

$$\frac{1}{mN^\circ}\frac{\partial p_{ij}^\circ}{\partial x_j}\frac{\partial f^\circ}{\partial v_i}$$

Let us now find the equation that must be satisfied by $\bar{f}'$. Let $U_i(t)$ be a small, first order velocity perturbation resulting from a small perturbation of the plasma.

$$\bar{f}(x_i, v_i, t) = \bar{f}^\circ(x_i, v_i - U_i(t)) + \bar{f}'(x_i, v_i, t) \tag{15}$$

After a Taylor expansion of $\bar{f}$ about $\bar{f}^\circ(x_i, v_i)$ and linearization, equation (1) becomes:

$$\left(\frac{\partial}{\partial t} + v_j \frac{\partial}{\partial x_j} + A_j^\circ \frac{\partial}{\partial v_j} + \frac{e}{m} \epsilon_{ijk}\, v_j\, B_k^\circ \frac{\partial}{\partial v_i}\right) \bar{f}' + A_j' \frac{\partial \bar{f}^\circ}{\partial v_j} +$$

$$\frac{e}{m} \epsilon_{ijk}\, v_j\, B_k' \frac{\partial \bar{f}^\circ}{\partial v_i} = \left(\frac{\partial}{\partial t} + v_j \frac{\partial}{\partial x_j} + A_j^\circ \frac{\partial}{\partial v_j} + \frac{e}{m} \epsilon_{ijk}\, v_j\, B_k^\circ \frac{\partial}{\partial v_i}\right) U_l \frac{\partial \bar{f}^\circ}{\partial v_l} \qquad (16)$$

U_i is that part of the particle drift velocity due to the time-dependent component A_i' of A_i. Using the relation

$$\frac{\partial U_i}{\partial t} = A_i' + \frac{e}{m} \epsilon_{ijk} U_j B_k^\circ \qquad (17)$$

assuming the boundary condition that U_i vanishes in the stationary state of the plasma when A_i' is zero; assuming furthermore that A_i is independent of v_i, and neglecting the second order terms $A_i' \frac{\partial \bar{f}'}{\partial v_i}$ and $\frac{e}{m} \epsilon_{ijk} v_j B_k' \frac{\partial \bar{f}'}{\partial v_i}$.

we can eliminate A_i' and simplify the right-hand side of equation (16) to obtain

$$\mathcal{O}_2 \bar{f}' = -U_j \frac{\partial \bar{f}^\circ}{\partial x_j} + v_j \frac{\partial \bar{f}^\circ}{\partial v_k} \frac{\partial U_k}{\partial x_j} - \frac{e}{m} \epsilon_{ijk} v_j B_k' \frac{\partial \bar{f}^\circ}{\partial v_i} \qquad (18)$$

where $\mathcal{O}_2 \equiv \frac{\partial}{\partial t} + v_j \frac{\partial}{\partial x_j} + A_j^\circ \frac{\partial}{\partial v_j} + \frac{e}{m} \epsilon_{ijk}\, v_j\, B_k^\circ \frac{\partial}{\partial v_i}$ (19)

Assuming that $\bar{f}' \ll \bar{f}^o$ (20)

so that $N' \ll N^o$, (21)

and assuming further that

$$U_i \ll \bar{v}_i \ , \quad V_i^\circ \ll \bar{v}_i \ , \quad V_i^\circ \frac{\partial \overline{\bar{f}'(v)}}{\partial v} \ll \overline{\bar{f}'(v)} \tag{22}$$

where the heavy bars denote averaging over all particles for inequalities (20) and (21), and over all velocity space for inequalities (22), then the perturbation velocity U_i is related to the change in the local mean velocity by

$$V_i' = U_i + \frac{1}{N^\circ} \int \bar{f}' v_i \, d^3v = U_i + \frac{1}{N^\circ} \iiint (\zeta_i + \varrho \eta_i) \bar{f}'(s \, d\varphi) \, ds \, d\varrho \tag{23}$$

where $\vec{s}$ is the component of $\vec{v}$ that is perpendicular to $\vec{B}^\circ$.

To write equation (18) in terms of v_i , N° , $V_i{}^\circ$, and p°_{ij}, we need the momentum equation for $\bar{f}$ in order to introduce the pressure tensor. We must first write equation (1) in terms of these variables:

$$\left(\frac{\partial}{\partial t} + V_j^\circ \frac{\partial}{\partial x_j} + v_j \frac{\partial}{\partial x_j} + A_j \frac{\partial}{\partial v_j} \right) \bar{f} + \frac{e}{m} \epsilon_{k\ell m} V_\ell^\circ B_m \frac{\partial \bar{f}}{\partial v_k}$$
$$- \left(\frac{\partial V_k^\circ}{\partial t} + V_j^\circ \frac{\partial V_k^\circ}{\partial x_j} \right) \frac{\partial \bar{f}}{\partial v_k} + \frac{e}{m} \epsilon_{k\ell m} v_\ell B_m \frac{\partial \bar{f}}{\partial v_k} - v_j \frac{\partial V_k^\circ}{\partial x_j} \frac{\partial \bar{f}}{\partial v_k} = 0 \tag{24}^*$$

On taking the zero-order moment of this equation, we obtain the continuity equation

$$\frac{\partial N}{\partial t} + V_j^\circ \frac{\partial N}{\partial x_j} + N \frac{\partial V_j{}^\circ}{\partial x_j} + V_j' \frac{\partial N}{\partial x_j} + N \frac{\partial V_j'}{\partial x_j} = 0 \tag{25}$$

On taking the first-order moment of equation (24), using equation (25), and doing some partial integration, we obtain the momentum equation

$$\frac{\partial(Nm V_\kappa')}{\partial t} + \frac{\partial(Nm V_i^\circ V_\kappa')}{\partial x_i} + \frac{\partial p_{i\kappa}}{\partial x_i} +$$
$$Nm\left[\frac{\partial V_\kappa^\circ}{\partial t} + V_i^\circ \frac{\partial V_\kappa^\circ}{\partial x_i} + V_i' \frac{\partial V_\kappa^\circ}{\partial x_i} - A_\kappa - \frac{e}{m}\epsilon_{\kappa j\ell}(V_j^\circ + V_j')B_\ell\right] = 0 \qquad (26)$$

Using the time-independent terms of this equation to introduce the pressure tensor term, we can write equation (18) in terms of v_i to give the equation that must be solved for f' in terms of hydrodynamic-like variables:

$$\frac{\partial f'}{\partial t} + (v_j + V_j^\circ)\frac{\partial f'}{\partial x_j} + \left[\frac{e}{m}\epsilon_{ijk} v_j B_k^\circ + \frac{1}{mN^\circ}\frac{\partial p_{ij}^\circ}{\partial x_j} - v_j \frac{\partial V_i^\circ}{\partial x_j}\right]\frac{\partial f'}{\partial v_i} +$$
$$U_j\left(\frac{\partial f^\circ}{\partial x_j} - \frac{\partial f^\circ}{\partial v_\kappa}\frac{\partial V_\kappa^\circ}{\partial x_j}\right) - (v_j + V_j^\circ)\frac{\partial U_\kappa}{\partial x_j}\frac{\partial f^\circ}{\partial v_\kappa} + \frac{e}{m}\epsilon_{ijk}\frac{\partial f^\circ}{\partial v_i}(v_j + V_j^\circ)B_k' = 0 \qquad (27)$$

2.2 Time-independent solution of the Boltzmann equation

The general solution of equation (3) for the time-independent component f° will be sought first. We will use a perturbation method to solve equation (3) for f°. Let us then write f° as a power series in the smallness parameter η :

$$f^\circ \equiv f_0^\circ + \eta f_1^\circ + \eta^2 f_2^\circ + \cdots\cdots + \eta^\ell f_\ell^\circ + \cdots\cdots \qquad (28)$$

where $$\eta \equiv \frac{\bar{r}_\perp}{L} = \frac{m}{eB^\circ}\frac{\bar{v}_\perp}{L} = \frac{1}{\omega_c}\frac{\bar{v}_\perp}{L} \simeq \frac{\Omega}{\omega_c} \ll 1. \qquad (29)$$

L = characteristic length of plasma inhomogeneities

Ω = wave angular frequency

To collect terms of the same order in η we substitute equation (28) in equation (3). We then obtain the following sequence of differential equations which determine f_0°, f_1°, f_2°, ..., f_ℓ° , ...

$$\lambda \mathscr{L}_1 f_0^\circ = 0 \tag{30}$$

$$\mathscr{D}_1 f_0^\circ + \lambda \mathscr{L}_1 f_1^\circ = 0 \tag{31}$$

$$\vdots$$

$$\mathscr{D}_1 f_{\ell-1}^\circ + \lambda \mathscr{L}_1 f_\ell^\circ = 0 \qquad (\ell = 1, 2, 3, \cdots\cdots) \tag{32}$$

where $$\mathscr{D}_1 \equiv v_j \frac{\partial}{\partial x_j} + A_j \frac{\partial}{\partial v_j} \tag{33}$$

and $$\mathscr{L}_1 \equiv \frac{\bar{v}_i}{L} \epsilon_{ijk} v_j \eta_k \frac{\partial}{\partial v_i} = -\frac{\bar{s}}{L} \frac{\partial}{\partial \varphi} \tag{34}$$

Since f_ℓ° is periodic in φ with period 2π ,

$$\langle \mathscr{L}_1 f_\ell^\circ \rangle = 0 \qquad (\ell = 0, 1, 2, \cdots\cdots) \tag{35}^*$$

where, for any function $x(\varphi)$ of the azimuthal angle φ (around the direction of $\vec{B}^0$), the average over φ is indicated by the symbol $\langle\ \rangle$, so that

$$\langle x(\varphi) \rangle = \frac{1}{2\pi} \int_a^{a+2\pi} x(\varphi)\, d\varphi \tag{36}^*$$

Hence, on averaging the terms in equation (31) over

all directions of $\vec{s}$ (i.e., over φ), we find integrability conditions that must be further satisifed by f_0°, f_1°, f_2°, ...,

$$\langle \mathcal{D}_l \, f_l^\circ \rangle = 0 \qquad (l = 0, 1, 2, \cdots) \tag{37}$$

Let us find the form of the functional dependence of f_0° on x_i, s_i, and q, where q is the component of v_i parallel to $\vec{B}^0$. Assuming no time-independent external body force so that

$$A_j^\circ = 0 \tag{38}$$

equation (30) becomes, in vector form,

$$(\vec{\nabla}_v f_0^\circ) \cdot \vec{v} \times \vec{n} = 0 \tag{39}$$

Since this equation demands that f_0° be symmetrically dependent on $(\vec{v})_\perp$, or $\vec{s}$, we have

$$f_0^\circ \equiv f_0^\circ (x_i, s^2, q) \tag{40}$$

We then substitute equation (40) into the first integrability condition in equation (37) to obtain

$$n_j \frac{\partial f_0^\circ}{\partial x_j} + s^2 \frac{\partial n_j}{\partial x_j} \left(\frac{1}{2q} \frac{\partial f_0^\circ}{\partial q} - \frac{\partial f_0^\circ}{\partial s^2} \right) = 0 \tag{41}$$

From one of Maxwell's equations, we evaluate the divergence of $\vec{n}$ as

$$\frac{\partial \eta_j}{\partial x_j} = -\frac{1}{B^\circ}\eta_j \frac{\partial B^\circ}{\partial x_j} \tag{42}$$

Substituting this into the preceding equation, we can now solve the first integrability condition equation (41) by the method of characteristics to obtain the general solution

$$f_o^\circ \equiv f_o^\circ \left(H, \mu, \int_{\vec{r}_o}^{\vec{r}} d\vec{r} \times \frac{\vec{B}^\circ}{B^\circ}\right) \tag{43}$$

where $H = w_\parallel + w_\perp$ = the sum of the parallel and perpendicular components of the total kinetic energy of a particle, a constant (44)

$$\mu = \frac{s^2}{2H B^\circ \times \text{a constant}} = \frac{w_\perp}{B^\circ} \tag{45}$$

= the magnetic moment of a particle a constant

$\int_{\vec{r}_o}^{\vec{r}} d\vec{r} \times \frac{\vec{B}^\circ}{B^\circ}$ = a vector which is constant along a magnetic line of force. (46)

With this knowledge of the functional form of f_o° we can find the first-order part, f_1°, of f° from equation (14). Since we will do much averaging over all directions of $\vec{s}$, let us write equation (14) in terms of $\vec{s}$ and q:

$$\partial_4 f^\circ + \frac{1}{\eta}\lambda \mathcal{L}_1 f^\circ = 0 \tag{47}$$

where $$\mathcal{D}_4 \equiv (S_j + q n_j + V_j^\circ)\left[\frac{\partial}{\partial x_j} - \left(n_i S_\kappa \frac{\partial n_\kappa}{\partial x_j} + q \frac{\partial n_i}{\partial x_j}\right)\frac{\partial}{\partial S_i} + S_\kappa \frac{\partial n_\kappa}{\partial x_j}\frac{\partial}{\partial q}\right] + \left[\frac{1}{m N^\circ}\frac{\partial p_{ij}}{\partial x_j} - (S_j + q n_j)\frac{\partial V_i^\circ}{\partial x_j}\right]\left[(\delta_{ij} - n_i n_j)\frac{\partial}{\partial S_j} + n_i \frac{\partial}{\partial q}\right] \quad (48)^*$$

Substituting equation (28) into equation (47), we obtain the sequence of equations (30)...(32) for f_0°, f_1°, f_2°, ... in a form convenient for averaging over all directions of $\vec{s}$. The equation to be solved for f_1° is

$$-\mathcal{L}_1(\lambda f_1^\circ) = \mathcal{D}_4 f_0^\circ - \langle \mathcal{D}_4 f_0^\circ \rangle \quad (49)^*$$

From the equivalence of the operators $\mathcal{D}_1$ and $\mathcal{D}_4$ we note from the integrability condition for f_0° given in equations (37) that the last term on the right-hand side of equation (49) vanishes. Equation (49) reduces to

$$-\epsilon_{ijk}\frac{\partial(\lambda f_1^\circ)}{\partial S_i} S_j n_\kappa = \left[S_j \Phi_j + (S_i S_j - \langle S_i S_j \rangle)\Phi_{ij}\right] \quad (50)$$

where $$\Phi_i \equiv \frac{\partial f_0^\circ}{\partial x_i} + 2q(q n_j + V_j^\circ)\frac{\partial n_i}{\partial x_j}\left(\frac{1}{2q}\frac{\partial}{\partial q} - \frac{\partial}{\partial S^2}\right) f_0^\circ + \frac{2}{m N^\circ}\frac{\partial p_{ij}}{\partial x_j}\frac{\partial f_0^\circ}{\partial S^2} - 2q n_j\left(\frac{\partial V_i^\circ}{\partial x_j}\frac{\partial}{\partial S^2} + \frac{\partial V_j^\circ}{\partial x_i}\frac{\partial}{\partial q^2}\right) f_0^\circ \quad (51)$$

which is a vector that is independent of the direction of $\vec{s}$,

and

$$\Phi_{ij} = g\left(\frac{\partial \eta_i}{\partial x_j} + \frac{\partial \eta_j}{\partial x_i}\right)\left(\frac{1}{2g}\frac{\partial}{\partial g} - \frac{\partial}{\partial s^2}\right) f_o^\circ - \left(\frac{\partial V_i^\circ}{\partial x_j} + \frac{\partial V_j^\circ}{\partial x_i}\right)\frac{\partial f_o^\circ}{\partial s^2} \qquad (52)$$

which is a constant tensor that is symmetric in its indices. A particular integral $(\lambda f_1^\circ)_p$ of equation (50) is then

$$(\lambda f_1^\circ)_p = \epsilon_{ijk}\left(\Phi_i + \tfrac{1}{2}\Phi_{il}\, S_l\right) S_j \eta_k \qquad (53)$$

The complementary solution $(\lambda f_1^\circ)_c$ of equation (50) must be a function of the independent variables (x_i, S^2, g) because (λf_1°) must also be a complementary solution of the equivalent equation (49), i.e.,

$$\mathcal{L}_1 (\lambda f_1^\circ)_c = -\frac{\vec{S}}{L}\frac{\partial(\lambda f_1^\circ)}{\partial \varphi} = 0 \qquad (54)$$

Hence, $$f_1^\circ = \frac{1}{\lambda}\epsilon_{ijk}\left(\Phi_i + \tfrac{1}{2}\Phi_{il}\, S_l\right) S_j \eta_k + (f_1^\circ)_c \qquad (55)$$

so that the stationary state solution of equation (1), correct to first order in η, is

$$f^\circ = f_o^\circ(x_i, S^2, g) + \frac{\eta}{\lambda}\epsilon_{ijk}\left(\Phi_i + \tfrac{1}{2}\Phi_{il}\, S_l\right) S_j \eta_k + \eta\left[f_1^\circ(x_i, S^2, g)\right]_c \qquad (56)^*$$

A differential equation for a fuller determination of $(f_1^\circ)_c$ can be obtained by substituting $(\lambda f_1^\circ)_p$ just found in equation (53) into the integrability condition (37), which now has the form

$$\langle \mathcal{O}_1 (f_1^\circ)_c \rangle + \frac{1}{\lambda} \langle \mathcal{O}_1 (\lambda f_1^\circ)_p \rangle + \langle (\lambda f_1^\circ)_p \mathcal{O}_1 (\tfrac{1}{\lambda}) \rangle = 0 \qquad (57)^*$$

However, for the purpose of obtaining the zero-order non-stationary deviation f_0', the information that $(f_1^\circ)_c$ depends on the independent variables x_i, s^2, q suffices.

2.3 Time-dependent solution of the Boltzmann equation

We are now ready to seek the solution of equation (27) for the time-dependent component f'. We will use a perturbation method to give f' in the form of a sum of terms of increasing order in η. To collect terms of the same order in η we substitute

$$f^\circ(x_i, s_i, q) = f_0^\circ(x_i, s^2, q) + \eta f_1^\circ(x_i, s_i, q) + \eta^2 f_2^\circ(x_i, s_i, q) + \cdots \qquad (58)^*$$

and

$$f'(x_i, s_i, q, t) = f_0'(x_i, s_i, q, t) + \eta f_1'(x_i, s_i, q, t) + \eta^2 f_2'(x_i, s_i, q, t) + \cdots \qquad (59)$$

into equation (27).

We will divide the left-hand side of equation (27) into two parts, the first of which will consist of terms of lowest order in η whose average over all directions of $\vec{s}$ is zero. The terms left over make up the second part.

We now restrict our considerations to cases in which the dominant terms are those which contain $\vec{B}^\circ$ or $\vec{B}'$ as a factor (these cases have $\eta \ll 1$). The first part of equation (27) is

$$\frac{eB^\circ}{m}\epsilon_{ijk}\frac{\partial f_o'}{\partial s_i}S_j\eta_k - \frac{e}{m}\left\{2q\left(\frac{\partial f_o^\circ}{\partial q^2} - \frac{\partial f_o^\circ}{\partial S^2}\right)\epsilon_{ijk}B_i'S_j\eta_k + 2\frac{\partial f_o^\circ}{\partial S^2}\epsilon_{ijk}V_i^\circ S_j B_k'\right\} \tag{60}$$

and can be written as

$$\frac{1}{\eta}\lambda\mathcal{L}_1 f_o' + \frac{1}{\eta}\lambda|b_k'|\mathcal{L}_2 f_o^\circ \tag{61}^*$$

where

$$\mathcal{L}_1 \equiv \frac{\vec{v}_\perp}{L}\epsilon_{ijk}v_j\eta_k\frac{\partial}{\partial v_i} = -\frac{\vec{S}}{L}\frac{\partial}{\partial\varphi} \tag{62}^*$$

$$\mathcal{L}_2 \equiv \frac{\sqrt{S_i S_\ell}}{L}\left\{2q\left(\frac{\partial}{\partial q^2} - \frac{\partial}{\partial S^2}\right)\epsilon_{ijk}\eta_i S_j m_k - 2\frac{\partial}{\partial S^2}\epsilon_{ijk}V_i^\circ S_j m_k\right\} \tag{63}^*$$

$$|b_k'| \equiv \frac{|B_k'|}{B^\circ} \tag{64}^*$$

and $\vec{m}$ is a unit vector in the direction of $\vec{B}^\circ$. The second part of equation (27) is

$$\mathcal{O}_2(f_o' + \eta f_1' + \eta^2 f_2' + \cdots) + \mathcal{O}_3(f_o^\circ + \eta f_1^\circ + \eta^2 f_2^\circ + \cdots) + \frac{1}{\eta}\lambda\mathcal{L}_1(\eta f_1' + \eta^2 f_2' + \eta^3 f_3' + \cdots) + \frac{1}{\eta}\lambda|b_k'|\mathcal{L}_2(\eta f_1^\circ + \eta^2 f_2^\circ + \cdots) \tag{65}^*$$

where $$\mathcal{O}_2 \equiv \frac{\partial}{\partial t} + (v_j + V_j^\circ)\frac{\partial}{\partial x_j} + \left[\frac{1}{mN^\circ}\frac{\partial p_{ij}^\circ}{\partial x_j} - v_j\frac{\partial V_i^\circ}{\partial x_j}\right]\frac{\partial}{\partial v_i} \tag{66}^*$$

$$\mathcal{O}_3 \equiv U_i\left(\frac{\partial}{\partial x_j} - \frac{\partial V_k^\circ}{\partial x_j}\frac{\partial}{\partial v_k}\right) - (v_j + V_j^\circ)\frac{\partial U_k}{\partial x_j}\frac{\partial}{\partial v_k} + 2\frac{qe}{m}\epsilon_{ijk}\eta_i V_j^\circ B_k'\frac{\partial}{\partial q^2} \tag{67}^*$$

Collecting terms of the same order in η in equation (27), and equating to zero each of the coefficients of the

various powers of η , we obtain the following sequence of approximating equations for f_0', f_1', f_2', etc.

$$\lambda \mathcal{L}_1 f_0' + \lambda |b_k'| \mathcal{L}_2 f_0^\circ = 0 \qquad (68)^*$$

$$\mathcal{D}_2 f_0' + \mathcal{D}_3 f_0^\circ + \lambda \mathcal{L}_1 f_1' + \lambda |b_k'| \mathcal{L}_2 f_1^\circ = 0 \qquad (69)^*$$

$$\mathcal{D}_2 f_1' + \mathcal{D}_3 f_1^\circ + \lambda \mathcal{L}_1 f_2' + \lambda |b_k'| \mathcal{L}_2 f_2^\circ = 0 \qquad (70)^*$$

Since the operators $\mathcal{L}_1$ and $\mathcal{L}_2$ were defined (cf. equation 35) so that

$$\langle \mathcal{L}_1 f_\ell' \rangle = 0 \qquad (\ell = 0, 1, 2, \ldots) \qquad (71)^*$$

$$\langle \mathcal{L}_2 f_0^\circ \rangle = 0 \qquad (72)^*$$

on taking the average of equations (69) and (70) over all directions of $\vec{s}$ we obtain integrability conditions on f_0' and f_1'.

$$\langle \mathcal{D}_2 f_0' + \mathcal{D}_3 f_0^\circ + \lambda |b_k'| \mathcal{L}_2 f_1^\circ \rangle = 0 \qquad (73)^*$$

$$\langle \mathcal{D}_2 f_1' + \mathcal{D}_3 f_1^\circ + \lambda |b_k'| \mathcal{L}_2 f_2^\circ \rangle = 0 \qquad (74)^*$$

With f_0° given by equation (40), we can find f_0' from equation (68) and from the integrability condition (73).

With f_0' known, we can find f_1' from equation (69) and the integrability condition (74). Equation (68) can be written as

$$\epsilon_{ijk} s_j n_k \frac{\partial (f_0')_p}{\partial s_i} = -\frac{|B_k'|}{B_0} \left[2q \epsilon_{ijk} n_i s_j m_k \left(\frac{\partial}{\partial q^2} - \frac{\partial}{\partial s^2} \right) - 2 \epsilon_{ijk} V_i^0 s_j m_k \frac{\partial}{\partial s^2} \right] f_0^0 (x_i, s^2, q) \tag{75}$$

where $(f_0')_p$ is a particular solution of this equation. It can be verified that we may take

$$(f_0')_p = \frac{2}{p^0} \vec{s} \cdot \left[\vec{B}' q \left(\frac{\partial f_0^0}{\partial q^2} - \frac{\partial f_0^0}{\partial s^2} \right) + \vec{n} \times (\vec{V}^0 \times \vec{B}') \frac{\partial f_0^0}{\partial s^2} \right] \tag{76}$$

The complementary solution $(f_0')_c$ of equation (75) satisfies the equation

$$\epsilon_{ijk} s_j n_k \frac{\partial (f_0')_c}{\partial s_i} = 0 \tag{77}^*$$

Following the same reasoning which gave us the functional dependence of f_0^0 on its independent variables in equation (40), we find that

$$(f_0')_c = f_0' (x_i, s^2, q, t)_c \tag{78}^*$$

$$\text{Since} \quad f_0' = (f_0')_p + (f_0')_c \tag{79}^*$$

a fuller determination of $(f_0')_c$ may be obtained by sub-

stituting equation (79) into the integrability condition (73). The resulting equation is

$$\langle \mathcal{D}_2 (f_0')_c \rangle = - \langle \mathcal{D}_2 (f_0')_p \rangle - \langle \mathcal{D}_3 f_0^\circ \rangle - \lambda |b_\kappa'| \langle \mathcal{L}_2 f_1^\circ \rangle \qquad (80)^*$$

where, for ease in averaging over the azimuthal angle φ, we write

$$\begin{aligned}\mathcal{D}_2 \equiv \frac{\partial}{\partial t} &+ (S_j + g n_j + V_j^\circ)\left[\frac{\partial}{\partial x_j} - (n_i S_\kappa \frac{\partial n_\kappa}{\partial x_j} + g \frac{\partial n_i}{\partial x_j}) \frac{\partial}{\partial s_i} + S_\kappa \frac{\partial n_\kappa}{\partial x_j} \frac{\partial}{\partial g}\right] \\ &+ \left\{\frac{1}{m N^\circ}\left[\frac{\partial p_{ij}^\circ}{\partial x_j} - (n_i S_\kappa \frac{\partial n_\kappa}{\partial x_j} + g \frac{\partial n_i}{\partial x_j}) \frac{\partial p_{ij}^\circ}{\partial s_i} + S_\kappa \frac{\partial n_\kappa}{\partial x_j} \frac{\partial p_{ij}^\circ}{\partial g}\right]\right. \\ &- (S_j + g n_j)\left[\frac{\partial V_i^\circ}{\partial x_j} - (n_i S_\kappa \frac{\partial n_\kappa}{\partial x_j} + g \frac{\partial n_i}{\partial x_j}) \frac{\partial V_i^\circ}{\partial s_i} + S_\kappa \frac{\partial n_\kappa}{\partial x_j} \frac{\partial V_i^\circ}{\partial g}\right] \cdot \\ &\left.\left[(\delta_{ij} - n_i n_j) \frac{\partial}{\partial s_j} + n_i \frac{\partial}{\partial g}\right]\right\}\end{aligned} \qquad (81)^*$$

$$\begin{aligned}\mathcal{D}_3 \equiv\ & U_i \left[\frac{\partial}{\partial x_j} - (n_i S_\kappa \frac{\partial n_\kappa}{\partial x_j} + g \frac{\partial n_i}{\partial x_j}) \frac{\partial}{\partial s_i} + S_\kappa \frac{\partial n_\kappa}{\partial x_j} \frac{\partial}{\partial g}\right] \\ & - U_i \left[\frac{\partial V_\kappa^\circ}{\partial x_j} - (n_i S_\kappa \frac{\partial n_\kappa}{\partial x_j} + g \frac{\partial n_i}{\partial x_j}) \frac{\partial V_\kappa^\circ}{\partial s_i} + S_\kappa \frac{\partial n_\kappa}{\partial x_j} \frac{\partial V_\kappa^\circ}{\partial g}\right] \\ & \left[(\delta_{ij} - n_i n_j) \frac{\partial}{\partial s_j} + n_i \frac{\partial}{\partial g}\right] + (S_j + g n_j + V_j^\circ)\left[\frac{\partial U_\kappa}{\partial x_j}\right. \\ & - (n_i S_\kappa \frac{\partial n_\kappa}{\partial x_j} + g \frac{\partial n_i}{\partial x_j}) \frac{\partial U_\kappa}{\partial s_i} + S_\kappa \frac{\partial n_\kappa}{\partial x_j} \frac{\partial U_\kappa}{\partial g}\Big] \left[(\delta_{ij} - n_i n_j) \frac{\partial}{\partial s_j}\right. \\ & \left. + n_i \frac{\partial}{\partial g}\right] + 2 g \epsilon_{ijk} n_i V_j^\circ B_\kappa' \frac{\partial}{\partial g^2}\end{aligned} \qquad (82)^*$$

Equation (80) gives us a first order partial differential equation for determining $(f_o')_c$. For convenience in certain classes of problems, we may express $(f_o')_c$ as the sum of an even and of an odd function of q:

$$(f_o')_c = C_1(x_i, S^2, \xi^2, t) + \xi C_2(x_i, S^2, \xi^2, t) \tag{83}$$

When we separate the even and the odd parts of the various terms in equation (80), we find that the even part C_1 contributes to the first-order change in the pressure tensor p_{ij}, the odd part qC_2 contributes to the first-order change in the mean velocity V_i.

The system of first-order partial differential equations which have to be solved for C_1 and C_2 are, in mixed vector and Cartesian tensor notation,

$$\frac{\partial C_1}{\partial t} + V_j^\circ \frac{\partial C_1}{\partial x_j} + \frac{S^2}{D}\left[\tfrac{1}{2}C_2 + \xi^2\left(\frac{\partial C_2}{\partial \xi^2} - \frac{\partial C_2}{\partial S^2}\right) - 2\xi^2(\nabla_{11}\cdot\vec{V}^\circ)\frac{\partial C_1}{\partial \xi^2}\right.$$
$$\left. - S^2(\nabla_1\cdot\vec{V}^\circ)\frac{\partial C_1}{\partial S^2} + \xi^2 n_j \frac{\partial C_2}{\partial x_j} + \frac{2}{mN^\circ}(div\,\vec{\vec{P}}^\circ)_{11}\left(\tfrac{1}{2}C_2 + \xi^2\frac{\partial C_2}{\partial \xi^2}\right)\right.$$
$$+ Q_1 = G_1(\vec{U}) \tag{84}$$

$$\frac{\partial C_2}{\partial t} + V_j^\circ \frac{\partial C_2}{\partial x_j} + \frac{S^2}{D}\left(\frac{\partial C_1}{\partial \xi^2} - \frac{\partial C_1}{\partial S^2}\right) - 2(\nabla_{11}\cdot\vec{V}^\circ)\left(\tfrac{1}{2}C_2 + \xi^2\frac{\partial C_2}{\partial \xi^2}\right)$$
$$- S^2(\nabla_1\cdot\vec{V}^\circ)\frac{\partial C_2}{\partial S^2} + n_j\frac{\partial C_1}{\partial x_j} + \frac{2}{mN^\circ}(div\,\vec{\vec{P}}^\circ)_{11}\frac{\partial C_1}{\partial \xi^2} + Q_2$$
$$= G_2(\vec{U}) - \frac{2e}{m}\frac{\partial f^\circ}{\partial \xi^2}\vec{n}\cdot(\vec{V}^\circ\times\vec{B}') \tag{85}$$

where $\frac{1}{D} \equiv div\,\vec{n} = -\frac{1}{B^\circ} n_j \frac{\partial B^\circ}{\partial x_j} = -(\vec{n}\cdot grad)\log|\vec{B}^\circ|$ (86)

$$Q_1 \equiv \frac{1}{B^\circ}\left(s^2\frac{\partial f_0^\circ}{\partial s^2} - 2q^2\frac{\partial f_0^\circ}{\partial s^2}\right)\left(\frac{\partial V_i^\circ}{\partial x_j} + \frac{\partial V_j^\circ}{\partial x_i}\right)(\vec{B}_\perp')_i n_j + s^2\frac{\partial X_i}{\partial x_i}\frac{\partial f_0^\circ}{\partial s^2}$$
$$- X_i\left\{\frac{\partial f_0^\circ}{\partial x_i} - n_j\frac{\partial n_i}{\partial x_j}\left(s^2\frac{\partial f_0^\circ}{\partial s^2} - 2q^2\frac{\partial f_0^\circ}{\partial q^2}\right)\right\} \qquad (87)$$

$$Q_2 \equiv s^2\left[\nabla_\perp\cdot\left(\frac{\vec{B}'}{B^\circ}\right) - \frac{\vec{n}\cdot\vec{B}'}{B^\circ}\frac{\partial n_j}{\partial x_j} - n_j\frac{\partial n_i}{\partial x_j}\frac{(\vec{B}_\perp')_i}{B^\circ}\right]\left(\frac{\partial f_0^\circ}{\partial q^2} - \frac{\partial f_0^\circ}{\partial s^2}\right)$$
$$+ \frac{1}{B^\circ}\left(\frac{\partial f_0^\circ}{\partial x_i} + \frac{2}{mN^\circ}\frac{\partial p_{ij}^\circ}{\partial x_j}\frac{\partial f_0^\circ}{\partial q^2}\right)(\vec{B}_\perp')_i$$
$$+ 2X_i\left(n_j\frac{\partial V_j^\circ}{\partial x_i} - V_j^\circ\frac{\partial n_i}{\partial x_j}\right)\frac{\partial f_0^\circ}{\partial q^2} \qquad (88)$$

$$\vec{X} \equiv \frac{\vec{n}\times(\vec{V}^\circ\times\vec{B}')}{B^\circ} \qquad (89)$$

$$G_1(U) \equiv -U_j\frac{\partial f_0^\circ}{\partial x_j} + 2(\nabla_\parallel\cdot\vec{U})\,q^2\frac{\partial f_0^\circ}{\partial q^2} + (\nabla_\perp\cdot\vec{U})\,s^2\frac{\partial f_0^\circ}{\partial s^2} \qquad (90)$$

$$G_2(\vec{U}) \equiv 2\left(U_j \frac{\partial V_k^\circ}{\partial x_j} n_k + V_j^\circ \frac{\partial U_k}{\partial x_j} n_k\right) \frac{\partial f_o^\circ}{\partial q^2} \tag{91}$$

$$\overset{\bullet}{p}_{ij} \equiv p_{\parallel}^\circ n_i n_j + p_\perp^\circ (\delta_{ij} - n_i n_j) \tag{92}$$

$$p_{\parallel}^\circ \equiv \frac{m}{2} \iint q^2 f_o^\circ \, dq \, ds^2 \tag{93}^*$$

$$p_\perp^\circ \equiv \frac{m}{4} \iint s^2 f_o^\circ \, dq \, ds^2 \tag{94}$$

with f_o° normalized so that

$$N^\circ = \frac{1}{2} \iint f_o^\circ \, dq \, ds^2 \tag{95}$$

$$\operatorname{div} \overset{\leftrightarrow}{p}^\circ = \vec{n} (\operatorname{div} \overset{\leftrightarrow}{p}^\circ)_\parallel + (\operatorname{div} \overset{\leftrightarrow}{p}^\circ)_\perp \tag{96}$$

$$(\operatorname{div} \overset{\leftrightarrow}{p}^\circ)_\parallel = n_j \frac{\partial p_{\parallel}^\circ}{\partial x_j} + (p_{\parallel}^\circ - p_\perp^\circ) \frac{\partial n_j}{\partial x_j} = n_j \frac{\partial p_{\parallel}^\circ}{\partial x_j} + \frac{p_{\parallel}^\circ - p_\perp^\circ}{D} \tag{97}$$

$$(\operatorname{div} \overset{\leftrightarrow}{p}^\circ)_\perp = \nabla_\perp p_\perp^\circ + (p_{\parallel}^\circ - p_\perp^\circ) n_j \frac{\partial n_i}{\partial x_j} \tag{98}$$

$$\nabla_\perp = \frac{\partial}{\partial x_i} - \eta_i \eta_j \frac{\partial}{\partial x_j} = (\delta_{ij} - \eta_i \eta_j) \frac{\partial}{\partial x_j} \tag{99}$$

The remaining unknown in equations (82) to (99) are $\vec{B}'$ and $\vec{U}$, both of which may be expressed in terms of the perturbation displacement $\vec{\xi}$ defined by

$$\vec{U}^+ = \frac{\partial \vec{\xi}}{dt} \tag{100}$$

where the superscript "+" denotes ions. $\vec{U}^+$ is related to $\vec{A}'$ and $\vec{B}^0$ by equation (17).

2.4 Derivation of the plasma equations of motion

We shall now express the electromagnetic variables in Maxwell's vacuum equations in terms of $\vec{\xi}$. First we break up equation (17) into two equations, one a relation between the components perpendicular to the ambient magnetic field $\vec{B}^0$, the other a relation between the parallel components. To the lowest order in η, the equation for the perpendicular components yield Ohm's law for an infinitely conducting plasma in a strong magnetic field,

$$\vec{A}_\perp' + \frac{e}{m} \vec{U}_\perp \times \vec{B}^\circ = 0 \tag{101}$$

Since $m\vec{A}' = e\vec{E}'$,

$$\vec{U}_\perp^+ = \vec{U}_\perp^- = \frac{\partial \vec{\xi}_\perp}{\partial t} \tag{102}$$

and $$U_\parallel^- = -\frac{m^+}{m^-} U_\parallel^+ = -\frac{m^+}{m^-}\frac{\partial \xi_\parallel}{\partial t} \tag{103}$$

Substituting equation (100) into the defining equation (17), and using equation (101), we can write $\vec{E}'$ as

$$\vec{E}' = \frac{m^+}{|e|}\frac{\partial^2 \vec{\xi}}{\partial t^2} - \frac{\partial \vec{\xi}}{\partial t} \times \vec{B}^\circ \tag{104}$$

From the linearized Maxwell's equation for $\frac{\partial \vec{B}}{\partial t}$ and from equation (104) we find, after an integration, that

$$\vec{B}' = \text{curl}\,(\vec{\xi} \times \vec{B}^\circ) - \frac{m^+}{|e|}\,\text{curl}\left(\frac{\partial \vec{\xi}}{\partial t}\right) = \text{curl}\,(\vec{\xi} \times \vec{B}^\circ) - \frac{m^+}{|e|}\,\text{curl}\left[\frac{\partial (\vec{n}\,\xi_\parallel)}{\partial t}\right] \tag{105}$$

where we discarded the term $\frac{m^+}{|e|}\,\text{curl}\left(\frac{\partial \vec{\xi}_\perp}{\partial t}\right)$ because it was η times curl $(\vec{\xi} \times \vec{B}^\circ)$, and we retained the last term of equation (101) since it was the lowest order term for $\xi_\parallel$.

The equations of motion for the plasma as a whole are a set of equations for the components of the perturbation displacement $\vec{\xi}$ in terms of the moments of the non-stationary deviations f'^+ and f'^- (which were obtained from equation (76) and the solution of equations (83) to (85).

A combined momentum equation for ions and electrons

is obtained by adding the momentum equations (26) for each species of particle expressed in terms of the moments of the peculiar velocity v_i referred to the nonstationary local mean velocity V_i. When we assume that

$$A_i^{\pm} = g_i \pm \frac{|e|}{m^{\pm}} E_i \qquad (106)^*$$

the combined momentum equation becomes

$$m^+N^+\left(\frac{\partial V_i^+}{\partial t} + V_j^+ \frac{\partial V_i^+}{\partial x_j}\right) + m^-N^-\left(\frac{\partial V_i^-}{\partial t} + V_j^- \frac{\partial V_i^-}{\partial x_j}\right) = -\frac{\partial (p_{ij}^+ + p_{ij}^-)}{\partial x_j} + \rho g_i + \mathcal{E} E_i + \epsilon_{i\ell m} J_\ell B_m \qquad (107)$$

where g_i = gravitational force per unit mass

$$J_\ell \equiv |e|\,(N^+V_i^+ - N^-V_i^-) \quad = \text{current density} \qquad (108)$$

$$\rho \equiv m^+N^+ + m^-N^- \quad = \text{mean density} \qquad (109)$$

$$\mathcal{E} \equiv |e|\,(N^+ - N^-) \quad = \text{charge density} \qquad (110)$$

After linearization, extensive algebra, and an integration by parts, assuming that expressions of the form

$$\frac{|\vec{V}^\circ|\,|\vec{B}'|}{|\vec{B}^\circ|}\,, \quad (\vec{V}^\circ \cdot \text{grad})\,\vec{V}'\,, \quad (\vec{V}' \cdot \text{grad})\,\vec{V}^\circ \quad \text{and} \quad (\vec{V}^\circ \cdot \text{grad})\,\vec{V}^\circ$$

are small, the perpendicular component of the equation of motion for the plasma as a whole, equation (107), becomes

$$\rho^\circ\left(1+\epsilon_\circ\frac{|\vec{B}^\circ|^2}{\rho^\circ}\right)\frac{\partial^2\vec{\xi}_\perp}{\partial t^2} = -\left(\operatorname{div}\overleftrightarrow{p}'^{+}+\operatorname{div}\overleftrightarrow{p}'^{-}\right)_\perp+\varepsilon^\circ\vec{E}'_\perp+\varepsilon'\vec{E}^\circ_\perp + (\vec{J}^\circ\times\vec{B}')_\perp+\left[\operatorname{curl}\left(\frac{\vec{B}'}{\mu_\circ}\right)\right]\times\vec{B}^\circ+\rho'\vec{g}_\perp \tag{111}$$

If we make the further assumption that

$$|\vec{E}^\circ_{\parallel}| \ll |\vec{B}^\circ| \quad \text{and} \quad |\vec{g}_{\parallel}| \ll \left|\frac{e}{m}\vec{B}^\circ\right|, \tag{112}^*$$

we find that the equation of motion for the parallel component of $\vec{\xi}$ is

$$\frac{\epsilon_\circ m^+}{|e|}\left(\frac{\partial^2}{\partial t^2}+\omega_p^{2^+}+\omega_p^{2^-}\right)\frac{\partial^2\xi_\parallel}{\partial t^2} = \sum_{+,-}\frac{e^\pm}{m^\pm}\left\{(\operatorname{div}\overleftrightarrow{p}')_\parallel - e^\pm N^\circ(\vec{V}^\circ\times\vec{B}')_\parallel\right\} + \frac{1}{\mu_\circ}\left[\operatorname{curl}\left(\frac{\partial\vec{B}'}{\partial t}\right)\right]_\parallel \tag{113}$$

In the above equations

$$\omega_p = \left(\frac{N^\circ e^2}{\epsilon_\circ m}\right)^{\frac{1}{2}} \quad = \text{plasma frequency} \tag{114}$$

The divergence of the nonstationary pressure deviation is

$$\begin{aligned}\frac{\partial p_{ij}'}{\partial x_j} = {} & \left\{n_i\left[n_j\frac{\partial p'_{\parallel;c}}{\partial x_j}+\left(p'_{\parallel;c}-p'_{\perp;c}\right)\frac{\partial n_j}{\partial x_j}\right]+\left(\delta_{ij}-n_in_j\right)\frac{\partial p'_{\perp;c}}{\partial x_j}\right. \\ & \left.+\left(p'_{\parallel;c}-p'_{\perp;c}\right)n_j\frac{\partial n_i}{\partial x_j}\right\}+\left\{\left[2n_in_jn_\kappa B'_\kappa-n_iB'_j-n_jB'_i\right]\left[\frac{(p^\circ_{\parallel}-p^\circ_{\perp})}{(B^\circ)^2}\frac{\partial B^\circ}{\partial x_j}\right.\right. \\ & \left.+\frac{1}{B^\circ}\left(\frac{\partial p^\circ_{\parallel}}{\partial x_j}-\frac{\partial p^\circ_{\perp}}{\partial x_j}\right)\right]+\left[n_i\frac{\partial B'_j}{\partial x_j}+n_j\frac{\partial B'_i}{\partial x_j}+B'_\kappa\frac{\partial n_i}{\partial x_\kappa}+B'_i\frac{\partial n_j}{\partial x_j}\right. \\ & -2B'_\kappa n_in_\kappa\frac{\partial n_j}{\partial x_j}-2n_in_jn_\kappa\frac{\partial B'_\kappa}{\partial x_j}-2B'_\kappa n_jn_\kappa\frac{\partial n_i}{\partial x_j} \\ & \left.\left.-2B'_\kappa n_in_j\frac{\partial n_\kappa}{\partial x_j}\right]\frac{(p^\circ_{\parallel}-p^\circ_{\perp})}{B^\circ}\right\}\end{aligned} \tag{115}^*$$

where $p'_{11;c} = \frac{m}{2} \iint g^2 C_1 \, dg \, ds^2$ (116)

$$p'_{1;c} = \frac{m}{4} \iint s^2 C_1 \, dg \, ds^2 \tag{117}$$

$$\frac{\partial n_j}{\partial x_j} = -(\vec{n} \cdot \text{grad}) \log |\vec{B}^o| \tag{118}$$

$$n_j \frac{\partial n_i}{\partial x_j} = \frac{\hat{l}_1}{R_1} \tag{119}$$

$\hat{l}_1$ = unit vector normal to $\vec{n}$ and in the direction of the principal normal to the line of force $\vec{B}^o$

R_1 = radius of curvature of the line of force.

CHAPTER 3

DISPERSION EQUATION FOR HYDROMAGNETIC WAVES

This chapter outlines the derivation of the dispersion equation for hydromagnetic waves in a collisionless (Vlasov) plasma immersed in a magnetic field strong enough (see equation (2.29)) to make the cyclotron radius of protons much smaller than characteristic lengths of inhomogeneities and their gyrofrequencies much less than characteristic frequencies of perturbations. The dispersion equation is obtained by setting the determinant of the coefficients of the perturbation displacement $\vec{\xi}$ in the equations of motion equal to zero. When we refer to equations in other chapters we write "equation (2.29)" to refer to equation (29) in chapter 2. Asterisks mark new or unpublished equations.

3.1 Equations of motion for a homogeneous plasma in a uniform magnetic field

When we neglect the gravitational acceleration $\vec{g}$, the bulk motion $\vec{V}^o$, the external electric field $\vec{E}$, and the stationary current density $\vec{J}^o$, the equations of motion derived in Chapter 2 (equations (2.111) and (2.113)) simplify to

$$\rho^o\left[1+\frac{c_A^2}{c^2}\right]\frac{\partial^2\vec{\xi}_\perp}{\partial t^2} = -(\mathrm{div}\,\overleftrightarrow{P}')_\perp + \left[\mathrm{curl}\left(\frac{\vec{B}'}{\mu_o}\right)\right]\times\vec{B}^o \qquad (1)$$

$$\frac{\epsilon_o m^+}{|e|}\left(\frac{\partial^2}{\partial t^2}+\omega_p^{2^+}+\omega_p^{2^-}\right)\frac{\partial^2\xi_\parallel}{\partial t^2} = |e|\left[\frac{1}{m^+}(\mathrm{div}\,\overleftrightarrow{p}'^+)_\parallel - \frac{1}{m^-}(\mathrm{div}\,\overleftrightarrow{p}'^-)_\parallel\right] + \frac{1}{\mu_o}\left[\mathrm{curl}\left(\frac{\partial\vec{B}'}{\partial t}\right)\right]_\parallel \qquad (2)$$

where

$$\left[\frac{\epsilon_0 |\vec{B}^\circ|^2}{\rho^\circ}\right]^{\frac{1}{2}} = \frac{C_A}{C} = \text{ratio of Alfven speed to vacuum speed of light} \tag{3}$$

$$\overleftrightarrow{p}' = \overleftrightarrow{p}'^{+} + \overleftrightarrow{p}'^{-} = \text{deviation in total pressure (with } v^{o+} = v^{o-}) \tag{4}$$

$$\overleftrightarrow{p}' = \overleftrightarrow{p}_c' + \overleftrightarrow{p}_p'$$

$$= \begin{pmatrix} p_{\perp;c}' & 0 & 0 \\ 0 & p_{\perp;c}' & 0 \\ 0 & 0 & p_{\parallel;c}' \end{pmatrix} + \frac{(p_{\parallel}^\circ - p_{\perp}^\circ)}{B^\circ} \begin{pmatrix} 0 & 0 & B_1' \\ 0 & 0 & B_2' \\ B_1' & B_2' & 0 \end{pmatrix} \tag{5}$$

$$p_{\parallel}^\circ = \tfrac{1}{2} m \iint q^2 f_o^\circ \, dq \, ds^2 \tag{2.93}$$

$$p_{\perp}^\circ = \tfrac{1}{4} m \iint s^2 f_o^\circ \, dq \, ds^2 \tag{2.94}$$

$$p_{\perp;c}' = \tfrac{1}{4} m \iint s^2 C_1 \, dq \, ds^2 \tag{2.116}$$

$$p_{\parallel;c}' = \tfrac{1}{2} m \iint q^2 C_1 \, dq \, ds^2 \tag{2.117}$$

$$\vec{B}' = \operatorname{curl}(\vec{\xi} \times \vec{B}^\circ) - \frac{m^+}{|e|} \operatorname{curl}\left[\frac{\partial(\vec{n}\,\xi_n)}{\partial t}\right] \tag{2.105}$$

and C_1 in eqs. (2.116) and (2.117) is a solution of the system of partial differential equations (2.84) and (2.85). The uniform stationary state plasma and the uniform external magnetic field which we are assuming allow us to make the following further simplifications in the differential equations for C_1:

$$\frac{\partial f_0^\circ}{\partial x_i} = 0 \qquad (6)^*$$

$$\frac{1}{D} = \frac{\partial n_i}{\partial x_i} = 0 \qquad (7)^*$$

$$(\mathrm{div}\, \overleftrightarrow{p}^\circ)_{\parallel} = 0 \qquad (8)^*$$

Equations (2.84) and (2.85) for C_1 and C_2 simplify to

$$\frac{\partial C_1}{\partial t} + q^2 n_j \frac{\partial C_2}{\partial x_j} = G_1(\vec{U}) \qquad (9)$$

$$\frac{\partial C_2}{\partial t} + n_j \frac{\partial C_1}{\partial x_j} = -Q_2 \qquad (10)$$

where

$$G_1^+(\vec{U}^+) = 2(\nabla_\parallel \cdot \vec{U}^+) q^2 \frac{\partial f_o^{o+}}{\partial q^2} + (\nabla_\perp \cdot \vec{U}^+) s^2 \frac{\partial f_o^{o+}}{\partial s^2}$$

$$= 2 \frac{\partial^2 \xi_3}{\partial t \partial x_3} q^2 \frac{\partial f_o^{o+}}{\partial q^2} + \frac{\partial^2 \xi_1}{\partial t \partial x_1} s^2 \frac{\partial f_o^{o+}}{\partial s^2} + \frac{\partial^2 \xi_2}{\partial t \partial x_2} s^2 \frac{\partial f_o^{o+}}{\partial s^2} \qquad (11)^*$$

$$G_1^-(\vec{U}^-) = -2 \frac{m^+}{m^-} \frac{\partial^2 \xi_3}{\partial t \partial x_3} q^2 \frac{\partial f_o^{o-}}{\partial q^2} + \frac{\partial^2 \xi_1}{\partial t \partial x_1} s^2 \frac{\partial f_o^{o-}}{\partial s^2} + \frac{\partial^2 \xi_2}{\partial t \partial x_2} s^2 \frac{\partial f_o^{o-}}{\partial s^2} \qquad (12)^*$$

and we have used equations (2.102) and (2.103) in substituting $\vec{\xi}$ for $\vec{U}$. The difference in form between G_1^+ and G_1^- is not pointed out in the original publications, and this omission may be a cause of confusion. In equation (10) above,

$$Q_2 = s^2 \left[\nabla_\perp \cdot \left(\frac{\vec{B}'}{B^o} \right) \right] \left(\frac{\partial f_o^o}{\partial q^2} - \frac{\partial f_o^o}{\partial s^2} \right) \qquad (13)$$

3.2 Dispersion equation for waves with real propagation vector and complex frequency

To obtain a simple form of the dispersion relation, we will apply a Fourier transformation to the equation of motion in order to eliminate differentiation with respect to position and apply a Laplace transformation to eliminate differentiation with respect to time. If $A(\vec{x})$ is any function of position $\vec{x}$, its Fourier transform is

$$A_{\vec{k}}(\vec{K}) = \int_{-\infty}^{\infty}\int_{-\infty}^{\infty}\int_{-\infty}^{\infty} e^{-i\vec{k}\cdot\vec{x}} A(\vec{x})\, d^3x \qquad (14)$$

provided this integral exists. The inverse Fourier transform is

$$A(\vec{x}) = \frac{1}{(2\pi)^3} \int_{-\infty}^{\infty}\int_{-\infty}^{\infty}\int_{-\infty}^{\infty} e^{i\vec{k}\cdot\vec{x}} A_{\vec{k}}(\vec{k})\, d^3k \qquad (15)$$

If B(t) is an almost piecewise continuous function of time t, of exponential order σ_o, its one-sided Laplace transform is

$$B_{\Omega}(\Omega) = \int_0^{\infty} e^{-\Omega t} B(t)\, dt \qquad (Re\ \Omega > \sigma_o) \qquad (16)$$

The inverse Laplace transform is

$$u(t)\, B(t) = \frac{1}{i2\pi} \int_{-i\infty+\sigma}^{i\infty+\sigma} e^{\Omega t} B_{\Omega}(\Omega)\, d\Omega \qquad (\sigma > \sigma_o) \qquad (17)$$

where u(t) is the unit step function and $\sigma = Re\,\Omega$. This last integration is to be performed along a straight line running parallel to the imaginary (vertical) axis, and to the right of all singularities of $B_{\Omega}(\Omega)$ on the complex Ω plane.

We will approach our problem as an initial value problem so that in definition (14), $\vec{k}$ is the wave number and will be

considered to be real; and $A_{\vec{k}}$ is the amplitude of the k^{th} component of $A(\vec{x})$, a component with spatial dependence proportional to $\cos(\vec{k} \cdot \vec{x})$. In definition (16), the complex Laplace transform variable $\mathcal{S}$ is related to the complex wave frequency $\omega = \omega_r + i\omega_i$ by

$$\mathcal{S} = -i\omega \tag{18}$$

Hence, wave-like quantities are proportional to $e^{i(\vec{k}\cdot\vec{x} - \omega t)}$, and

$$Re\,\mathcal{S} = Im\,\omega = \omega_i\,, \qquad -Im\,\mathcal{S} = Re\,\omega = \omega_k \tag{19}$$

For stable waves, $\omega_i \leq 0$, assuming that $\omega_r > 0$.

The Fourier-Laplace transformed form of the variables involved in the equations of motion (1) and (2) are given below. For the sake of simplicity, we will drop the subscript $\vec{k}$ for the amplitude of the k^{th}-component of Fourier transformed variables and the subscript $\mathcal{S}$ for Laplace transformed variables.

$$\frac{\partial^2 \vec{\xi}_\perp}{\partial t^2} \rightarrow \mathcal{S}^2 \vec{\xi}_\perp \quad + \quad \text{a function of initial values} \tag{20}$$

$$\frac{\partial^4 \xi_\parallel}{\partial t^4} \rightarrow \mathcal{S}^4 \xi_\parallel \quad + \quad \text{a function of initial values} \tag{21}$$

$$\frac{\partial^2 \xi_{\parallel}}{\partial t^2} \rightarrow \Omega^2 \xi_{\parallel} + \text{a function of initial values} \qquad (22)$$

$$\left\{\left[\text{curl}\left(\frac{\vec{B}'}{\mu_0}\right)\right] \times \vec{B}^0\right\} \cdot \hat{a}_1 = (B^0)^2 \left\{\left[K_1 K_2 \frac{\Omega}{\omega_{c+}} - (K_1^2 + K_3^2)\right] \xi_1' - \left[(K_1^2 + K_3^2)\frac{\Omega}{\omega_{c+}} + K_1 K_2\right] \xi_2'\right.$$

$$\left. + K_2 K_3 \frac{\Omega}{\omega_{c+}} \xi_3' + \text{a function of initial values}\right\} \qquad (23)^*$$

$$\left\{\left[\text{curl}\left(\frac{\vec{B}'}{\mu_0}\right)\right] \times \vec{B}^0\right\} \cdot \hat{a}_2 = (B^0)^2 \left\{\left[(K_2^2 + K_3^2)\frac{\Omega}{\omega_{c+}} - K_1 K_2\right] \xi_1' - \left[(K_2^2 + K_3^2) - K_1 K_2 \frac{\Omega}{\omega_{c+}}\right] \xi_2'\right.$$

$$\left. - K_1 K_3 \frac{\Omega}{\omega_{c+}} \xi_3' + \text{a function of initial values}\right\} \qquad (24)^*$$

$$\left[\text{curl}\left(\frac{\partial \vec{B}'}{\partial t}\right)\right]_{\parallel} \rightarrow B^0 \left\{\left(K_1 K_3 \frac{\Omega}{\omega_{c+}} + K_2 K_3\right)\Omega \xi_1' - \left(K_2 K_3 \frac{\Omega}{\omega_{c+}} + K_1 K_3\right)\Omega \xi_2'\right.$$

$$\left. - (K_1^2 + K_2^2)\frac{\Omega}{\omega_{c+}} \xi_3' + \text{a function of initial values}\right\} \qquad (25)^*$$

To lowest order in η , the Fourier-Laplace transformed simultaneous partial differential equations which determine the solutions C_1 and C_2 for the nonstationary deviation f_0' are,

for ions: (26)*

$$\Omega C_1^+ + iK_3 q^2 C_2^+ = i\Omega (K_1 \xi_1 + K_2 \xi_2) s^2 \frac{\partial f_0^{o+}}{\partial s^2} + i2K_3 \Omega \xi_3 q^2 \frac{\partial f_0^{o+}}{\partial q^2}$$

+ a function of initial values

(27)*

$$\Omega C_2^+ + iK_3 C_1^+ = s^2 [K_1 K_3 \xi_1 + K_2 K_3 \xi_2] [\frac{1}{2q} \frac{\partial f_0^{o+}}{\partial q} - \frac{\partial f_0^{o+}}{\partial s}]$$

+ a function of initial values

for electrons:

(28)*

$$\Omega C_1^- + iK_3 q^2 C_2^- = i\Omega (K_1 \xi_1 + K_2 \xi_2) s^2 \frac{\partial f_0^{o-}}{\partial s^2} - i2K_3 \Omega \frac{m^+}{m^-} \xi_3 q^2 \frac{\partial f_0^{o-}}{\partial q^2}$$

+ a function of initial values

(29)*

$$\Omega C_2^- + iK_3 C_1^- = s^2 [K_1 K_3 \xi_1 + K_2 K_3 \xi_2] [\frac{1}{2q} \frac{\partial f_0^{o-}}{\partial q} - \frac{\partial f_0^{o-}}{\partial s^2}]$$

+ a function of initial values

After eliminating C_2, we find that

$$C_1^{+} = i\frac{1}{\Omega^2 + K_3^2 g^2}\Big\{\Omega^2\Big[S^2\frac{\partial f_0^{o+}}{\partial S^2}(K_1\xi_1' + K_2\xi_2') + 2g^2\frac{\partial f_0^{o+}}{\partial g^2}K_3\xi_3'\Big] - K_3 g^2 S^2\Big[\frac{\partial f_0^{o+}}{\partial g^2} - \frac{\partial f_0^{o+}}{\partial S^2}\Big]\Big[K_1K_3\xi_1' + K_2K_3\xi_2'\Big] + \text{a function of initial values} \tag{30}$$

$$C_1^{-} = i\frac{1}{\Omega^2 + K_3^2 g^2}\Big\{\Omega^2\Big[S^2\frac{\partial f_0^{o-}}{\partial S^2}(K_1\xi_1' + K_2\xi_2') - 2\frac{m^+}{m^-}g^2\frac{\partial f_0^{o-}}{\partial g^2}K_3\xi_3'\Big] - K_3 g^2 S^2\Big[\frac{\partial f_0^{o-}}{\partial g^2} - \frac{\partial f_0^{o-}}{\partial S^2}\Big]\Big[K_1K_3\xi_1' + K_2K_3\xi_1'\Big] + \text{a function of initial values.} \tag{31}$$

The initial values do not enter into the time asymptotic limit which gives the expression for the dispersion relation for waves which the medium can support. Hence, we will no longer retain the initial values in our expressions (Bernstein, 1958).

When C_1 given in eqs. (30) and (31) is used in the integrals (2.116) and (2.117) to define the pressure deviation components $p'_{\perp;c}$ and $p'_{\parallel;c}$, we obtain the following formulas for the Fourier-Laplace transformed pressure deviations,

for ions:

$$p'^{+}_{\perp;c} \rightarrow iK_3 \xi_3 J_1^{+} + (\nabla_\perp \cdot \vec{\xi}_\perp) J_2^{+} + iK_3 \frac{\nabla_\perp \cdot \vec{B}'_\perp}{B^\circ} J_3^{+} \qquad (32)$$

$$p'^{+}_{\parallel;c} \rightarrow iK_3 \xi_3 I_1^{+} + (\nabla_\perp \cdot \vec{\xi}_\perp) I_2^{+} + iK_3 \frac{\nabla_\perp \cdot \vec{B}'_\perp}{B^\circ} I_3^{+} \qquad (33)$$

for electrons:

$$p'^{-}_{\perp;c} \rightarrow -i \frac{m^+}{m^-} K_3 \xi_3 J_1^{-} + (\nabla_\perp \cdot \vec{\xi}_\perp) J_2^{-} + iK_3 \frac{\nabla_\perp \cdot \vec{B}'_\perp}{B^\circ} J_3^{-} \qquad (34)^*$$

$$p'^{-}_{\parallel;c} \rightarrow (I_2^{-} - K_3^2 I_3^{-})(\nabla_\perp \cdot \vec{\xi}_\perp) - i \frac{m^+}{m^-} K_3 I_1^{-} \xi_3 \qquad (35)^*$$

where, if we denote

$$\Omega^2 + K_3^2 q^2 = \Lambda \qquad (36)^*$$

we define

$$I_1^{\pm} = \tfrac{1}{2} m^{\pm} \iint \frac{2\Omega^2 q^4}{\Lambda} \frac{\partial f_o^{\circ\pm}}{\partial q^2} dq\, ds^2 \qquad (37)$$

$$I_2^{\pm} = \tfrac{1}{2} m^{\pm} \iint \frac{\Omega^2 q^2 s^2}{\Lambda} \frac{\partial f_o^{\circ\pm}}{\partial s^2} dq\, ds^2 \qquad (38)$$

$$I_3^{\pm} = \tfrac{1}{2} m^{\pm} \iint \frac{q^4 s^2}{\Lambda} \left(\frac{\partial f_o^{\circ\pm}}{\partial q^2} - \frac{\partial f_o^{\circ\pm}}{\partial s^2} \right) dq\, ds^2 \qquad (39)$$

$$J_1^{\pm} = \frac{1}{4} m^{\pm} \iint \frac{2\Omega^2 q^2 s^2}{\Lambda} \frac{\partial f_0^{o\pm}}{\partial q^2} dq\, ds^2 \tag{40}$$

$$J_2^{\pm} = \frac{1}{4} m^{\pm} \iint \frac{\Omega^2 s^4}{\Lambda} \frac{\partial f_0^{o\pm}}{\partial s^2} dq\, ds^2 \tag{41}$$

$$J_3^{\pm} = \frac{1}{4} m^{\pm} \iint \frac{q^2 s^4}{\Lambda} \left(\frac{\partial f_0^{o\pm}}{\partial q^2} - \frac{\partial f_0^{o\pm}}{\partial s^2} \right) dq\, ds^2 \tag{42}$$

The integrals (37) to (42) are of the form

$$J(K_3, \Omega) = \int_{-\infty}^{\infty} \frac{\phi(q^2, K_3, \Omega)}{\Omega^2 + K_3^2 q^2} dq \tag{43}$$

where ϕ is an entire function of Ω . Let us define the complex quantity

$$\sigma \equiv + \frac{i\Omega}{K_3} \tag{44}$$

The integral (43) may then be written as

$$J = \frac{1}{2\sigma K_3^2} \int_{-\infty}^{\infty} \left(\frac{1}{q-\sigma} - \frac{1}{q+\sigma} \right) \phi \, dq$$

$$= \frac{1}{\omega K_3} \int_{-\infty}^{\infty} \frac{\phi \, dq}{q - \omega/K_3} \qquad (\mathrm{Im}\,\omega > 0) \qquad (45)$$

where we have used eq. (18) in the last integral. In the complex q plane, J is evaluated with the path of integration passing along the real axis (under the singularity in q). When Im $\omega \leq 0$ as in the case of stable waves, the analytic continuation of J is obtained by making the path of integration loop under the singularity.

Substituting eqs. (32) to (35) into eqs. (4) and (5), we find that the Fourier-Laplace transform of $(\mathrm{div}\,\vec{P}')_\perp$ is

$$\begin{aligned}(\mathrm{div}\,\vec{\vec{P}}')_\perp \rightarrow\ & \hat{a}_1 \Big[s P_\perp^\circ (K_1^2 \xi_1' + K_1 K_2 \xi_2') - (J_1^+ - \tfrac{m^+}{m^-} J_1^-) K_1 K_3 \xi_3' \\ & - (P_{11}^\circ - P_\perp^\circ) \left(K_3^2 \xi_1' - \tfrac{\Omega}{\omega_c^+} K_2 K_3 \xi_3' \right) \Big] \\ & + \hat{a}_2 \Big[s P_\perp^\circ (K_1 K_2 \xi_1' + K_2^2 \xi_2') - \left(J_1^+ - \tfrac{m^+}{m^-} J_1^- \right) K_2 K_3 \xi_3' \\ & - (P_{11}^\circ - P_\perp^\circ) \left(K_3^2 \xi_2' + \tfrac{\Omega}{\omega_c^+} K_1 K_3 \xi_3' \right) \Big] \qquad (46)^*\end{aligned}$$

where

$$\begin{aligned} P_{11}^\circ &= P_{11;1}^\circ + P_{11;2}^\circ + \cdots, \\ P_\perp^\circ &= P_{\perp;1}^\circ + P_{\perp;2}^\circ + \cdots. \end{aligned} \qquad (47a)$$

$$SP_{\perp}^{\circ} = S^{+}\mathcal{P}_{\perp}^{\circ +} + S^{-}\mathcal{P}_{\perp}^{\circ -} = -\left[(J_2^{+} - K_3^2 J_3^{+}) + (J_2^{-} - K_3^2 J_3^{-})\right] \qquad (47)$$

Furthermore,

$$(div\, \overleftrightarrow{\mathcal{P}}^{\prime +})_{\parallel} \longrightarrow -\left[(K_1 K_3\, \xi_1' + K_2 K_3\, \xi_2')\, J_1^{+} + K_3^2 I_1^{+}\, \xi_3'\right] \qquad (48)^{*}$$

$$(div\, \overleftrightarrow{\mathcal{P}}^{\prime -})_{\parallel} \longrightarrow -\left[(K_1 K_3\, \xi_1' + K_2 K_3\, \xi_2')\, J_1^{-} - K_3^2 \frac{m^{+}}{m^{-}} I_1^{-}\, \xi_3'\right] \qquad (49)^{*}$$

On substituting the Fourier-Laplace transformed variables into eqs. (1) and (2), we obtain the equations of motion free of derivatives. Collecting components along each of the mutually perpendicular axes $\hat{a}_1$, $\hat{a}_2$, $\hat{a}_3$, with the externally applied magnetic field $\vec{B}^{0}$ along $\hat{a}_3$, we find:

along $\hat{a}_1$ -

$$\begin{aligned} \mathcal{P}^{\circ}\left[1 + \left(\frac{C_A}{C}\right)^2\right]\Omega^2 \xi_1' = -\Big[& SP_{\perp}^{\circ}(K_1^2 \xi_1' + K_1 K_2 \xi_2') + \left(\frac{m^{+}}{m^{-}} J_1^{-} - J_1^{+}\right) K_1 K_3 \xi_3' \\ & + \left(K_2 K_3 \frac{m^{+}\Omega}{|e|}\, \xi_3' - K_3^2 B^{\circ} \xi_1'\right)\left(\frac{P_{\parallel}^{\circ} - P_{\perp}^{\circ}}{B^{\circ}}\right)\Big] \\ & + \frac{B^{\circ}}{\mu_0}\Big(K_2 K_3 \frac{m^{+}\Omega}{|e|}\, \xi_3' - K_3^2 B^{\circ} \xi_1' - K_1^2 B^{\circ} \xi_1' \\ & - K_1 K_2 B^{\circ} \xi_2'\Big) \end{aligned} \qquad (50)^{*}$$

along $\hat{a}_2$ -

$$\rho^0\left[1+\left(\frac{c_A}{c}\right)^2\right]\Omega^2\xi_2' = -\left[SP_\perp^0\left(K_1K_2\xi_1' + K_2^2\xi_2'\right) + \left(\frac{m^+}{m^-}J_1^- - J_1^+\right)K_2K_3\xi_3'\right.$$
$$\left.-\left(K_1K_3\frac{m^+\Omega}{|e|}\xi_3' + K_3^2B^0\xi_2'\right)\left(\frac{P_{11}^0-P_\perp^0}{B^0}\right)\right] \qquad (51)^*$$
$$-\frac{(B^0)^2}{\mu_0}\left(K_1K_2\xi_1' + K_2^2\xi_2' + K_1K_3\frac{\Omega}{\omega_c^+}\xi_3' + K_3^2\xi_2'\right)$$

along $\hat{a}_3$ -

$$\epsilon_0\left(\Omega^2+\omega_p^{2^+}+\omega_p^{2^-}\right)\frac{m^+}{|e|}\Omega^2\xi_3' = -\frac{|e|}{m^+}\left[\left(K_1K_3\xi_1' + K_2K_3\xi_2'\right)J_1^+ + K_3^2I_1^+\xi_3'\right]$$
$$+\frac{|e|}{m^-}\left[\left(K_1K_3\xi_1' + K_2K_3\xi_2'\right)J_1^- - \frac{m^+}{m^-}I_1^-K_3^2\xi_3'\right] \qquad (52)^*$$
$$+\frac{B^0\Omega}{\mu_0}\left[K_2K_3\xi_1' - K_1K_3\xi_2' - \frac{\Omega}{\omega_c^+}\left(K_1^2+K_2^2\right)\xi_3'\right]$$

In the case we are considering, that of a uniform plasma in a uniform, externally applied magnetic field, the rotational symmetry around the magnetic field allows us to choose coordinate axes so that

$$K_2 = 0 \qquad (53)$$

without loss of generality.

Collecting similar terms in ξ_1', ξ_2' and ξ_3', we reduce the equations of motion to

$$[\rho^{*}\Omega^{2} + \mathrm{S}P_{\perp}^{\circ} K_1^{2} - K_3^{2}(P_{11}^{\circ} - P_{\perp}^{\circ}) + \frac{(B^{\circ})^{2}}{\mu_0}(K_1^{2}+K_3^{2})]\xi_1 - (J_1^{+} - \frac{m^{+}}{m^{-}} J_1^{-})K_1 K_3 \xi_3 = 0 \qquad (54)^{*}$$

$$[\rho^{*}\Omega^{2} - (P_{11}^{\circ} - P_{\perp}^{\circ})K_3^{2} + \frac{(B^{\circ})^{2}}{\mu_0} K_3^{2}]\xi_2 + \{[\frac{(B^{\circ})^{2}}{\mu_0} - (P_{11}^{\circ} - P_{\perp}^{\circ})]\frac{\Omega}{\omega_c^{+}} K_1 K_3 \xi_3\} = 0 \qquad (55)^{*}$$

$$[|e|(\frac{J_1^{+}}{m^{+}} - \frac{J_1^{-}}{m^{-}})K_1 K_3]\xi_1 + \frac{B^{\circ}\Omega}{\mu_0} K_1 K_3 \xi_2 + \{[\Omega^{2} + \omega_p^{2+} + \omega_p^{2-}]\frac{\epsilon_0 m^{+}}{|e|}\Omega^{2} + \frac{B^{\circ}\Omega^{2}}{\mu_0 \omega_c^{+}} K_1^{2} + [\frac{I_1^{+}}{m^{+}} + (\frac{m^{+}}{m^{-}})\frac{I_1^{-}}{m^{-}}]|e| K_3^{2}\}\xi_3 = 0 \qquad (56)^{*}$$

where

$$\rho^{*} \equiv \rho^{\circ}[1 + (\frac{C_A}{C})^{2}] \qquad (57)^{*}$$

The equations of motion take a simpler form when written in terms of the angle of propagation (measured from the direction of the magnetic field $\vec{B}^{\circ}$), rather than in terms of the propagation vector $\vec{k}$, and when written in terms of plasma parameters given in dimensionless ratios.

Let $\tan\theta = \frac{K_1}{K_3}$ (58)

$$\xi_1 = K_1 \xi_1 \tag{59}$$

$$\xi_2 = K_1 \xi_2 \tag{60}$$

$$\xi_3 = K_3 \xi_3 \frac{\Omega}{\omega_c^+} \tag{61}$$

$$\delta = \frac{\omega}{c_A} \frac{1}{\sqrt{K_1^2 + K_3^2}} \tag{62}^*$$

$$\alpha = 1 + \frac{\mu_0 (P_\perp^\circ - P_{11}^\circ)}{(B^\circ)^2} \tag{63}$$

$$R = 1 + \frac{\mu_0 S P_\perp^\circ}{(B^\circ)^2} \tag{64}^*$$

$$\mathcal{J} = -i \frac{\omega_c^+}{\omega} \frac{\mu_0}{(B^\circ)^2} \left(J_1^+ - \frac{m^+}{m^-} J_1^- \right) \tag{65}^*$$

$$\mathcal{S} = \frac{1}{\delta^2} \left\{ - \frac{(-\omega^2 + \omega_p^{2+} + \omega_p^{2-})}{K^2 c^2} + \frac{\mu_0 |e|^2 \cos^2\theta}{m^+ \omega^2} \left[\frac{I_1^+}{m^+} + \left(\frac{m^+}{m^-} \right) \frac{I_1^-}{m^-} \right] \right\} \tag{66}^*$$

The equations of motion then take the form

$$\{\alpha \cos^2\theta - (1+\tfrac{C_A^2}{C^2})\delta^2 + [1+R]\sin^2\theta\}\xi_1 + \{J\sin^2\theta\}\xi_3 = 0 \qquad (67)$$

$$\{\alpha \cos^2\theta - (1+\tfrac{C_A^2}{C^2})\delta^2\}\xi_2 + \{\alpha \sin^2\theta\}\xi_3 = 0 \qquad (68)$$

$$\{-J\cos^2\theta\}\xi_1 + \{\cos^2\theta\}\xi_2 + \{\sin^2\theta - \delta^2\beta\}\xi_3 = 0 \qquad (69)$$

The dispersion relation is the condition for eq. (69) to (71) to have a non-vanishing solution vector (ξ_1, ξ_2, ξ_3). This condition is that the determinant of the coefficient matrix of this vector be equal to zero. The dispersion relation may then be written as

$$\mathcal{H}\mathcal{I} + \frac{J^2}{\delta^2\beta}(1+\tfrac{C_A^2}{C^2})\sin^4\theta\cos^2\theta = 0 \qquad (70)$$

where

$$\mathcal{H} \equiv (1+\tfrac{C_A^2}{C^2})\delta^2 + \frac{J^2}{\delta^2\beta}\cos^2\theta\sin^2\theta - [\alpha\cos^2\theta + (1+R)\sin^2\theta] \qquad (71)$$

$$\mathcal{I} \equiv (1+\tfrac{C_A^2}{C^2})\beta\delta^2 - [\alpha\beta\cos^2\theta + (1+\tfrac{C_A^2}{C^2})\sin^2\theta] \qquad (72)$$

For a plasma consisting of a superposition of bi-Maxwellian proton and electron populations (each population is identified by means of the subscript i), its distribution function is

$$f_0^\circ = \sum_i f_{0,i}^\circ = \sum_i \frac{2}{\sqrt{\pi}} N_i^\circ a_i \sqrt{b_i}\, e^{-a_i s^2} e^{-b_i \beta^2} \qquad (73)^*$$

where a_i and b_i are the reciprocals of the mean square perpendicular and parallel velocities, respectively, for the i^{th} particle population, i.e., $a_i = \frac{m_i}{2KT_{\perp,i}}$, $b_i = \frac{m_i}{2KT_{\parallel,i}}$

$T_{\perp,i}$ = perpendicular temperature of i^{th} species,

$T_{\parallel,i}$ = parallel temperature

We will describe the plasma by means of the following dimensionless parameters. Subscript 1 refers to thermal protons. Odd subscripts refer to protons, while even subscripts refer to electrons.

$$\beta_\parallel = \frac{2\mu_0 P_\parallel^\circ}{(B^\circ)^2} \qquad \gamma = \frac{P_\perp^\circ}{P_\parallel^\circ} \qquad C_{A_1}^2 = \frac{(B^\circ)^2}{\mu_0 m_1 N_1^\circ}$$

$$\lambda_i = \frac{P_{\perp,i}^\circ}{P_\perp^\circ} \qquad \tau_i = \frac{P_{\parallel,i}^\circ}{P_\parallel^\circ} \qquad K = \frac{K C_{A_1}}{\omega_{p_1}} \qquad (74)$$

$$P_{11,i}^{\circ} = \frac{m_i N_i^{\circ}}{2 b_i} = K T_{11;i} N_i^{\circ} \qquad (2.93)$$

and

$$P_{\perp,i}^{\circ} = \frac{m_i N_i^{\circ}}{2 a_i} = K T_{\perp;i} N_i^{\circ} \qquad (2.94)$$

$$\psi_1 = \frac{N_1^{\circ}}{N_1^{\circ}} = 1 \qquad \psi_2 = \frac{N_2^{\circ}}{N_1^{\circ}} \qquad \psi_i = \frac{N_i^{\circ}}{N_1^{\circ}} \quad (i > 2) \qquad (75)^*$$

where

$$P_{11}^{\circ} = P_{11,1}^{\circ} + P_{11,2}^{\circ} + \cdots \qquad P_{\perp}^{\circ} = P_{\perp,1}^{\circ} + P_{\perp,2}^{\circ} + \cdots \qquad (76)^*$$

$$\lambda_1 + \lambda_2 + \lambda_3 + \cdots + \lambda_i = 1 \qquad (77)^*$$

$$\tau_1 + \tau_2 + \tau_3 + \cdots + \tau_i = 1 \qquad (78)^*$$

To evaluate the integrals J_1, J_2, J_3, I_1, I_2, I_3, we may use the following theorem (Jackson, 1960):

If we define the analytic function I(z) of the complex variable z by the integral along the real v-axis,

$$I(z) = \int_{-\infty}^{\infty} \frac{f(v)\,dv}{v - z} \qquad (Im\, z > 0) \qquad (79)$$

where f(v) is a real function of v such that the integral exists for finite z, then the n^{th} derivative of $I(z_0)$ can

be expressed in terms of the n^{th} derivative of f(v),

$$I^{(n)}(z_0) = \int_{-\infty}^{\infty} \frac{f^{(n)}(v)\,dv}{v - z_0} \qquad Im\ z_0 > 0 \tag{80}$$

For Im $z_0 \leq 0$, we can take the analytic continuation of the above functions.

Let us denote by y_i the ratio of the parallel component of the velocity of particles in resonance with a wave, to the root mean square (thermal) velocity of the i^{th} particle population:

$$y_i = \frac{\omega \sqrt{b_i}}{k_3} \tag{81}$$

By using bi-Maxwellian distributions, we are enabled to evaluate the integrals $J_1, \ldots, I_3$, in terms of the plasma dispersion function (Fried and Conte, 1961)

$$Z(y_i) = \frac{1}{\sqrt{\pi}} \int_{-\infty}^{\infty} \frac{e^{-x^2}}{x - y_i}\,dx \tag{82}$$

After lengthy computations, we find that

$$R(y) = \gamma \beta_{11} \left\{ 1 + \tfrac{1}{2}\gamma \left[\frac{\lambda_1^2}{\tau_1} Z'(y_1) + \frac{\lambda_2^2}{\tau_2} Z'(y_2) + \cdots \right] \right\} \tag{83}^{*}$$

$$\mathcal{S}(y) = \frac{C_{A_1}^2}{c^2} - \frac{C_{A_1}^2}{\beta_{11} K_1^2 c^2 \cos^2\theta} \left[\psi_1^2 \frac{z'(y_1)}{\tau_1} + \psi_2^2 \frac{z'(y_2)}{\tau_2} + \psi_3^2 \frac{z'(y_3)}{\tau_3} + \cdots \right] \quad (84)^*$$

$$\mathcal{T}(y) = i \frac{\gamma \beta_{11}}{2\omega} \left\{ |\omega_c^+| \left[\lambda_1 y_1^2 z'(y_1) + \lambda_3 y_3^2 z'(y_3) + \cdots \right] - |\omega_c^-| \left[\lambda_2 y_2^2 z'(y_2) + \lambda_4 y_4^2 z'(y_4) + \cdots \right] \right\} \quad (85)^*$$

$$\alpha = 1 + \frac{\beta_{11}}{2} (\gamma - 1) \quad (86)$$

3.3 Dispersion equations for the guided and unguided Alfven waves

The condition for the validity of our approximations, that the radius of gyration of protons be small compared to the characteristic length of inhomogeneities, say, a wavelength, means that

$$\frac{\overline{v_1^2}}{\omega_c^2} \frac{K^2}{(2\pi)^2} = \frac{\lambda_i \gamma \beta_{11} N_1 m_i K_1^2 c^2}{4\pi^2 N_i m_1 C_{A_1}^2} = \eta^2 << 1 \quad (87)^*$$

For magnetospheric plasma parameters this implies that the coefficient of the square brackets in eq. (84) is much greater than unity. Hence, unless the quantity in the square brackets vanishes, we conclude that

$$|\delta(y)| >> 1 \qquad (88)^*$$

Barnes (1966) found that for a bi-Maxwellian plasma with no "superthermal tail" the quantity in the square brackets vanishes near certain isolated frequencies corresponding to the k = 0 Fried and Gould ion waves.

From the properties of the plasma dispersion function $z(y_i)$ we deduce that the quantity inside the square brackets is never very small unless

$$|y_i| >> 1 \quad \text{and} \quad \frac{Im(y_i)}{|Re(y_i)|} > -1 \qquad (89)$$

In the following diagram of the complex y_i - plane, Fig. 3.1, the region defined by (89) is marked Σ .

When y_i is in region Σ ,

$$z'(y_i) \sim \frac{1}{y_i^2} \qquad (90)$$

After considerable computations we find that when y_i is in the region Σ the second term on the left-hand side of eq. (70) may be neglected in comparison with the first term. Outside of Σ ,

$$|\delta(y)| >> 1 \qquad (91)^*$$

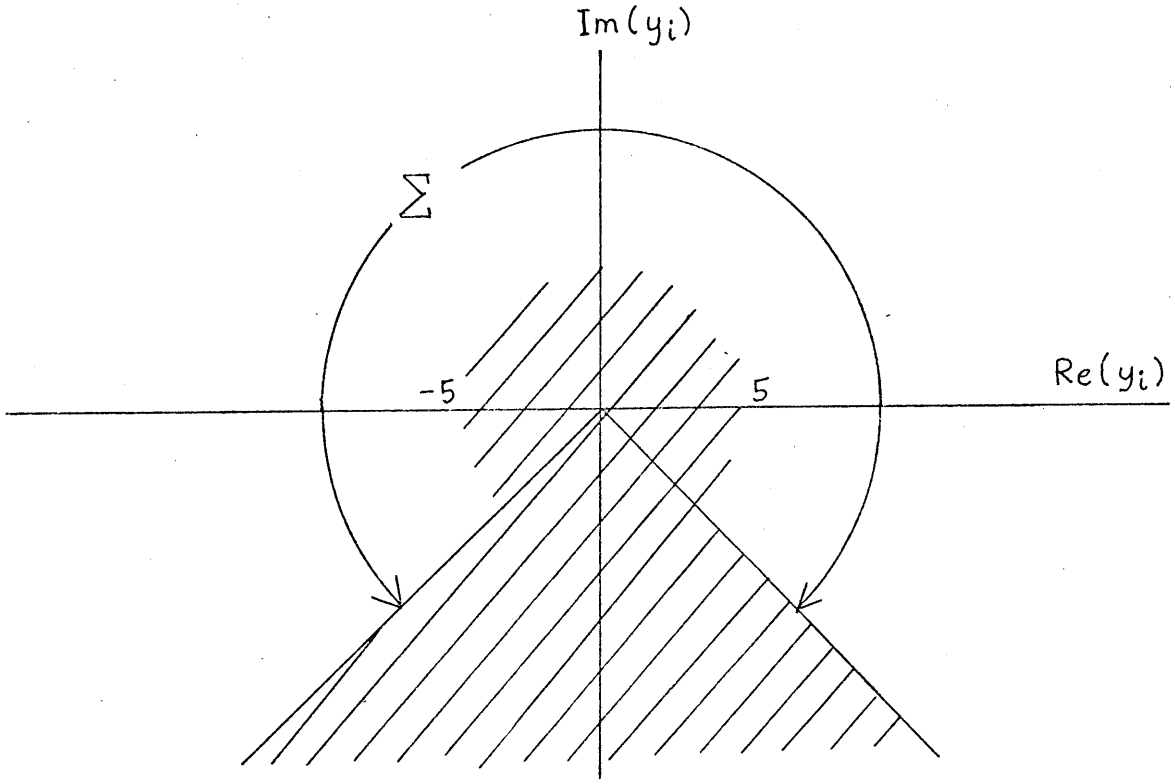

Figure 3.1

and the term $\left(\frac{\mathcal{T}^2}{\delta^2 \mathcal{S}}\right)\left(\sin^4\theta\right)\left(\cos^2\theta\right)$ in eq. (70) is much smaller than the terms $\left(\alpha \frac{\mathcal{T}^2}{\delta^2}\right)\left(\sin^2\theta\right)\left(\cos^4\theta\right)$ or $\left(\mathcal{T}^2 \sin^2\theta\right)\left(\cos^2\theta\right)$ in the product $\mathcal{H}\mathcal{S}$, unless both $|\alpha| \ll 1$ and $|\delta^2| \ll 1$. Since these last two conditions are unlikely in the magnetosphere, we may neglect the second term in eq. (70). Hence, the dispersion relation (70) factors into

$$\mathcal{S}(\delta, \theta) = 0 \tag{92}$$

$$\mathcal{H}(\delta, \theta) = 0 \tag{93}$$

The condition that the wave frequency ω be small compared with the ion gyrofrequency ω_{c^+} means that

$$\left(\frac{\omega}{\omega_{c^+}}\right)^2 = \frac{\delta_1^2 K_{\parallel}^2 C^2}{C_{A_1}^2} = \eta^2 \ll 1 \tag{94}$$

For the magnetospheric plasma this relation leads to the conclusion that in the expression (84) for $\mathcal{S}(y)$, the first term may be neglected in comparison with the second term for all values of y_i not very close to the origin. Hence,

$$\mathcal{S}(y) \cong -\frac{C_{A_1}^2}{C^2 \beta_{11} K_1^2 \cos^2\theta}\left[\psi_1^2 \frac{Z'(y_1)}{\tau_1} + \psi_2^2 \frac{Z'(y_2)}{\tau_2} + \psi_3^2 \frac{Z'(y_3)}{\tau_3} + \cdots\right] \tag{95}^*$$

Going back to eq. (92), we find that unless the angle of propagation is so close to $\frac{\pi}{2}$ so that $|\theta - \frac{\pi}{2}| \leq \frac{m_2}{m_1}$,

then $|\mathcal{S}(y)| >> 1$, and eq. (92) reduces to

$$\left(\frac{\omega}{k_3}\right)^2 = \frac{\alpha C_A^2}{(1 + C_A^2/c^2)} \tag{96}$$

which is the well-known dispersion relation for the guided Alfven wave. Equation (93) is the dispersion relation for the unguided Alfven (magnetosonic) mode. For a cold plasma it reduces to the usually given expression

$$\frac{\omega^2}{k^2} \simeq C_A^2 \tag{97}$$

When the dispersion relation (70) factors into eqs. (92) and (93), the guided and unguided Alfven modes are uncoupled.

Since C_A^2/c^2 may be neglected compared with unity, the dispersion relation for the unguided Alfven mode becomes, in terms of hydrodynamic-like plasma parameters and the derivative of the plasma dispersion function,

$$\frac{(1 + R) - m}{u^2 - \alpha} = \frac{\cos^2\theta}{\sin^2\theta} \tag{98}^*$$

Let the subscript 1 refer to the thermal proton population, 3 to resonant protons, and 4 to resonant electrons .

Then,

$$R = \gamma\beta_{11}\left\{1 + \tfrac{1}{2}\gamma\left[\frac{\lambda_3^2}{\tau_3}z'(y_3) + \frac{\lambda_4^2}{\tau_4}z'(y_4)\right]\right\} \qquad (99)^*$$

$$m = \frac{\gamma^2\beta_{11}}{4}\left\{\frac{\lambda_3^2}{\tau_3}z'(y_3) + \frac{\lambda_4^2}{\tau_4}z'(y_4) - \frac{\left[2\lambda_3\lambda_4\psi_3\psi_4 + \lambda_3^2\psi_4^2 + \lambda_4^2\psi_3^2\right]z'(y_3)z'(y_4)}{\left[\frac{\psi_3^2}{\tau_3}z'(y_3) + \frac{\psi_4^2}{\tau_4}z'(y_4)\right]\tau_3\tau_4}\right. \qquad (100)^*$$

$$\mu = \frac{\omega}{k_3 C_{A_1}} = \frac{\text{wave phase speed}}{C_{A_1}\cos\theta} = \frac{\delta_1}{\cos\theta} = \frac{y_i}{C_{A_1}\sqrt{b_i}} \qquad (101)^*$$

$$\alpha = 1 + \frac{\mu_0\left(P_\perp^\circ - P_\parallel^\circ\right)}{(B^\circ)^2} \qquad (102)$$

$$y_i = \frac{1}{k(\cos\theta)C_{A_1}}\sqrt{\frac{m_i\psi_i}{m_1\tau_i\beta_{11}}}\left(Re\ \omega + i\,Im\,\omega\right) \qquad (103)^*$$

3.4 The number of solutions of the dispersion equation for the unguided Alfven mode

The dispersion equation for the unguided Alfven mode is given by equation (104)

$$\mathcal{D} \equiv (1+\frac{c_A^2}{c^2})\delta^2 + \frac{\mathcal{I}^2}{\delta^2 \mathcal{S}}(\cos^2\theta)(\sin^2\theta) - [\alpha \cos^2\theta + (1+R)\sin^2\theta] = 0 \quad (104)$$

By observing the form of the expressions involving the independent variable y_i, i.e., δ^2, $\mathcal{I}^2$, $\mathcal{S}$, and R, we conclude that there are an infinite number of isolated roots of the dispersion equation in the complex y_i-plane. Except for δ^2, none of these expressions, since they are transcendental expressions, can be written as a finite polynomial in y_i. Since the expression $\mathcal{I}^2/(\delta^2 \mathcal{S})$ is a meromorphic function of finite order, the left-hand side of the dispersion equation is also a meromorphic function of finite order. An extension of Hadamard's factorization theorem to meromorphic functions (Titchmarsh, 1939) implies that the left-hand side of the dispersion equation has an infinite number of zeros and poles in the complex y_i-plane. Furthermore, these zeros and poles are isolated (see Theorem 43 in Kaplan, 1966), since each one of the transcendental expressions is an entire function (see Clemmow and Dougherty, 1969, page 269). Hence the dispersion equation has an infinite number of isolated roots. This means that the plasma can support many separate wave modes.

3.5 Comments on the analytic continuation of the dispersion equation to complex values of the propagation vector $\vec{k}$

For initial-value problems the wave propagation vector $\vec{k}$

is taken to be real and the frequency ω is allowed to be complex. The dispersion equation for hydromagnetic waves in a Vlasov plasma immersed in a strong magnetic field was derived in the preceding sections for real $\vec{k}$ and complex ω. On the other hand, for boundary-value problems ω is real and $\vec{k}$ is allowed to become complex. We cannot simply analytically continue the dispersion equation just derived into the complex $\vec{k}$ region because the dispersion equation for a Vlasov plasma composed of particle populations with non-zero temperature maxwellian distributions is not an analytic function of $\vec{k}$. It has a branch cut in the complex $\vec{k}$ space which prevents integration of the inverse Fourier transform expression along the Fourier contour.

Derfler (1962) showed that when the particle distribution function is cut off at a finite velocity the branch cut opens to allow a path for the integration of the inverse Fourier transform. Except in the vicinity of the branch points the solutions of the dispersion equation for plasmas with finite cut-off distribution functions may be approximated by the solutions for maxwellian plasmas (Kusse, 1964). For complex $\vec{k}$, integration alongside the branch cuts reveals a continuum of spatial van Kampen mode solutions. In the rest of this study we will disregard, for simplicity, these continuous modes and only look at the approximate discrete mode solutions from the zeros of the dispersion equation for maxwellian plasmas.

To do the analytic continuation of the dispersion equation to complex values of $\vec{k}$, we replace $\sin\theta$ by k_1/k, $\cos\theta$ by

k_3/k, and $\tan\theta$ by k_1/k_3, where $k=\sqrt{k_1^2+k_3^2}$. Then we allow k_1 and k_3 to become complex.

CHAPTER 4

PHYSICAL CONSIDERATIONS IN WAVE-PARTICLE INTERACTIONS

4.1 The magnetic moment-magnetic field gradient interaction

In the hydromagnetic regime, where the wave frequency is much less than the ion gyrofrequency and the wave length is much larger than the radius of gyration, the magnetic moment of a charged particle, $mv_\perp^2/(2B^o)$, is an adiabatic invariant. The parallel equation of motion for the particle is

$$m\frac{dv_\parallel}{dt} = eE_\parallel - m\frac{V_\perp^2}{2B^o}\frac{\partial B_\parallel}{\partial x_3}$$

where m and e are the mass and charge of the particle, $v_\parallel$ and $v_\perp$ are its velocity components parallel and perpendicular to the ambient magnetic field $\vec{B}^o$, where $E_\parallel$ and $B_\parallel$ are the parallel components of the self-consistent electric field and the magnetic field acting on the particle, and x_3 is the distance measured in the direction of the ambient magnetic field $\vec{B}^o$.

If the second term on the right-hand side is negligible, there remains only the Coulomb force equation, which leads to the well-known phenomenon of Landau damping. If the first term is negligible, the second term gives rise to an interaction which is the magnetic analogue of Landau damping, with the electric charge replaced by the magnetic moment and electric field replaced by the magnetic field gradient. While Landau damping applies to longitudinal (electrostatic) waves, its magnetic analogue, the magnetic moment-magnetic field gradient(MMMFG) interaction,

applies to transverse (electromagnetic) waves. Energy exchange with the particle occurs by means of the electric field. Even in the absence of an ambient electric field, the magnetic acceleration due to the interaction tends to produce charge separation in the plasma, which results in a restoring electric field $E_{\parallel}$ (Barnes, 1967). This field, on the average, cancels the magnetic acceleration and prevents charge build-up. By means of the quasilinear theory of hydromagnetic waves in a magnetized plasma, Barnes (1968) showed that energy from the damped waves enhances the resonant particle kinetic temperature parallel to the ambient magnetic field $\vec{B}^{o}$, but does not affect the transverse temperature.

4.2 Velocity space diagram of wave-particle resonances

In this section, we will study the effect of a propagating wave on an individual particle, with the motion of the particle through the wave field being taken into account. First, let us find a moving frame of reference in which the wave is static. Since motion across the ambient magnetic field $\vec{B}^{o}$ would introduce a uniform electric field, for simplicity let us take a frame of reference moving parallel to $\vec{B}^{o}$. An electromagnetic wave (either guided or unguided Alfven wave) with phase velocity V_p and angle of propagation θ (measured from the direction of $\vec{B}^{o}$) will be static in a frame of reference moving with a velocity $a = V_p / \cos\theta$ parallel to $\vec{B}^{o}$ (see Figure 4.1). In this moving reference frame, the wave being static, the electric field will have a potential which varies sinusoidally with wave phase. A particle moving in exact resonance with the wave (represented by a point on either

one of the Landau resonance lines) will see no electric field and cannot exchange energy with the wave. Since particles of constant energy in the moving frame have velocity space trajectories which are arcs of circles drawn from the origin o' in the moving frame (full arcs in Figure 4.1), particles in resonance with the wave have velocity space trajectories in the stationary reference frame which lie on such arcs. For comparison, the dashed arcs represent velocities of particles with equal energies relative to the stationary reference frame.

A particle in resonance with a wave may have a parallel component of velocity a = (wave phase velocity)/ cos θ . For the guided Alfven (cyclotron) wave, such particles have velocities represented by points on the Landau resonance line through o' in Figure 4.1. In this figure, V_{pg} stands for the phase speed of the guided Alfven wave, V_{pu} stands for the unguided wave phase speed, V_a stands for the Alfven speed. For resonance with the unguided Alfven wave, such particles have velocities represented by points on the Landau resonance line which is also labeled as the magnetic moment-magnetic field gradient resonance line. The angle of propagation for the unguided Alfven wave is given by ϕ .

For ion cyclotron resonance with the guided Alfven (cyclotron) wave, a particle must have a parallel component of velocity (b-a) such that the pitch of the particles' helical trajectory $v_{\parallel} \frac{2\pi}{\Omega_c}$ divided by (λ /cos) is an integer. We designate $v_{\parallel}$ to be the parallel component of the particle velocity, Ω_c the ion angular gyrofrequency and λ the wavelength for the guided Alfven wave.

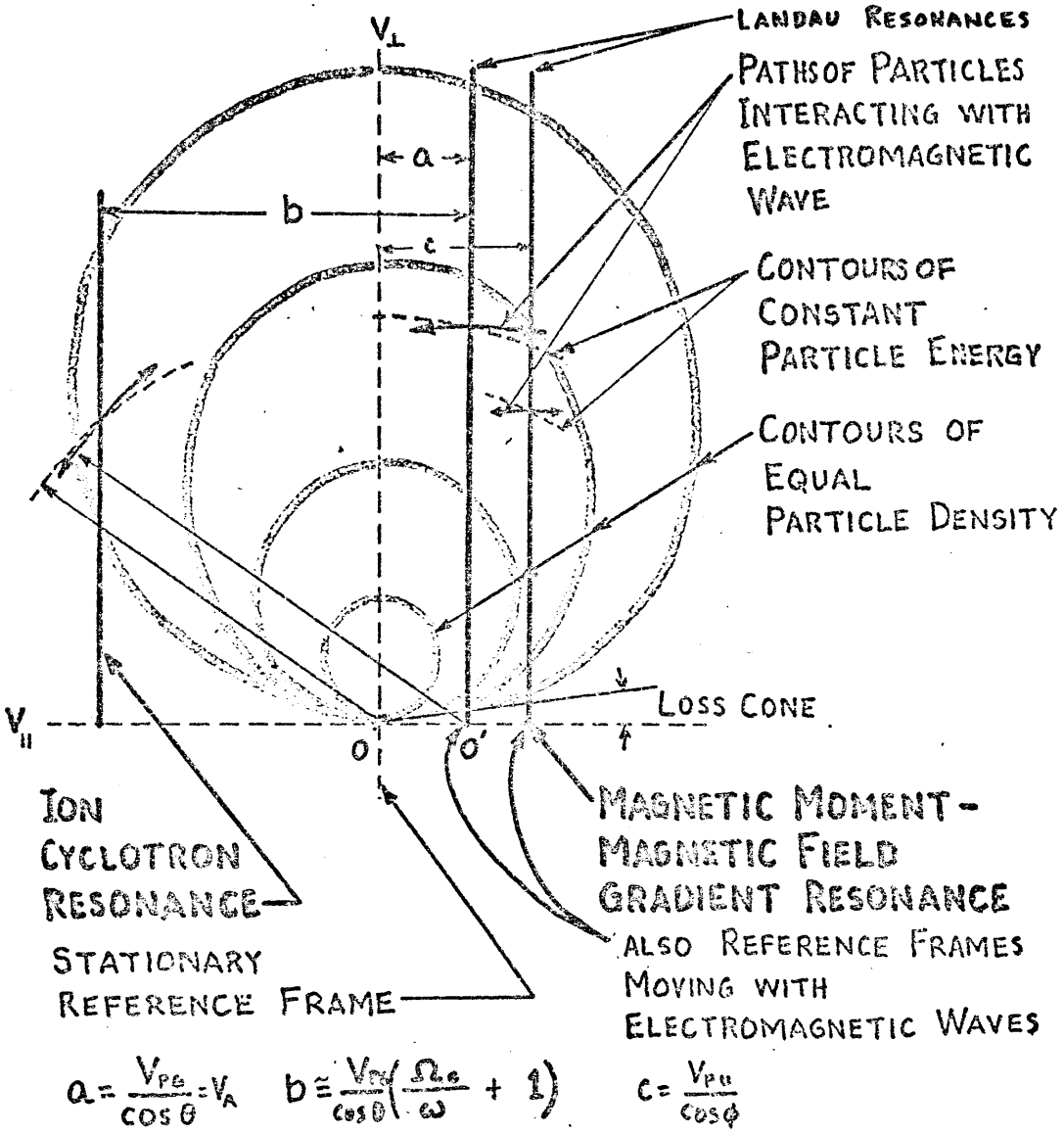

WAVE - PARTICLE INTERACTION DIAGRAM IN VELOCITY SPACE

Figure 4.1

4.3 Intuitive determination as to whether a wave is damped or amplified at a resonance

To determine whether a particle in resonance tends to gain or lose energy in an interaction, we see if, when it moves along the allowed trajectory in velocity space (full arcs in Figure 4.1) to diffuse in the direction that tends to produce a ledge in the density contour, it moves away from, or towards, the origin O in the stationary reference frame. It is well known from quasi-linear theory (Dungey, 1961; Barnes, 1968) that particles in resonance with a wave diffuse in velocity space so as to decrease the slope of the number density profile in the vicinity of the resonance velocity.

In the example presented in Figure 4.1 for a "loss-cone" particle velocity distribution, it can be seen that in resonance interactions represented by lines to the right of the stationary origin O, the density contour slopes are such that more particles gain energy from the wave than lose energy to it. On the other hand, in resonance interactions represented by lines to the left of the stationary origin, more particles lose energy to the wave than gain energy from it. Hence, for the "loss-cone" distribution, the guided Alfven wave is damped by the Landau resonance and amplified by the ion cyclotron resonance. The net effect on the wave depends on which of the competing interactions predominates. The form of the particle velocity distribution enters into these considerations. Other resonance lines exist for the guided Alfven wave, but the resonant velocities are so high that the

density of particles at such velocities are negligible in the magnetosphere.

Similarly, it can be seen that the "loss cone" distribution damps the unguided Alfven wave through the MMMFG resonance, which is represented by a resonance line on the right-hand side of the origin.

Hence, depending on the form of the particle distribution, it can simultaneously amplify the guided Alfven wave and damp the unguided Alfven wave (possibly exemplified by the "damping event" shown in Figure 1.2 from 16:45 to 17:45 EST), or damp the guided Alfven wave and amplify the unguided Alfven wave. Different combinations of damping and amplification are also possible depending on the form of the particle velocity distribution, on the resulting phase velocities, on the angles of propagation, and on the frequency of the guided Alfven wave relative to the ion gyrofrequency.

Kennel and Wong (1967) find that the strength of all resonances at Doppler shifted integral harmonics of the gyrofrequency depend on anisotropies in the resonant particle distribution, while the strength of the Landau resonances (including the MMMFG resonance) depends on the gradient in the distribution of parallel velocities. Kennel and Wong's study is limited to weakly resonant wave-particle interactions in which the damping rate ω_i/ω_r is much less than unity. The results of the present investigation (Chapter 3) are free of that limitation.

The polarizations of guided and unguided Alfven waves propagating in directions different from that of the external magnetic field $\vec{B}_o$ are shown schematically in Figure 4.2. These wave modes are circularly polarized when propagating in directions parallel to $\vec{B}_o$, but become plane polarized when propagating in other directions.

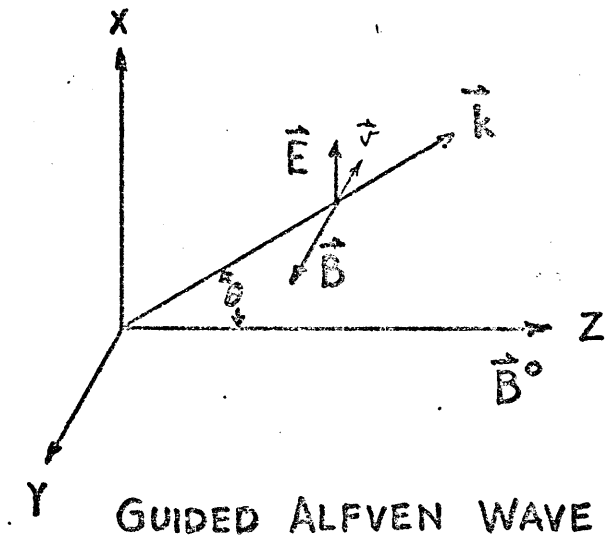

GUIDED ALFVEN WAVE

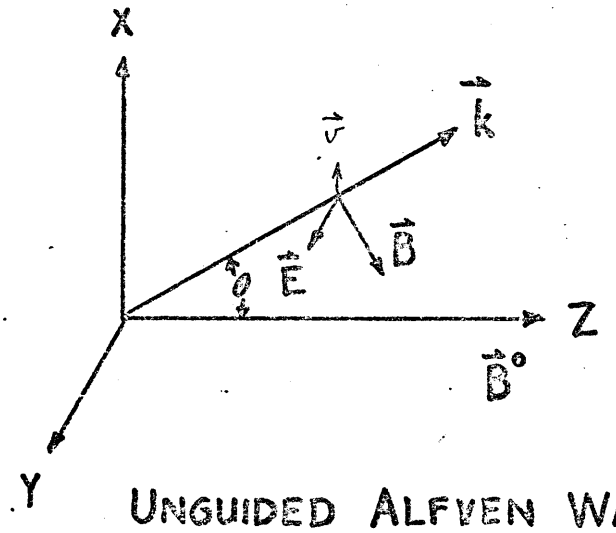

UNGUIDED ALFVEN WAVE

POLARIZATION OF PLANE HYDROMAGNETIC WAVES

Figure 4.2

CHAPTER 5

SOLUTIONS OF THE DISPERSION EQUATIONS FOR THE MAGNETOSPHERIC PLASMA

In this chapter we will present a model of the magnetospheric plasma in the vicinity of the geomagnetic equator when the M.I.T. telluric station in New Hampshire is at midnight. The models give plasma parameters representative of quiet periods ($K_p < 1^+$) and of slightly disturbed periods ($K_p = 2$). Solutions of the dispersion equations for the magnetospheric models for the unguided Alfven mode will be given in the form of graphs from which the numerical values can be scaled.

5.1 The damping rate

The damping rate is a measure of the rate of wave attenuation. For waves with real propagation vector $\vec{k}$ and complex frequency ω, the damping rate is the ratio ω_i/ω_r of the imaginary part of the frequency ω_i to the real part of the frequency ω_r. For waves with real ω and complex $\vec{k}$, the real part of $\vec{k}$, $\vec{k}_r$, and the imaginary part of $\vec{k}$, $\vec{k}_i$, are both vectors, but not necessarily parallel vectors. Wave-like quantities are proportional to $e^{i\vec{k}\cdot\vec{x}} = e^{i(\vec{k}_r + i\vec{k}_i)\cdot\vec{x}} = e^{i\vec{k}_r\cdot\vec{x}}\, e^{-\vec{k}_i\cdot\vec{x}} = e^{i\vec{k}_r\cdot\vec{x}}\, e^{-|\vec{k}_r|\vec{\alpha}\cdot\vec{x}}$ where $\vec{\alpha} = \vec{k}_i/|\vec{k}_r|$. Hence $\vec{\alpha}$ is the analogue of the damping rate ω_i/ω_r previously defined for waves with real $\vec{k}$ and complex ω. For loss-free media $\vec{k}\cdot\vec{k}$ is real. If $\vec{k}_i = 0$ the wave is not attenuated. If $\vec{k}_r = 0$ the wave is evanescent. These ideas are further discussed and applied in section 5.4 and chapter 6.

The damping rate depends on both the wave parameters and the parameters that characterize the medium. The wave

parameters are frequency ω and the propagation vector $\vec{k}$. The propagation vector, in turn, is characterized by an angle of propagation θ (which we will measure relative to the direction of the ambient magnetic field $\vec{B}^o$) and the wave number $|\vec{k}|$.

For the sake of simplicity we have assumed a spatially uniform and time invariant medium. The parameters relevant to the wave-particle interaction we are considering (the MMMFG interaction) are the strength of the ambient magnetic field $\vec{B}^o$, the number of component populations that make up the plasma, and for each component, the number density N, the temperature $T_{\parallel}$ in the direction of the magnetic field, and the temperature $T_{\perp}$ in the direction perpendicular to the magnetic field.

5.2 The magnetospheric plasma model

The ambient magnetic field was obtained from the satellite measurements of Sugiura, et al. (1972). They presented their measurements in terms of the deviations of the field from the International Geomagnetic Reference Field for 1966 (Cain, et al., 1967). As an indication of the need for this care in estimating the geomagnetic field, we note that Sugiura, et al., found that at the geomagnetic equator in the meridian plane of the M. I. T. telluric station in New Hampshire, the noon value of the magnetic field at a geocentric distance of 5.8 Re was more than 50% greater than the midnight value. If the average of the two values were to be used for estimating damping rates at 5.8 Re, the 25% inaccuracy in the field would result in a 56% inaccuracy in the damping rate. The reason for the escalation

in inaccuracy is that the damping rate depends on the ratio β between the particle pressure to the magnetic pressure, and this ratio varies inversely as the square of the magnetic field.

For the MMMFG interaction damping estimates, what is important is the slope of the number density vs. velocity curve for each particle population that is in resonance with the unguided Alfven wave, i.e., whose thermal spped is close to the parallel trace velocity of the unguided Alfven wave. The magnetosperic models are superpositions of double-maxwellian proton and electron populations. Since the equatorial plasma has often been found to have a pitch angle distribution with an intensity peak at a 90° pitch angle (Williams, et al., 1973) the perpendicular temperature $T_\perp$ was assumed to be 1.2 times the parallel temperature $T_\parallel$. The hot plasma double-maxwellian model has the same temperatures as the AP5 and AE2 models, but the number densities of the double-maxwellian model were adjusted to give the same gradient of number density with respect to parallel velocity as models AP5 and AE2.

The hot plasma population was estimated with the help of King's (1967) model AP5 for the low energy outer radiation belt protons, and Vette, Lucero and Wright's (1966) model AE2 for the low energy outer radiation belt electrons. These models are averages of the satellite measurements available at about the time they were constructed. King found that the average proton population with energies between .4 and 4 Mev had an energy distribution that could be represented by an exponential. The hot

proton temperatures of the magnetospheric models given in Tables IA, IB, IC, IIA, and IIB are taken from the e-folding energies given in the proton model AP5. Vette, et al. (1966) found that the hot electron populations in the outer radiation belt could be adequately modeled by a segmented exponential curve in a flux vs. energy diagram. For the sake of simplifying the calculations, only the lowest energy segments are used in the magnetospheric models adopted in this investigation.

The equatorial number densities for the thermal ($\sim$1.2 ev) component of the plasma are taken from Chappell, et al. (1970). Figure 5.1 shows this thermal plasma model.

For points not very far away from the equatorial plane, the thermal plasma was estimated by using a consequence of Liouville's theorem, which says that the distribution function behaves like an incompressible fluid in phase space. Hence, the thermal plasma at 20^{o} geomagnetic latitude was assumed to have the same number density as the equatorial plasma on the same magnetic field line. The hot electrons also show only a weak latitude dependence (Vette, et al., 1966).

The electron number density in the magnetosphere fluctuates considerably, and may drop to a hundredth of the values used in our models in a period of one to three weeks, then suddenly build up again to its former level, all because of geomagnetic storms. The proton number density is expected to be within a factor of two of its correct value (King, 1967). Substorms can increase the number density as much as ten times in ten min-

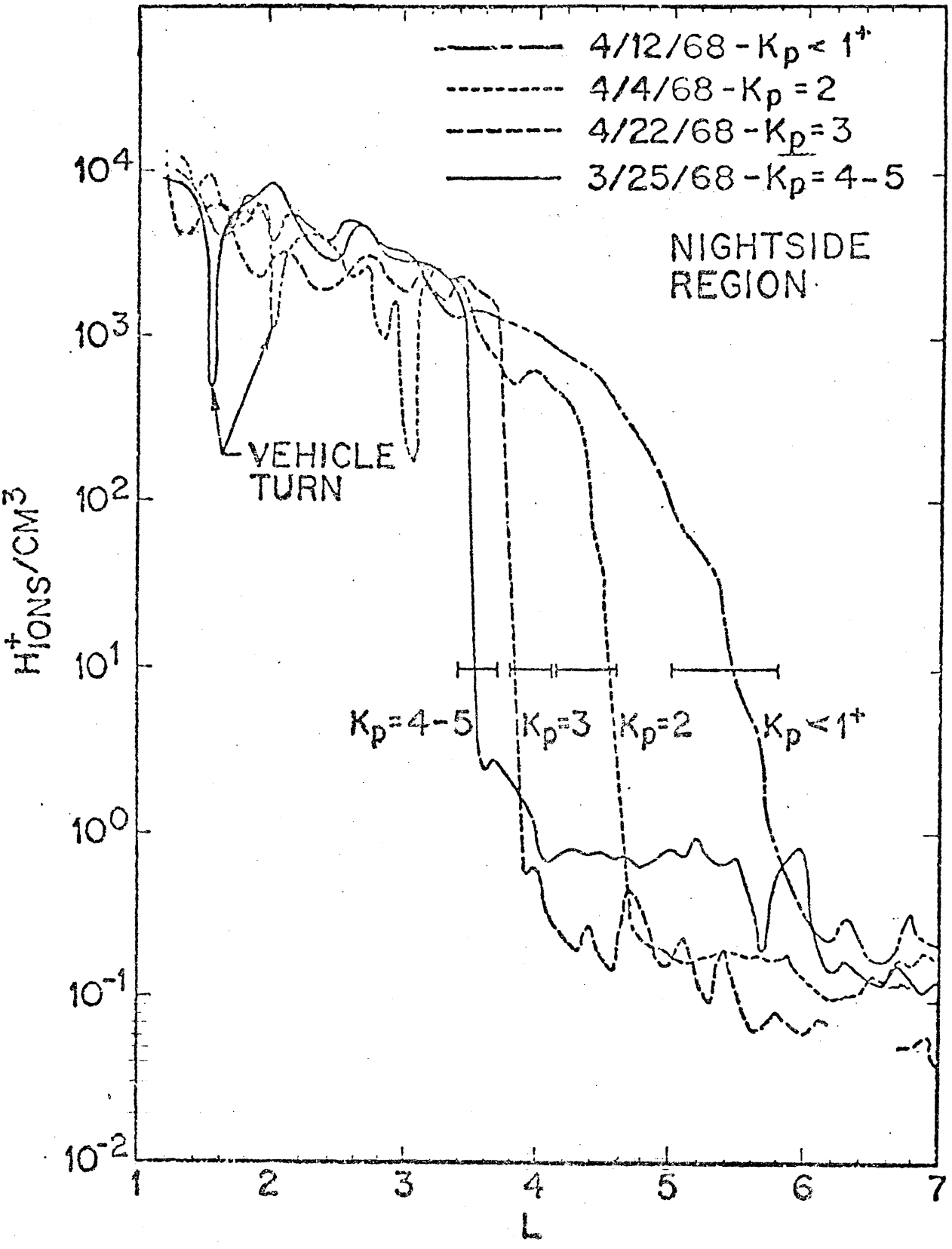

Figure 5.1 (from Chappell, et al., 1971)

utes.

Table IA summarizes the parameters of the magnetospheric plasma model for quiet conditions ($K_p < 1^+$) on the geomagnetic equator (latitude = 0°, geomagnetic) and in the meridian plane which passes through the M. I. T. telluric station in New Hampshire (288° longitude). All the models given in Tables IA, IB, IC, IIA, and IIB refer to conditions in the vicinity of the midnight meridian. The first column gives the geocentric distance of the magnetospheric region being modeled in terms of earth radii. The second column gives the total strength of the geomagnetic field in gauss. The third column gives the proton density in protons per $cm.^3$ The fourth column gives the proton temperatures parallel to the ambient magnetic field in electron volts. The fifth column gives the proton temperatures transverse to the magnetic field. The sixth column gives the electron density in electrons per cm^3. The seventh column gives the parallel electron temperature, while the eighth column gives the transverse electron temperature. Columns three to eight give two rows of values for each distance. The first row refers to the cooler plasma population, while the second row refers to the hotter population. The number densities are given to enough decimal places to satisfy the requirements for a neutral plasma.

Table IB gives plasma parameters for the same magnetospheric conditions as Table IA, but at 20° geomagnetic latitude. Tables IIA and IIB give magnetospheric plasma parameters for slightly disturbed conditions ($K_p = 2$). Table IIA gives equatorial values while Table IIB gives values for latitudes of 20°, geomagnetic.

TABLE IA: latitude = 0^{o} (geomagnetic), longitude = 288^{o}, Kp < 1^{+}, midnight sector

R (Re)	B (gauss)	N^{+}/cm^{3}	$T_{\parallel}$(ev)	$T_{\perp}$(ev)	N^{-}/cm^{3}	$T_{\parallel}$(ev)	$T_{\perp}$(ev)
3.4	.716 E-02	.130 E+04	.1 E+01	.12 E+01	.1301773 E+04	.1 E+01	.12 E+01
		.1775 E+01	.352 E+06	.423 E+06	.2 E-02	.769 E+05	.922 E+05
3.6	.599 E-02	.140 E+04	.1 E+01	.12 E+01	.1401358 E+04	.1 E+01	.12 E+01
		.1359 E+01	.320 E+06	.384 E+06	.1 E-02	.108 E+06	.1295 E+06
3.8	.506 E-02	.125 E+04	.1 E+01	.12 E+01	.1251000 E+04	.1 E+01	.12 E+01
		.1001 E+01	.290 E+06	.348 E+06	.1 E-02	.163 E+06	.1957 E+06
4.0	.431 E-02	.100 E+04	.1 E+01	.12 E+01	.1000693 E+04	.1 E+01	.12 E+01
		.694 E+00	.270 E+06	.324 E+06	.1 E-02	.226 E+06	.271 E+06
4.2	.368 E-02	.800 E+03	.1 E+01	.12 E+01	.8006069 E+03	.1 E+01	.12 E+01
		.608 E+00	.230 E+06	.276 E+06	.11 E-02	.250 E+06	.300 E+06
4.4	.318 E-02	.630 E+03	.1 E+01	.12 E+01	.6305175 E+03	.1 E+01	.12 E+01
		.519 E+00	.208 E+06	.250 E+06	.15 E-02	.276 E+06	.331 E+06
4.6	.274 E-02	.380 E+03	.1 E+01	.12 E+01	.3804747 E+03	.1 E+01	.12 E+01
		.476 E+00	.182 E+06	.218 E+06	.13 E-02	.288 E+06	.346 E+06
4.8	.239 E-02	.250 E+03	.1 E+01	.12 E+01	.2505947 E+03	.1 E+01	.12 E+01
		.596 E+00	.148 E+06	.1775 E+06	.13 E-02	.292 E+06	.350 E+06
5.0	.208 E-02	.100 E+03	.1 E+01	.12 E+01	.1006146 E+03	.1 E+01	.12 E+01
		.616 E+00	.130 E+06	.156 E+06	.14 E-02	.298 E+06	.347 E+06
5.2	.183 E-02	.600 E+02	.1 E+01	.12 E+01	.6056877 E+02	.1 E+01	.12 E+01
		.570 E+00	.120 E+06	.144 E+06	.123 E-02	.274 E+06	.329 E+06
5.4	.160 E-02	.220 E+02	.1 E+01	.12 E+01	.2250578 E+02	.1 E+01	.12 E+01
		.507 E+00	.114 E+06	.168 E+06	.122 E-02	.255 E+06	.306 E+06
5.6	.141 E-02	.520 E+01	.1 E+01	.12 E+01	.5606863 E+01	.1 E+01	.12 E+01
		.408 E+00	.112 E+06	.1344 E+06	.1137 E-02	.240 E+06	.288 E+06

TABLE IB: latitude = 20° (geomagnetic), longitude = 288°, Kp < 1, midnight sector

R (Re)	B (gauss)	N^+/cm^3	$T_{\parallel}$ (ev)	$T_{\perp}$ (ev)	N^-/cm^3	$T_{\parallel}$ (ev)	$T_{\perp}$ (ev)
3.2	.105 E-01	.140 E 04 .364 E 00	.10 E 01 .308 E 06	.12 E 01 .37 E 06	.1400363 E 04 .10 E-02	.10 E 01 .108 E 06	.12 E 01 .1295E 06
3.4	.871 E-02	.1188 E 04 .228 E 00	.10 E 01 .274 E 06	.12 E 01 .329 E 06	.1188227 E 04 .10 E-02	.10 E 01 .163 E 06	.12 E 01 .1955E 06
3.6	.736 E-02	.900 E 03 .233 E 00	.10 E 01 .24 E 06	.12 E 01 .288 E 06	.9002322 E 03 .8 E-03	.10 E 01 .237 E 06	.12 E 01 .284 E 06
3.8	.626 E-02	.715 E 03 .302 E 00	.10 E 01 .184 E 06	.12 E 01 .223 E 06	.7153011 E 03 .9 E-03	.10 E 01 .195 E 06	.12 E 01 .234 E 06
4.0	.538 E-02	.505 E 03 .407 E 00	.10 E 01 .144 E 06	.12 E 01 .173 E 06	.505406 E 03 .10 E-02	.10 E 01 .238 E 06	.12 E 01 .286 E 06
4.2	.466 E-02	.282 E 03 .453 E 00	.10 E 01 .118 E 06	.12 E 01 .142 E 06	.2824517 E 03 .13 E-02	.10 E 01 .292 E 06	.12 E 01 .35 E 06
4.4	.407 E-02	.100 E 03 .426 E 00	.10 E 01 .109 E 06	.12 E 01 .131 E 06	.1004246 E 03 .14072 E-02	.10 E 01 .289 E 06	.12 E 01 .347 E 06
4.6	.357 E-02	.600 E 02 .317 E 00	.10 E 01 .101 E 06	.12 E 01 .121 E 06	.6031567 E 02 .133 E-02	.10 E 01 .29 E 06	.12 E 01 .348 E 06
4.8	.316 E-02	.220 E 02 .255 E 00	.10 E 01 .105 E 06	.12 E 01 .126 E 06	.2225378 E 02 .1215 E-02	.10 E 01 .255 E 06	.12 E 01 .306 E 06

TABLE IC: latitude = 0° (geomagnetic), longitude = 288°, $K_p < 1$, midnight sector

R (Re)	B (gauss)	N^+/cm^3	$T_{\parallel}$(ev)	$T_{\perp}$(ev)	N^-/cm^3	$T_{\parallel}$(ev)	$T_{\perp}$(ev)
2.4	.206 E-01	.350 E+04	.10 E+01	.12 E+01	.3500525 E+04	.10 E+01	.12 E+01
		.538 E+00	.647 E+06	.776 E+06	.130 E-01	.713 E+05	.856 E+05
2.6	.162 E-01	.500 E+04	.10 E+01	.12 E+01	.5000929 E+04	.10 E+01	.12 E+01
		.938 E+00	.570 E+06	.684 E+06	.900 E-02	.564 E+05	.677 E+05
2.8	.130 E-01	.360 E+04	.10 E+01	.12 E+01	.3601484 E+04	.10 E+01	.12 E+01
		.149 E+01	.490 E+06	.588 E+06	.600 E-02	.482 E+05	.578 E+05
3.0	.105 E-01	.320 E+04	.10 E+01	.12 E+01	.3202114 E+04	.10 E+01	.12 E+01
		.212 E+01	.410 E+06	.492 E+06	.600 E-02	.500 E+05	.600 E+05
3.2	.863 E-02	.200 E+04	.10 E+01	.12 E+01	.2002126 E+04	.10 E+01	.12 E+01
		.213 E+01	.381 E+06	.458 E+06	.400 E-02	.602 E+05	.722 E+05
5.8	.125 E-02	.840 E+00	.10 E+01	.12 E+01	.1175916 E+01	.10 E+01	.12 E+01
		.337 E+00	.110 E+06	.132 E+06	.1084 E-02	.223 E+06	.268 E+06

TABLE IIA: latitude = 0° (geomagnetic), longitude = 288°, Kp = 2, midnight sector

R (Re)	B (gauss)	N^+/cm^3	$T_{\parallel}$(ev)	$T_{\perp}$(ev)	N^-/cm^3	$T_{\parallel}$(ev)	$T_{\perp}$(ev)
3.4	.698 E-02	.215 E+04	.1 E+01	.12 E+01	.2151772 E+04	.1 E+01	.12 E+01
		.1775 E+01	.352 E+06	.423 E+06	.3 E-02	.769 E+05	.923 E+05
3.6	.580 E-02	.900 E+03	.1 E+01	.12 E+01	.9013576 E+03	.1 E+01	.12 E+01
		.1359 E+01	.32 E+06	.384 E+06	.1396 E-02	.108 E+06	.1296 E+06
3.8	.486 E-02	.550 E+03	.1 E+01	.12 E+01	.5510001 E+03	.1 E+01	.12 E+01
		.1001 E+01	.29 E+06	.348 E+06	.9 E-03	.163 E+06	.1955 E+06
4.0	.411 E-02	.630 E+03	.1 E+01	.12 E+01	.6306931 E+03	.1 E+01	.12 E+01
		.694 E+00	.27 E+06	.324 E+06	.9 E-03	.226 E+06	.271 E+06
4.2	.349 E-02	.43 E+03	.1 E+01	.12 E+01	.4306069 E+03	.1 E+01	.12 E+01
		.608 E+00	.23 E+06	.276 E+06	.11 E-02	.250 E+06	.300 E+06
4.4	.301 E-02	.75 E+02	.1 E+01	.12 E+01	.7551752 E+02	.1 E+01	.12 E+01
		.519 E+00	.208 E+06	.250 E+06	.148 E-02	.276 E+06	.331 E+06
4.6	.259 E-02	.26 E+01	.1 E+01	.12 E+01	.3074663 E+01	.1 E+01	.12 E+01
		.476 E+00	.182 E+06	.218 E+06	.1337 E-02	.288 E+06	.346 E+06
4.8	.225 E-02	.23 E+00	.1 E+01	.12 E+01	.9046850 E+00	.1 E+01	.12 E+01
		.596 E+00	.148 E+06	.1775 E+06	.1315 E-02	.292 E+06	.351 E+06
5.0	.196 E-02	.21 E+00	.1 E+01	.12 E+01	.8245840 E+00	.1 E+01	.12 E+01
		.616 E+00	.13 E+06	.156 E+06	.1416 E-02	.289 E+06	.347 E+06
5.2	.172 E-02	.18 E+00	.1 E+01	.12 E+01	.7487660 E+00	.1 E+01	.12 E+01
		.570 E+00	.12 E+06	.144 E+06	.1234 E-02	.274 E+06	.329 E+06
5.4	.151 E-02	.20 E+00	.1 E+01	.12 E+01	.7057780 E+00	.1 E+01	.12 E+01
		.507 E+00	.14 E+06	.168 E+06	.1222 E-02	.255 E+06	.306 E+06
5.6	.133 E-02	.19 E+00	.1 E+01	.12 E+01	.5968630 E+00	.1 E+01	.12 E+01
		.408 E+00	.112 E+06	.1344 E+06	.1137 E-02	.240 E+06	.288 E+06

TABLE IIB: latitude = 20° (geomagnetic), longitude = 288°, Kp=2, midnight sector

R (Re)	B gauss	N^+/cm^3	$T_{\parallel}$(ev)	$T_{\perp}$(ev)	N^-/cm^3	$T_{\parallel}$(ev)	$T_{\perp}$(ev)
3.2	.1043 E-01	.900 E+03	.1 E+01	.12 E+01	.9003627 E+03	.1 E+01	.12 E+01
		.364 E+00	.308 E+06	.370 E+06	.13 E-02	.108 E+06	.1295 E+06
3.4	.866 E-02	.550 E+03	.1 E+01	.12 E+01	.5502271 E+03	.1 E+01	.12 E+01
		.228 E+00	.274 E+06	.329 E+06	.9 E-03	.163 E+06	.1955 E+06
3.6	.732 E-02	.630 E+03	.1 E+01	.12 E+01	.6302322 E+03	.1 E+01	.12 E+01
		.233 E+00	.240 E+06	.288 E+06	.8 E-03	.237 E+06	.284 E+06
3.8	.624 E-02	.253 E+03	.1 E+01	.12 E+01	.2533011 E+03	.1 E+01	.12 E+01
		.302 E+00	.184 E+06	.223 E+06	.9 E-03	.195 E+06	.234 E+06
4.0	.537 E-02	.388 E+02	.1 E+01	.12 E+01	.3920599 E+02	.1 E+01	.12 E+01
		.407 E+00	.144 E+06	.173 E+06	.101 E-02	.238 E+06	.286 E+06
4.2	.463 E-02	.142 E+01	.1 E+01	.12 E+01	.1871707 E+01	.1 E+01	.12 E+01
		.453 E+00	.118 E+06	.142 E+06	.1293 E-02	.292 E+06	.350 E+06
4.4	.402 E-02	.210 E+00	.1 E+01	.12 E+01	.6345928 E+01	.1 E+01	.12 E+01
		.426 E+00	.109 E+06	.131 E+06	.14072 E-02	.289 E+06	.347 E+06
4.6	.356 E-02	.180 E+00	.1 E+01	.12 E+01	.4956728 E+00	.1 E+01	.12 E+01
		.317 E+00	.101 E+06	.121 E+06	.13272 E-02	.290 E+06	.348 E+06
4.8	.314 E-02	.200 E+00	.1 E+01	.12 E+01	.4537850 E+01	.1 E+01	.12 E+01
		.255 E+00	.105 E+06	.126 E+06	.1215 E-02	.255 E+06	.306 E+06

5.3 Solutions of the dispersion equation for real $\vec{k}$ and complex ω

The dispersion equation (3.70) (together with equations (3.83) to (3.86)) for hydromagnetic waves in a strong magnetic field was solved numerically for magnetospheric plasma parameters corresponding to various locations in the midnight meridian in the vicinity of the geomagnetic equator. Magnetospheric parameters used were for quiet conditions ($K_p < 1^+$) and for slightly disturbed conditions ($K_p = 2$).

The phase velocity diagram for the unguided Alfven wave for $K_p < 1^+$, geomagnetic latitude = 0^o, geocentric distance = 4.6 Re is shown in Figure 5.2. This is a polar plot where the ambient magnetic field is directed along the abscissa. The radius vector is the magnitude of the phase velocity, and the polar angle θ is the angle between the propagation vector $\vec{k}$ and the ambient magnetic field $\vec{B}^o$. The rapid increase in phase velocity as the propagation angle increases beyond 80^o and its slight decrease as the propagation angle approaches 90^o is typical of the phase velocity diagrams. This feature is also found in Tajiri's (1967) corresponding phase velocity diagrams for the unguided Alfven wave in a Vlasov plasma in a magnetic field. Comparing Figure 5.2 with the phase velocity diagram for a Chew, Goldberger, Low (CGL) plasma, we note that although both phase velocity diagrams show little variation of velocity over most angles of propagation, the CKW velocities are some 25% lower than the CGL velocities. The rapid increase in velocities for angles of propagation beyond 80^o is peculiar to the microscopic CKW plasma.

Figure 5.3 shows the variation of the damping rate ω_i/ω_r

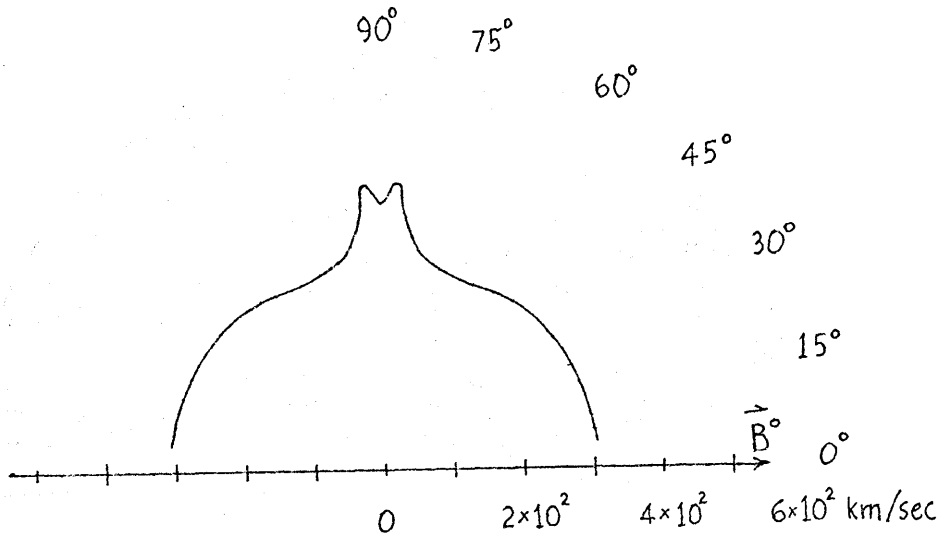

Figure 5.2

Phase Velocity Diagram

Real $\vec{k}$, complex w, $|\vec{k}| = .642E-09$ cm^{-1}

L = 4.6 Re, lat. = 0° (geomagnetic),

long. = 288° E(midnight), $K_p < 1^+$

Figure 5.3 Damping Rate Diagram

Real $\vec{k}$, complex w, $|\vec{k}| = .642E\text{-}09$ cm^{-1}

L = 4.6 Re, lat. = 0° (geomagnetic), long. = 288° E (midnight), $K_p < 1^+$

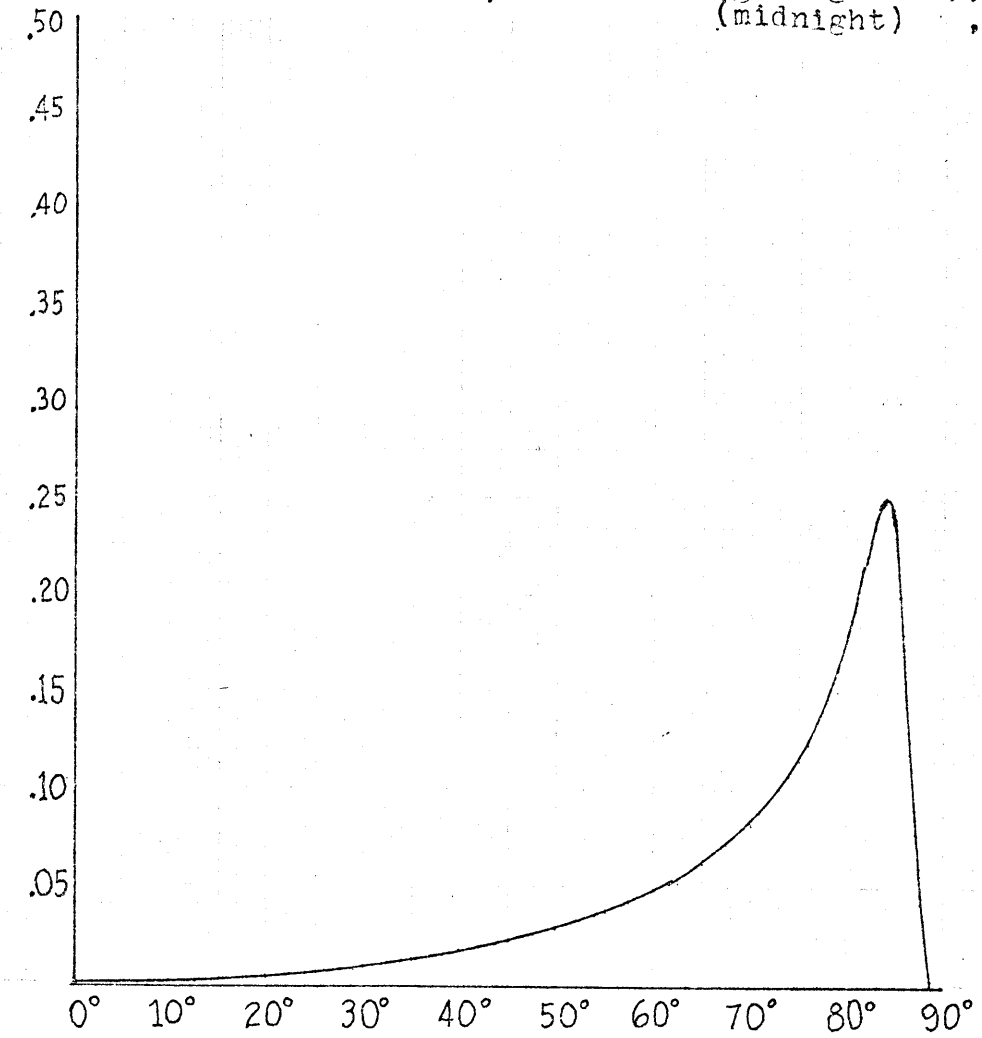

with propagation angle for the same plasma considered in Figure 5.2. A negative ω_i implies damping. The sharpness of the anisotropy, and the strength of the maximum damping is worthy of note. As a check on the computer program, some of Barnes' results were reproduced. To serve as a broad check on the dispersion equation, it was verified that the shapes of appropriate CKW damping rate vs. angle of propagation curves were similar to the one curve given by Hasegawa (1970). As noted previously, the shapes of the CKW phase velocity diagrams are similar to the shapes of the corresponding diagrams in Tajiri's (1967) paper. Since both Hasegawa and Tajiri started from Kutsenko and Stepanov's (1960) theory, which stands independently of the CKW theory used in the present study, the similarity in shapes of the curves serves as a check on the derivation of the dispersion equation.

5.4 Solutions of the dispersion equation for complex $\vec{k}$ and real ω

In situations where a wave propagates in space, solutions of the dispersion equation for real ω and complex $\vec{k}$ are usually more helpful than the solutions for real $\vec{k}$ and complex ω given in the preceding section. Since we will investigate the damping of a wave as it propagates earthward from beyond the plasmapause in the next chapter, we solved the dispersion equation (3.70) numerically for an inhomogeneous wave with real frequency ω and complex $\vec{k}$. In this section we shall present and discuss such solutions, but restrict ourselves again to the unguided Alfven wave.

The real part of the propagation vector, $\vec{k}_r$, is allowed to have various (real) propagation angles θ, where θ is measured

from the direction of the ambient magnetic field $\vec{B}^o$. However, the planes of constant amplitude of the wave are assumed to be parallel to $\vec{B}^o$ (and consequently, are parallel to the plasmapause). The spatial rate of wave attenuation in the direction perpendicular to the plasmapause, $\vec{k}_i$, is given by the imaginary part of $\vec{k}$. The planes of constant phase are perpendicular to $\vec{k}_r$.

The first set of solutions for complex $\vec{k}$ and real ω are given for quiet magnetospheric conditions with $K_p < 1^+$. Figure 5.4 shows the phase velocity vs. angle of propagation curve for the plasma on the geomagnetic equator at a geocentric distance of 5.8 Re (just outside the plasmapause). This curve is smaller than, and departs in shape considerably from, the oval that is the usual shape of the phase velocity curve for the unguided Alfven wave in a macroscopic plasma model like the CGL plasma (compare with Figure 5.17).

Figure 5.5 shows the curve for rate of wave attenuation $\vec{k}_{i\perp}$ in the direction perpendicular to the ambient magnetic field vs. angle of propagation θ for a wave frequency of .02 cps. The plasma involved here is the same plasma for which Figure 5.4 gives the phase velocity vs. propagation angle curve. Note the broad peak in attenuation rate at a propagation angle of 33^o. Figure 5.6 shows the curve for $\vec{k}_{i\perp}$ vs. θ for the same plasma to which Figure 5.4 applies, and with the same wave mode whose attenuation curve is given in Figure 5.5, but with four times the frequency. Note that the shape of the curve is similar to the curve in Figure 5.5, but the rates of attenuation is four times greater.

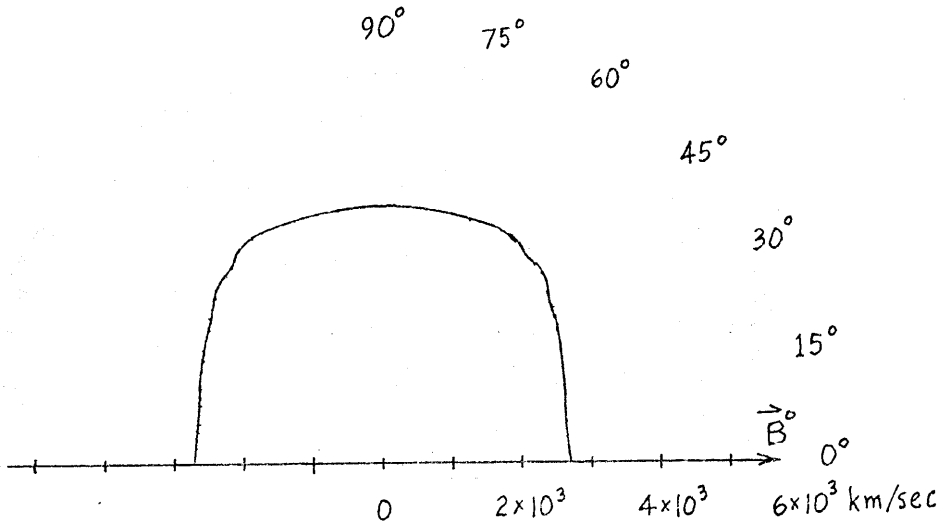

Figure 5.4

Phase Velocity Diagram

Real w, complex $\vec{k}$

L = 5.8 Re, lat. = 0° (geomagnetic)

long. = 288° E (midnight), $K_p < 1^+$

Figure 5.5 Perpendicular Attenuation Constant $k_{\perp i}$

Real w, complex $\vec{k}$, frequency = .02 cps
L = 5.8 Re, lat. = 0° (geomagnetic)
long. = 288° E (midnight), $K_p < 1^+$

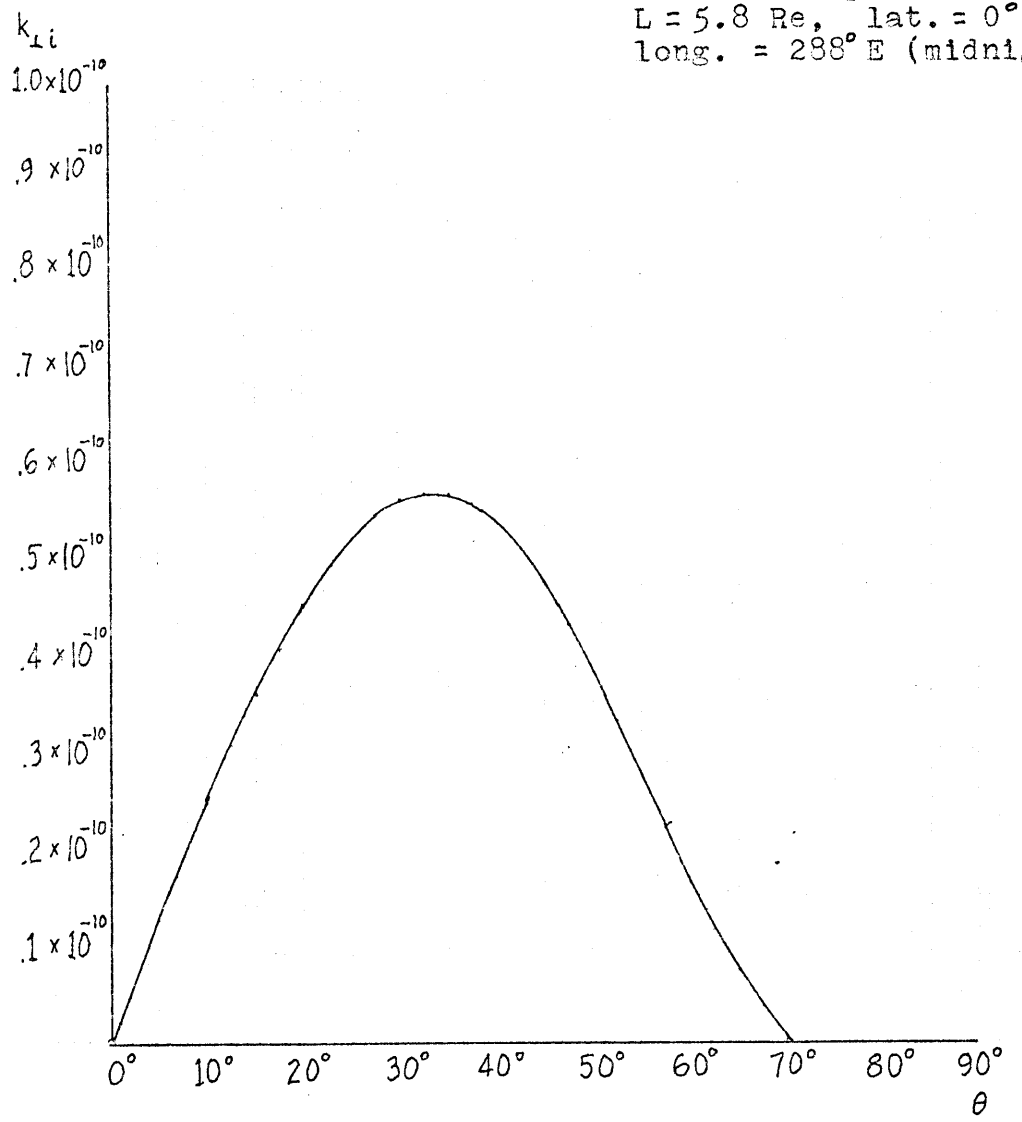

Figure 5.6 Perpendicular Attenuation Constant $k_{\perp i}$

Real w, complex $\vec{k}$, frequency = .08 cps
L = 5.8 Re, lat. = 0° (geomagnetic)
long. = 288° E (midnight), $K_p < 1^+$

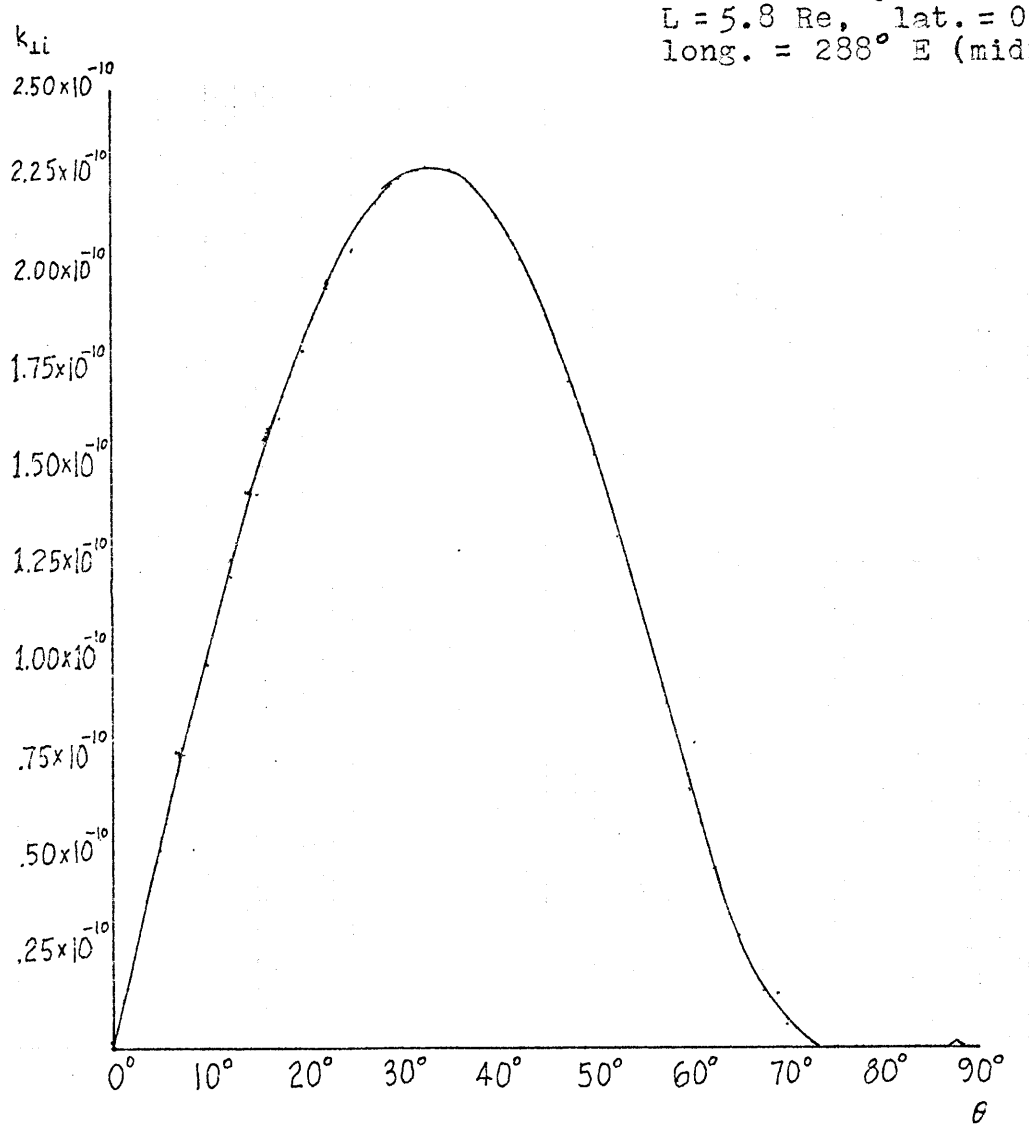

Figures 5.7 and 5.8 give the phase velocity and perpendicular attenuation rate curves for plasma at 4.6 Re (just inside the plasmapause) and for an unguided Alfven wave of .02 cps. frequency.

Figures 5.9 and 5.10 give the corresponding curves for plasma at 3.6 Re. Figures 5.11 and 5.12 give the same curves for plasma at 20° geomagnetic latitude. Figures 5.15 and 5.16 give the corresponding curves for a slightly disturbed magnetosphere ($K_p = 2$). Figures 5.17 and 5.18 give the phase velocity curves for a CGL plasma with the same parameters as those used with the CKW plasma in Figures 5.4 to 5.8 for the sake of comparison.

Figures 5.19 and 5.20 give the transmitted power below a slab 1 Re thick if an incident wave of unit power (.02 cps. frequency) were to enter the top of the slab and be subsequently damped by the slab. Figure 5.19 refers to plasma at 5.8 Re (just outside the plasmapause) and Figure 5.20 refers to plasma at 4.6 Re (just inside the plasmapause). One may note that the wave is hardly damped outside the plasmapause, but is heavily damped inside the plasmapause. The difference is easy to understand. The number density of the plasma outside the plasmapause is much lower than inside the plasmapause, thus making the wave phase velocities much higher outside than inside. Hence, there are more plasma particles at the lower velocity that resonate with the slower wave inside the plasmapause than there are particles at the higher velocity required to resonate with the much faster wave outside the plasmapause.

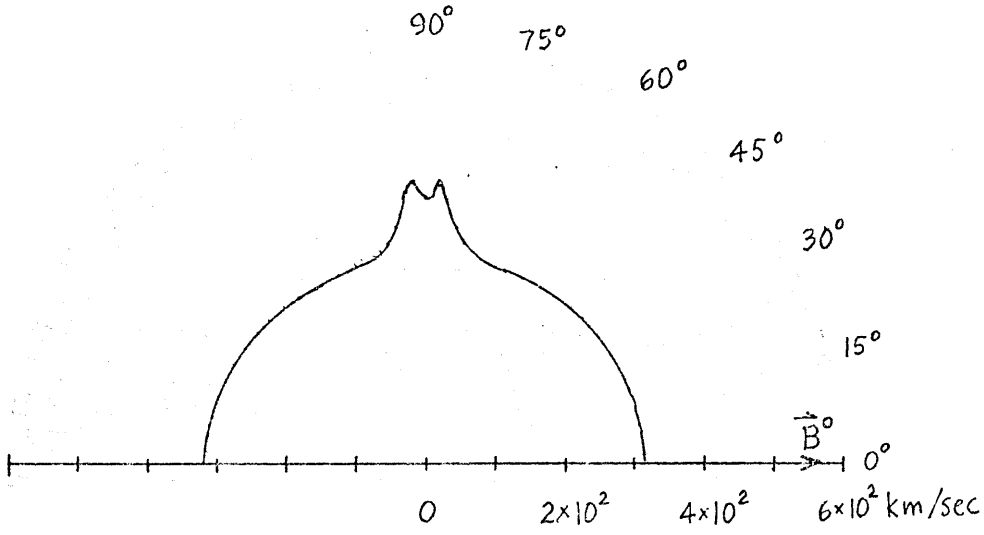

Figure 5.7

Phase Velocity Diagram

Real w, complex $\vec{k}$

L = 4.6 Re, lat. = 0° (geomagnetic)

long. = 288° E (midnight), $K_p < 1^+$

Figure 5.8 Perpendicular Attenuation Constant $k_{\perp i}$

Real w, complex $\vec{k}$, frequency = .02 cps
L = 4.6 Re, lat.= 0° (geomagnetic)
long., = 288° E (midnight), $K_p < 1^+$

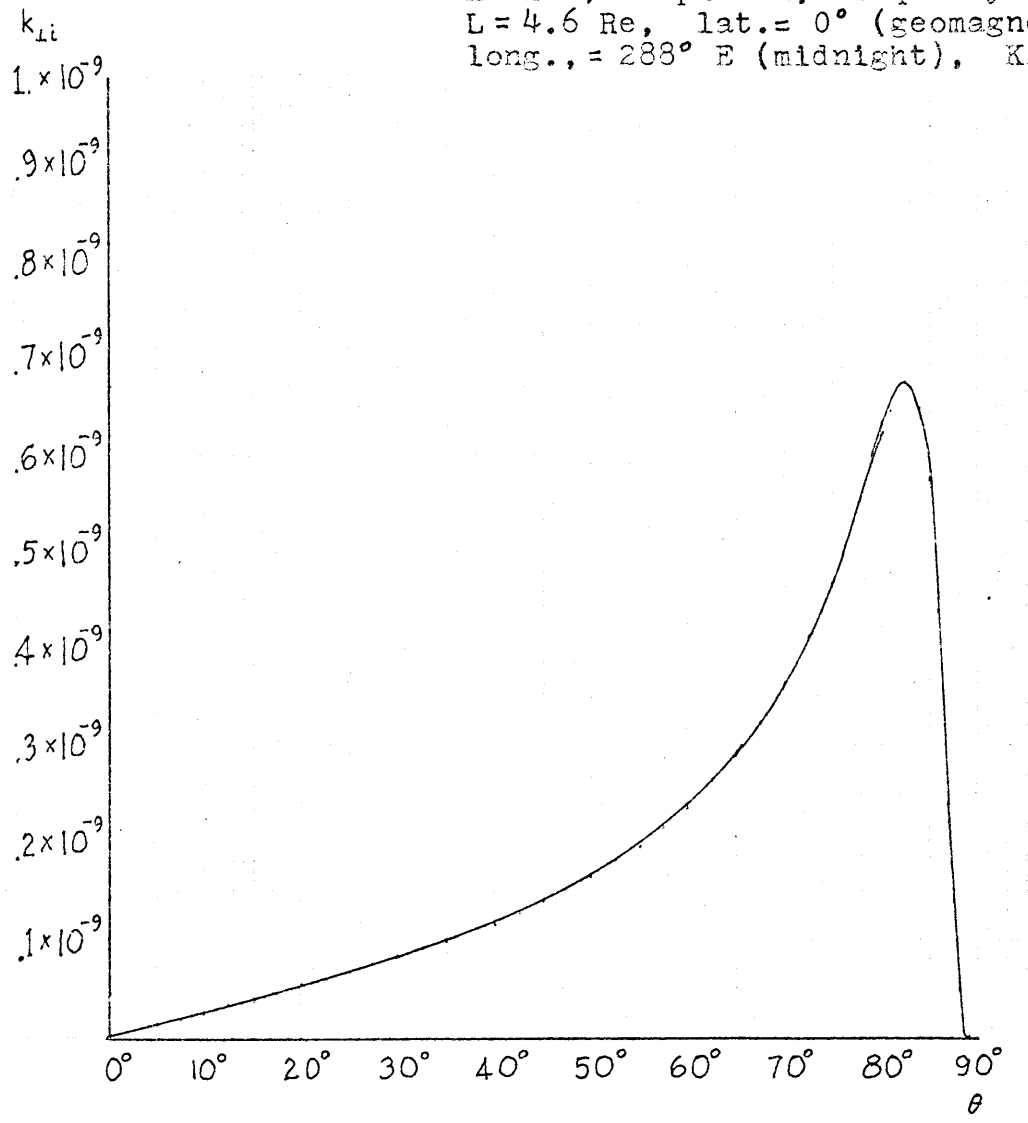

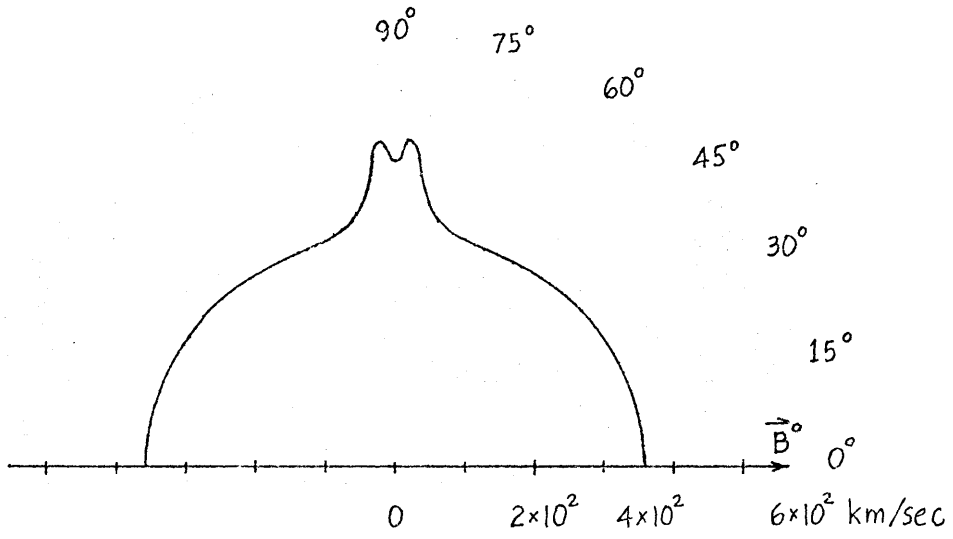

Figure 5.9

Phase Velocity Diagram

Real w, complex $\vec{k}$

L = 3.6 Re, lat. = 0° (geomagnetic)

long. = 288° E (midnight), $K_p < 1^+$

Figure 5.10 Perpendicular Attenuation Constant $k_{\perp i}$

Real w, complex $\vec{k}$, frequency = .02 cps
L = 3.6 Re, lat. = 0° (geomagnetic)
long. = 288° E (midnight), $K_p < 1^+$

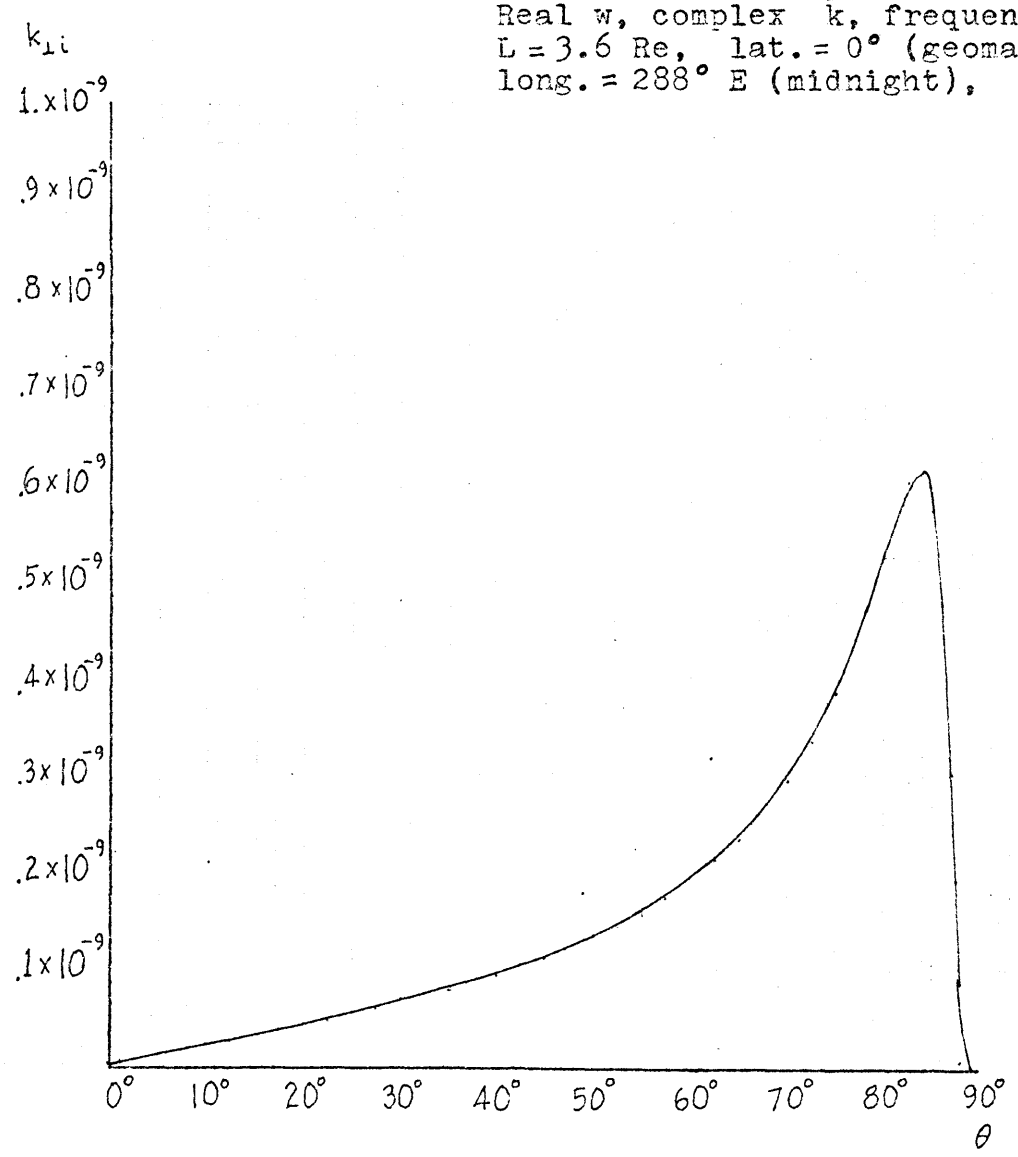

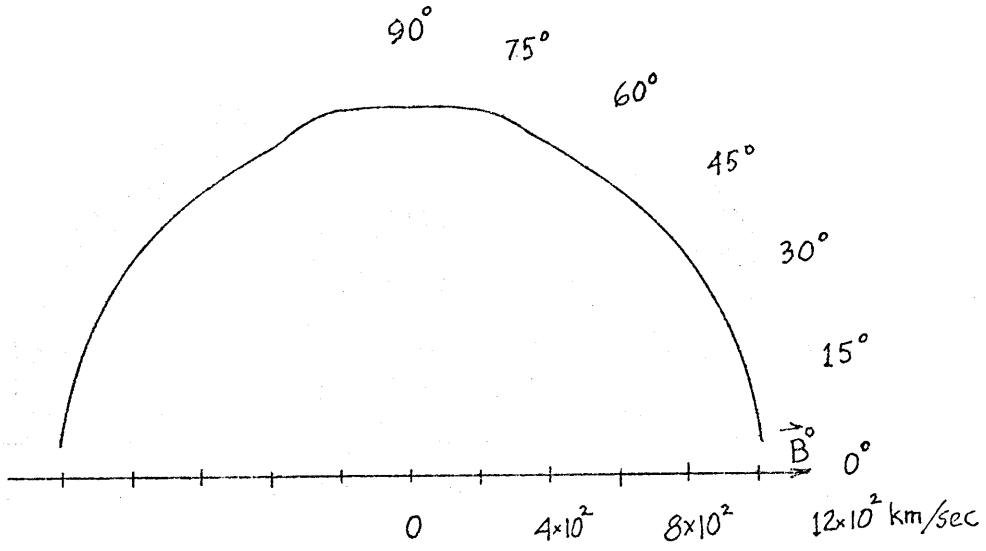

Figure 5.11

Phase Velocity Diagram

Real w, complex $\vec{k}$

L = 4.6 Re, lat. = 20° (geomagnetic)

long. = 288° E (midnight), $K_p < 1^+$

Figure 5.12 Perpendicular Attenuation Constant $k_{\perp i}$

Real w, complex $\vec{k}$, frequency = .02 cps
L = 4.6 Re, lat. = 20° (geomagnetic)
long. = 288°E (midnight), $K_p < 1^+$

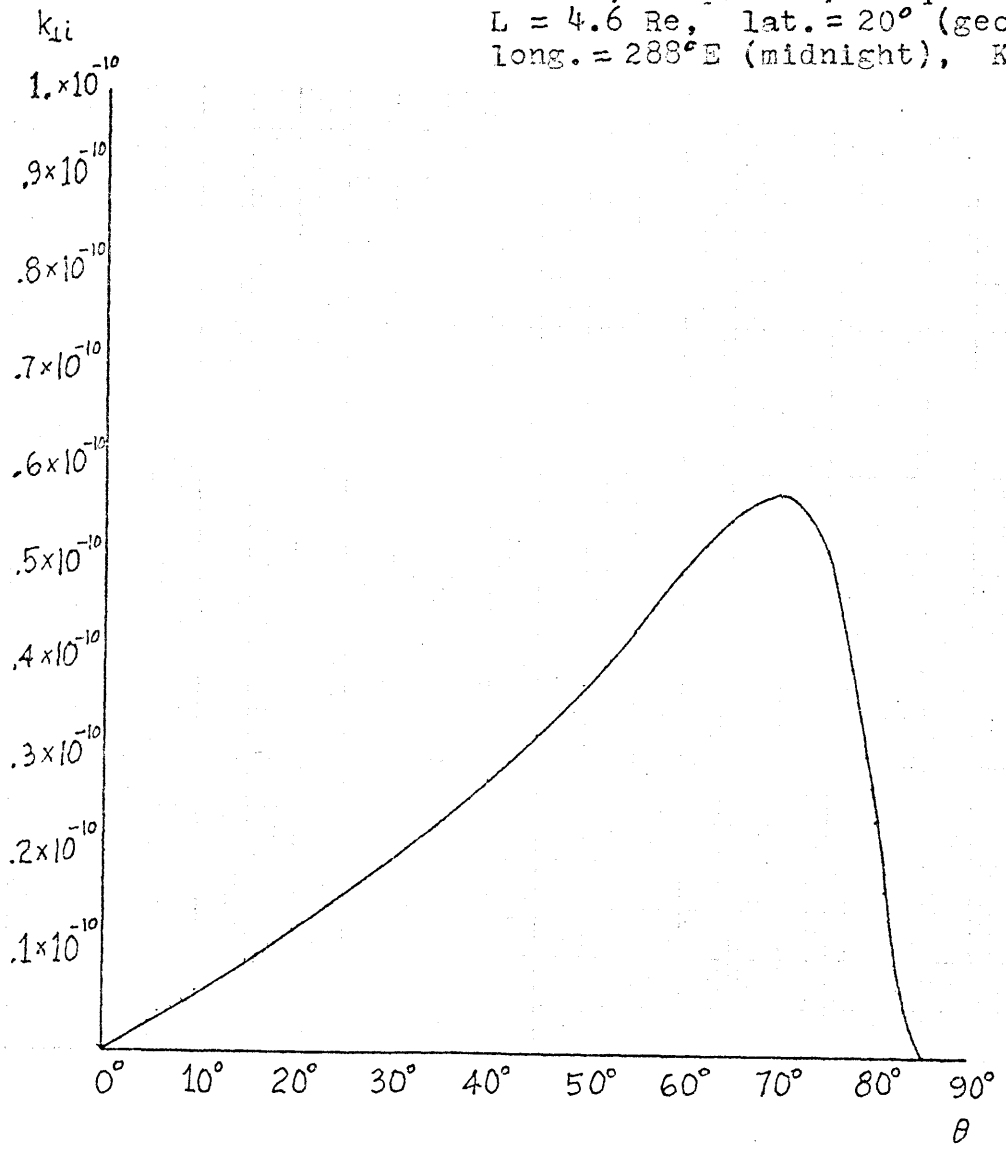

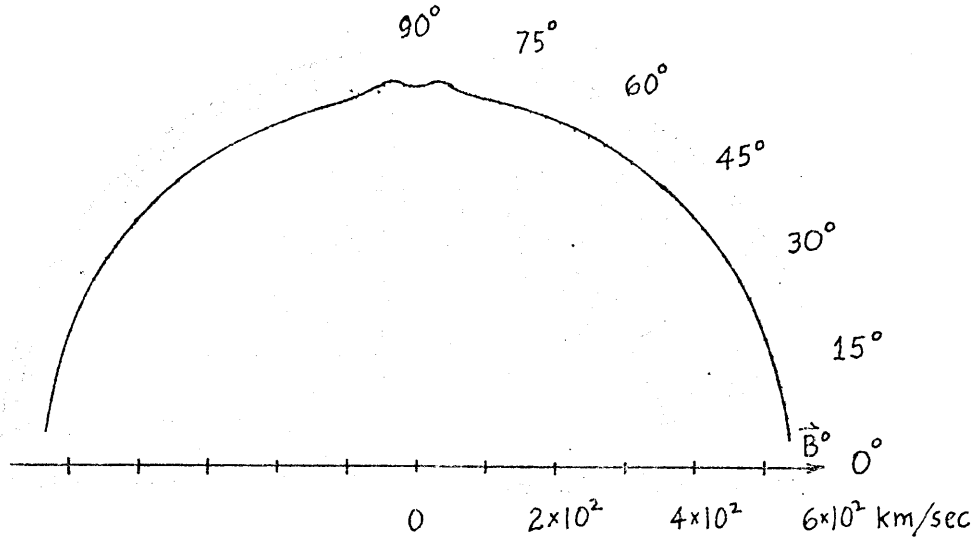

Figure 5.13

Phase Velocity Diagram

Real w, complex $\vec{k}$

L = 3.6 Re, lat. = 20° (geomagnetic)

long. = 288°E (midnight), $K_p < 1^+$

Figure 5.14 Perpendicular Attenuation Constant $k_{\perp i}$

Real ω, complex $\vec{k}$, frequency = .02 cps
L = 3.6 Re, lat. = 20° (geomagnetic)
long. = 288° E (midnight), $K_p < 1^+$

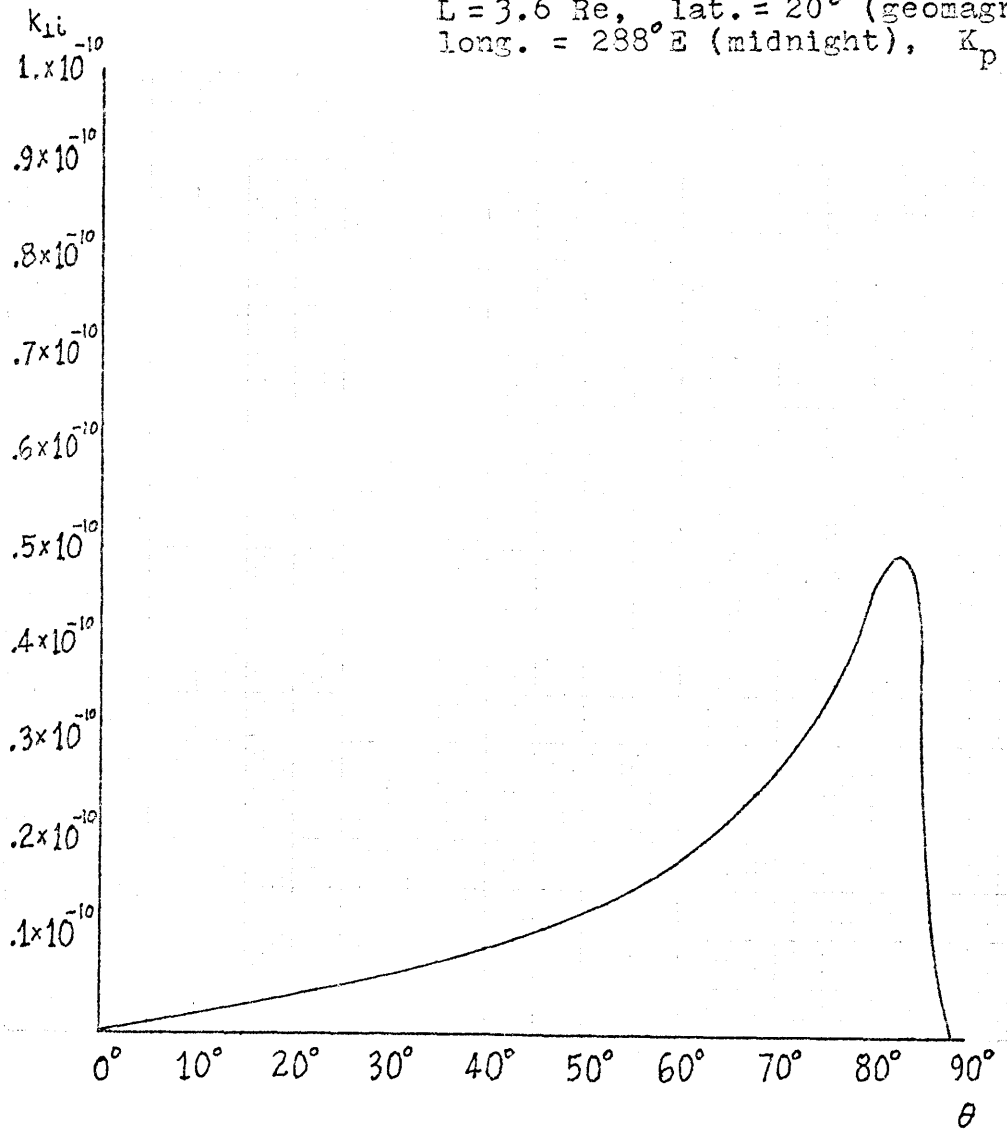

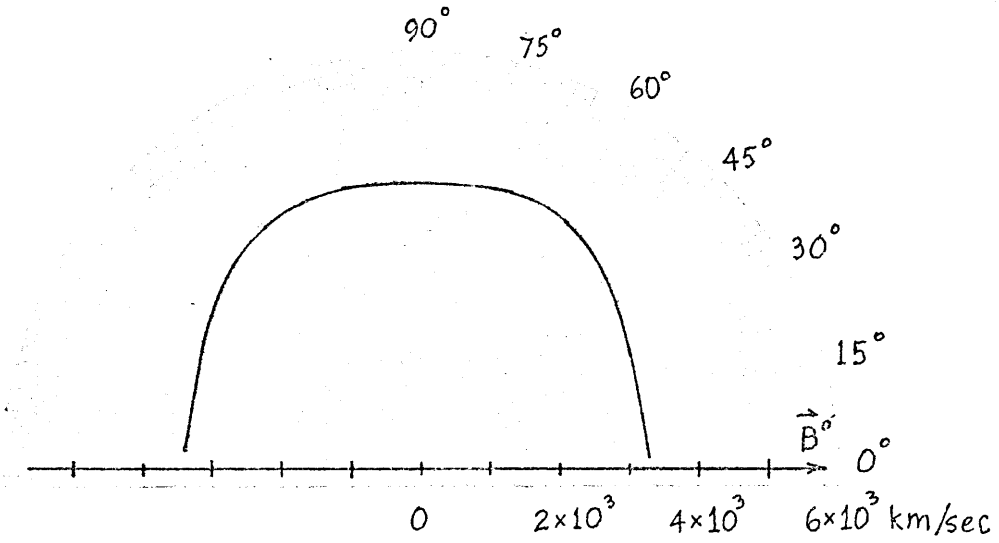

Figure 5.15

Phase Velocity Diagram

Real w, complex $\vec{k}$

L = 4.6 Re, lat. = 0° (geomagnetic)

long. = 288°E (midnight), K_p = 2

Figure 5.16 Perpendicular Attenuation Constant $k_{\perp i}$

Real w, complex $\vec{k}$, frequency = .02 cps
L = 4.6 Re, lat. = 0° (geomagnetic)
long. = 288°E (midnight), K_p = 2

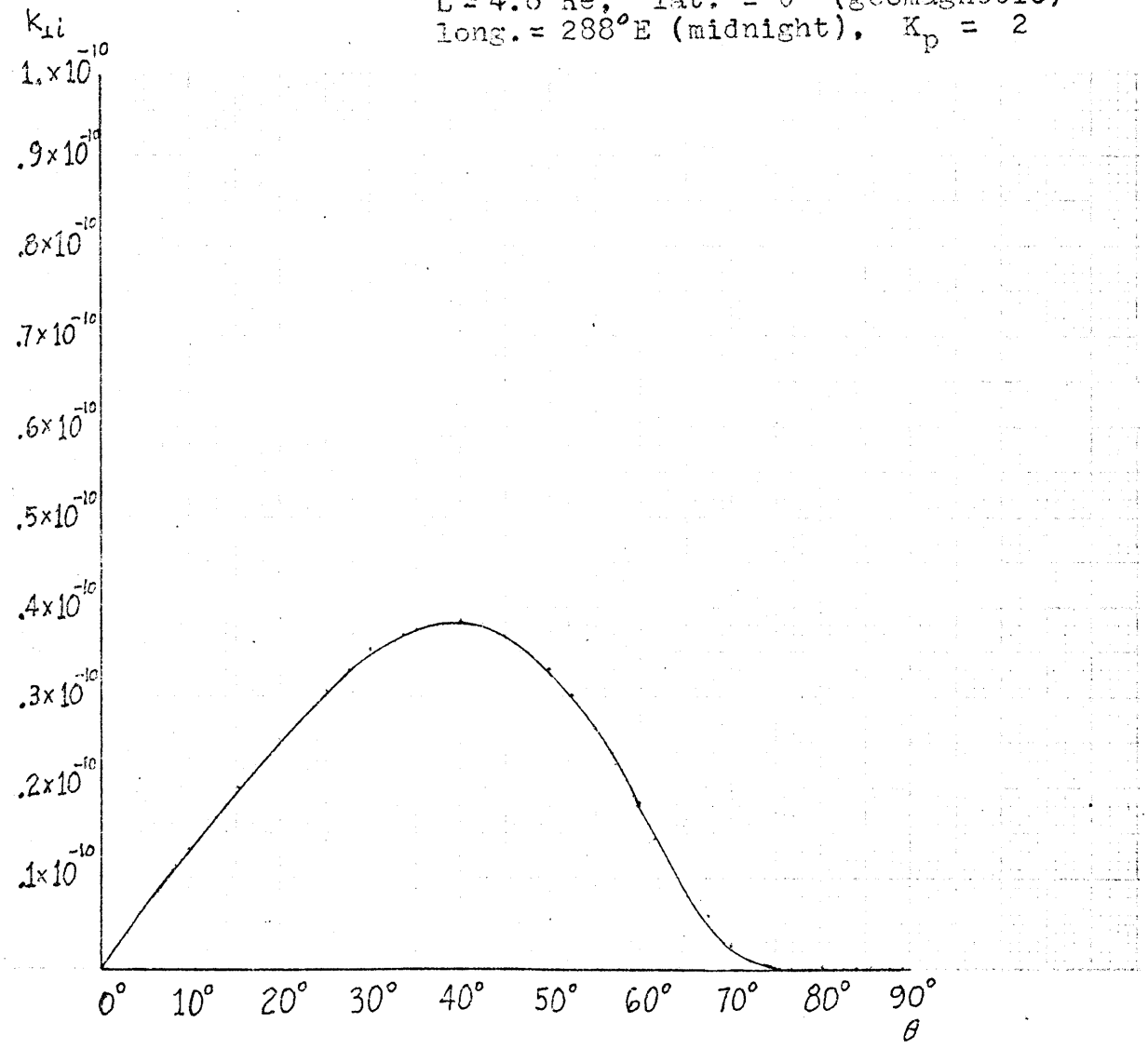

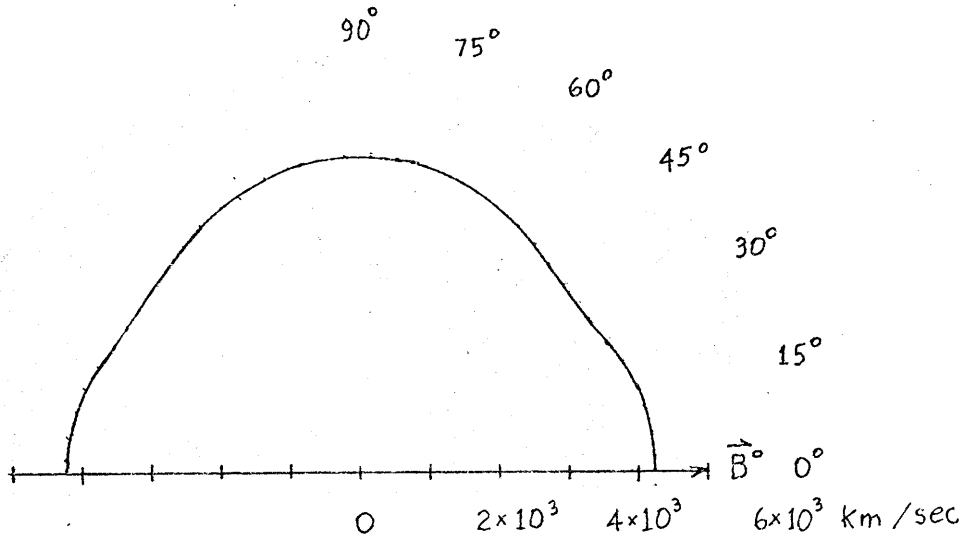

Figure 5.17

Phase Velocity Diagram for a Chew-Goldberger-Low (CGL) Plasma

L = 5.8 Re, lat. = 0° (geomagnetic)

long. = 283° E (midnight), $K_p < 1^+$.

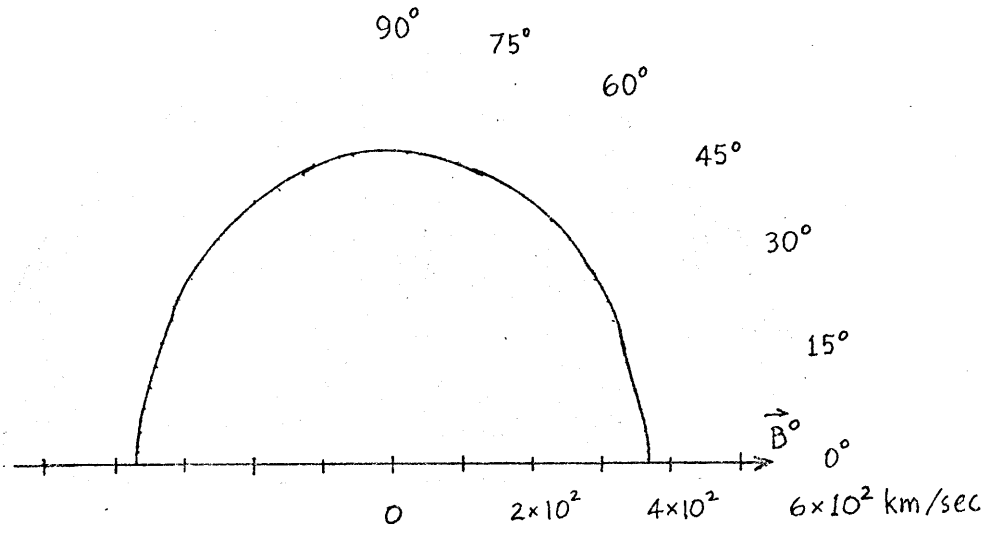

Figure 5.18

Phase Velocity Diagram for a Chew-Goldberger-Low (CGL) Plasma

L = 4.6 Re, lat. = 0° (geomagnetic)

long. = 288° E (midnight), $K_p < 1^+$

Figure 5.19 Relative Transmitted Power Below 1 Re Slab

Real w, complex $\vec{k}$, frequency = .02 cps
L = 5.8 Re, lat. = 0° (geomagnetic)
long. = 288° E (midnight), $K_p < 1^+$

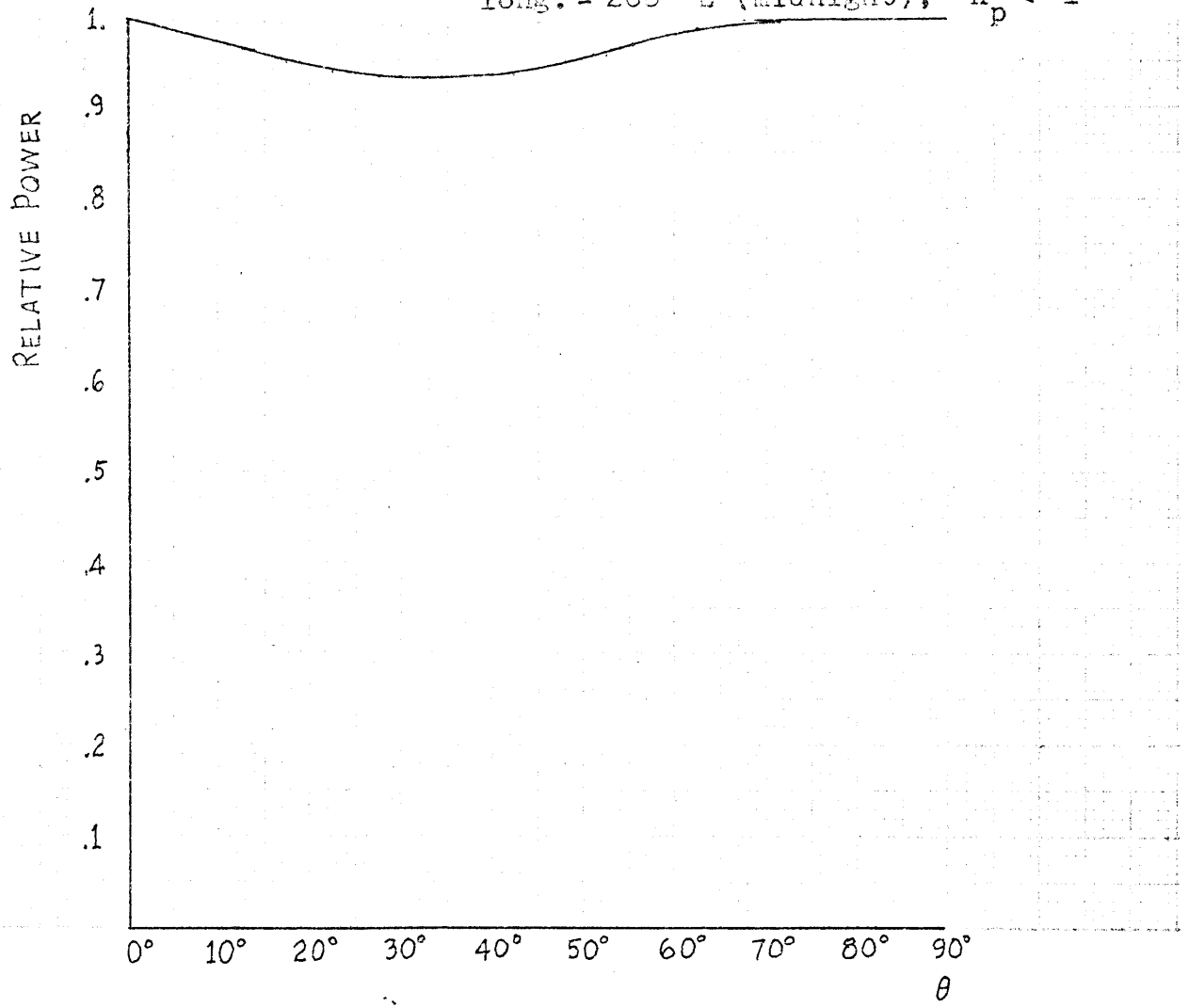

Figure 5.20 Relative Transmitted Power Below 1 Re Slab

Real w, complex $\vec{k}$, frequency = .02 cps
L = 4.6 Re, lat. = 0° (geomagnetic)
long. = 288° E (midnight), $K_p < 1^+$

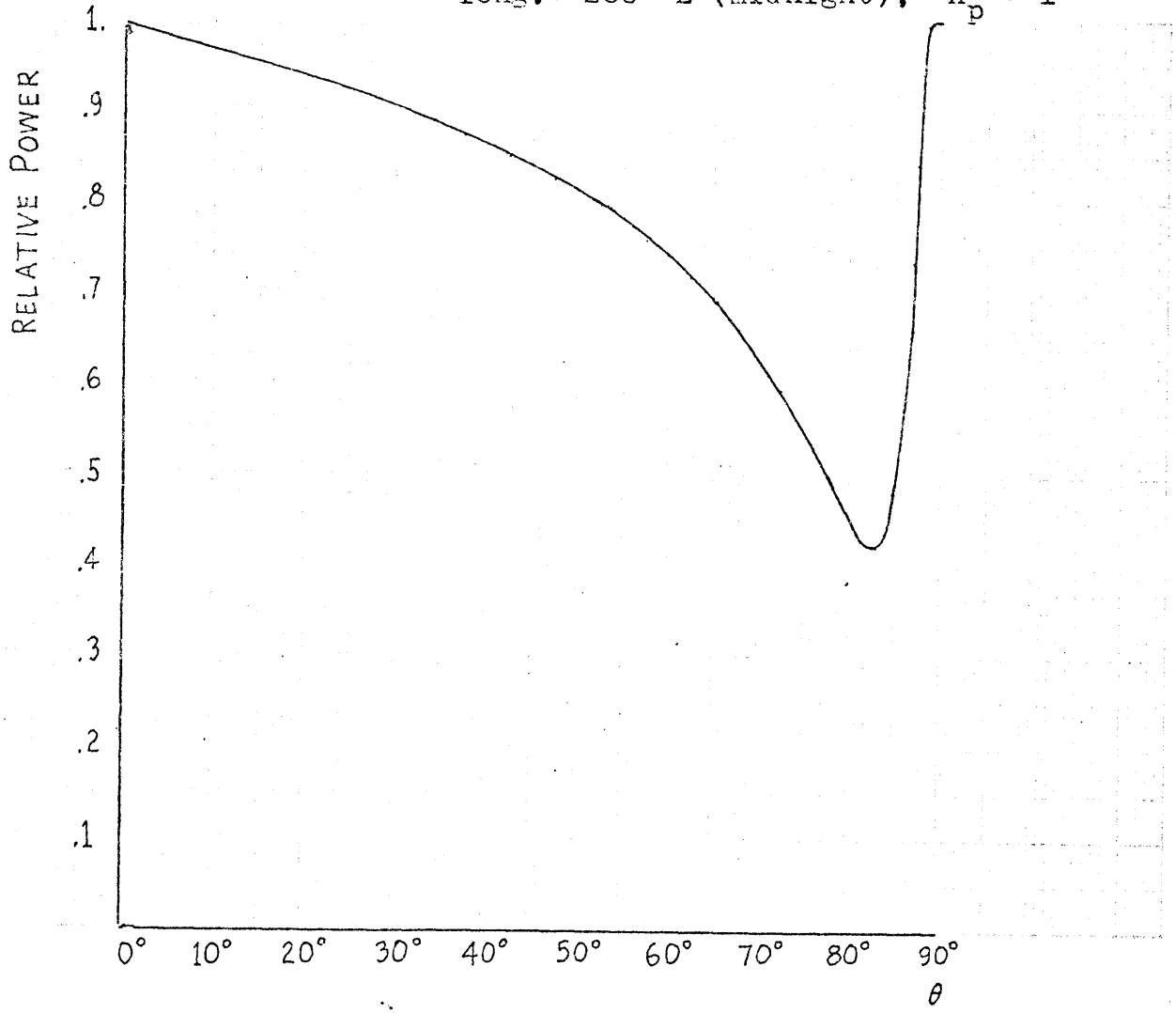

Figure 5.21 shows how doubling the number density of the hot proton component more than doubles the damping rate $\vec{\alpha} = \vec{k}_i / |\vec{k}_r|$ for most angles of propagation.

Since $\vec{k}_{\perp i} = |\vec{k}_r| \vec{\alpha}$, where $\vec{\alpha}$ is the analogue of the damping rate for complex $\vec{k}$; and since $|\vec{k}_r| = 2\pi f / |\vec{v}_{ph}|$, where $\vec{v}_{ph}$ is the wave phase velocity, if a plot of $\vec{v}_{ph}$ vs. angle of propagation θ is given, a plot of the perpendicular attenuation constant $|\vec{k}_{\perp i}|$ vs. θ yields information equivalent to a plot of $|\vec{\alpha}_\perp|$ vs. θ .

Figure 5.21 Comparison of Damping Rates When Hot Proton Number Density is Varied
Real w, complex k
L 4.6 Re, lat. 0° (geomagnetic),
long. 288° E (midnight), K_p 1

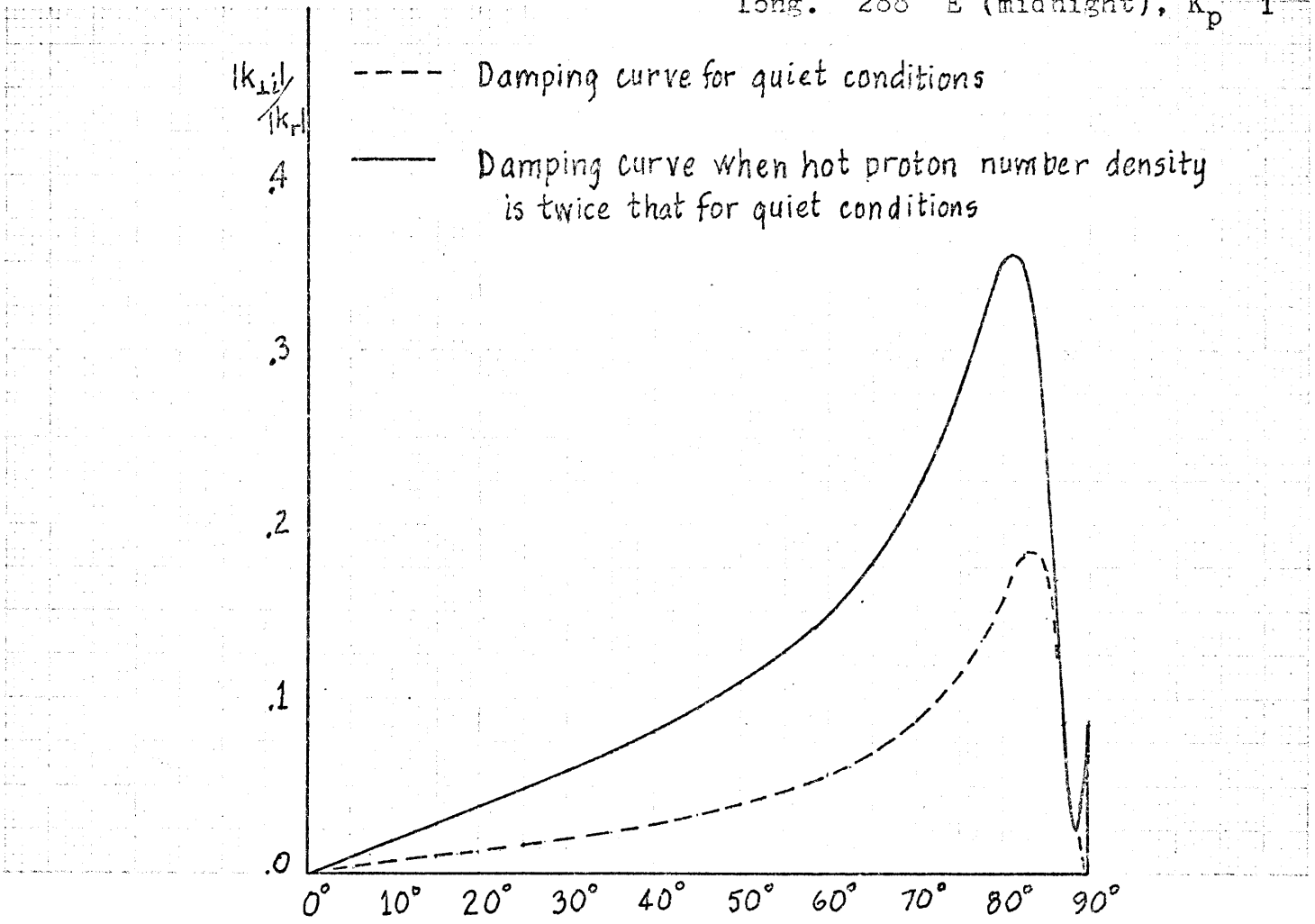

CHAPTER 6

GEOPHYSICAL IMPLICATIONS

6.1 Damping effects on micropulsations

This section focuses attention on waves with frequencies below about .2 cps, at which frequency modes other than the unguided Alfven mode begin to appear superimposed on that mode on the records from the M.I.T. telluric station in New Hampshire. Geomagnetically quiet periods are mostly discussed because then magnetospheric phenomena may be presumed to be at their simplest. For the same reason we have restricted this early phase of our investigation of damping only to the vicinity of the equatorial plane around the midnight meridian. The magnetospheric model encompasses the regions from 1 earth radius outside the plasmapause down to 2.1 earth radii (in geocentric coordinates), where damping is expected to diminish rapidly because the increasing magnetic field reduces rapidly the ratio β between plasma pressure and magnetic pressure.

We apply the damping theory to two cases of hydromagnetic waves propagating earthward through the inner magnetosphere. The first case concerns waves with sources outside the plasmapause, and the second, waves with sources just inside the plasmapause. We then relate the results to micropulsation

observations from a low latitude station in the Bermuda Islands, and to telluric observations from the M.I.T. mid-latitude station in New Hampshire.

6.2 Wave sources outside the plasmapause

In the first case, for sources outside the plasmasphere, we take a three-slab model of the inner magnetosphere. Each slab is of thickness one earth radius. The outermost slab represents the plasma just outside the plasmasphere. Its parameters are given in Table IC in Chapter 5, corresponding to plasma at 5.8 earth radii away from the center of the earth. The plasmapause is represented by the boundary between the first and second slabs. This second slab has parameters corresponding to plasma at 4.6 earth radii as given in Table IA. The third and innermost slab is described by the plasma parameters given for a point on the geomagnetic equator at 3.6 earth radii away from the center of the earth (Table IA).

We want to know how much damping a wave undergoes as it propagates earthward starting from near the top of the first slab and emerging at the bottom of the third slab. In this investigation, we are primarily interested in the damping effects. We have thus neglected partial reflections at the slab boundaries. In each slab we solve the dispersion equations for an inhomogeneous wave with real frequency ω and complex propagation constant $\vec{k}$. The planes of constant amplitude are assumed to be parallel to the plasmapause, i.e.,

the imaginary component of $\vec{k}$ is assumed to lie in the direction perpendicular to the plasmapause. The spatial rate of damping is proportional to this imaginary component. The planes of constant phase are perpendicular to the real component of $\vec{k}$, so that these planes propagate in the direction of this component. This real vector makes an angle θ with the earth's magnetic field, which in turn is parallel to the plasmapause. Snell's law determines the changes in the (real) propagation angle θ as the wave progresses from one slab to the next. Several characteristics of the waves in each slab are given in the preceding chapter.

The over-all damping is much affected by two features that characterize wave propagation from above the plasmapause: first, the focusing effect of the transmission across the plasmapause; and second, the highly anisotropic nature of the damping.

Since the phase velocities are much higher above the plasmapause than below it, waves at all angles of propagation above the plasmapause are refracted (Snell's law) into a narrow band of angles close to 90° in the plasma just below the plasmapause. The result is a focusing effect. With the plasma parameters in this study assumed for quiet period, midnight equatorial conditions, the wave phase speeds above the plasmapause (at 5.8 earth radii) are about 10 times the phase speeds just below the plasmapause at 4.6 earth radii, because of the sharp rise in density below the plasmapause. This speed change

refracts incoming waves at all propagation angles in the top slab into a narrow 7.5° range of propagation angles below the plasmapause from 82.5° to 90°.

Below the plasmapause, the phase speeds are so low compared to the thermal speeds of the hot plasma (see Chapter 5) that the propagation angles required for wave-particle resonance with the hot plasma are in the 80°'s. At such large angles of propagation, even wide variations in the parallel thermal speed of the hot plasma correspond to very small variations in the propagation angle required for resonance. Hence, there is not much variation in the angle of propagation for maximum damping rate.

In our magnetospheric plasma model, doubling the parallel temperature of the hot plasma component shifts the angle of maximum damping from 82.5° to 85°. This small change in refracted angle corresponds to a change in incident angle outside the plasmapause from 12.5° to 37.5°.

On the other hand, doubling the number density of the hot plasma component approximately doubles the damping rate and reduces slightly the angle of maximum damping (see Figure 5.21).

Since the unguided Alfven wave at a frequency of 0.08 cps has a wavelength of about $\frac{1}{2}$ earth radius inside the plasmapause, waves at lower frequencies could have wavelengths comparable to some characteristic lengths in the plasmasphere. Among the long wavelength effects which may be expected, but not considered in the computations, are resonance peaks in the spectra. However, since damping is a local wave-particle interaction, our estimates of damping rates are still valid at frequencies below 0.08 cps.

We computed the average power attenuation factor δ for unguided Alfven waves from outside the plasmapause which are incident on our magnetospheric model plasma slab, assuming that all incident wave directions are equally probable. The attenuation factor δ is proportional to the damping rate. The estimated average value of δ is 59, which indicates strong damping. Figure 6.1 shows how δ varies with the propagation angle θ of the incident wave above the plasmapause. Figure 6.2 shows the weighting function used in the averaging.

In this estimate, the change in angle of propagation as a wave moves down a slab due to the curvature of the dipole field lines is taken into account for angles 85° or greater. Below 85° the rate of change of damping rate with change of angle is considerably less than for angles of 85° and above. Hence, the change in angle of propagation as a wave moves down a slab is neglected for waves with propagation angles less than 85°.

For small geomagnetic latitudes λ, the change in angle of propagation $\Delta\theta$ as a wave moves down a distance Δr is given by (all angles in the equation below are to be in radians):

$$\Delta\theta = \left(1 + \frac{2}{1 + 4\lambda^2}\right)(2\lambda + \gamma)\frac{\Delta r}{r} \qquad (6.1)$$

where γ = angle of incidence at the top of the slab of thickness Δr

r = distance from the center of the earth to the middle of the slab

Figure 6.1 Power attenuation factor δ when source is above the plasmapause
Lat. = 0° (geomagnetic), Long. = 288°E, $K_p < 1^+$

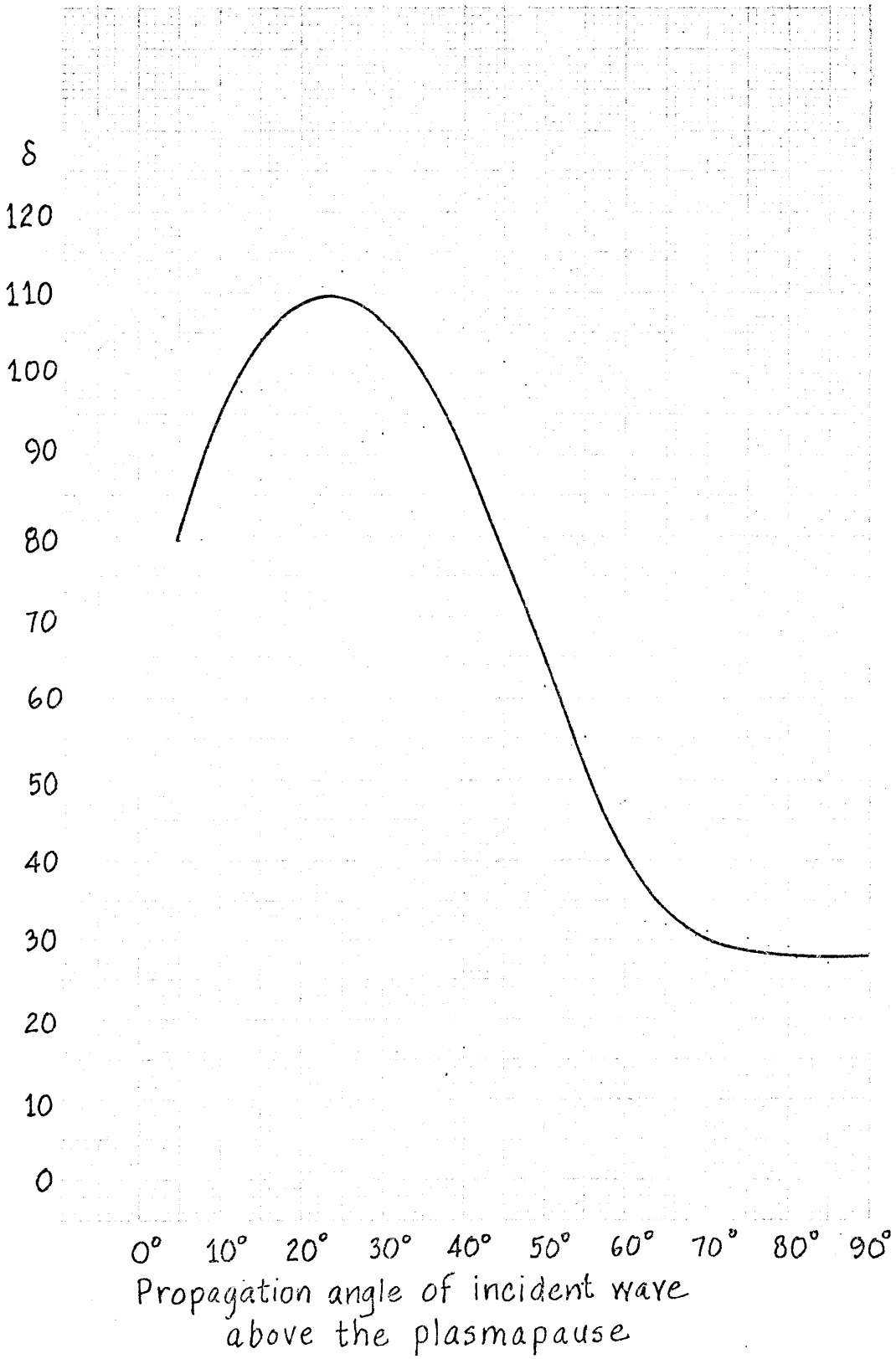

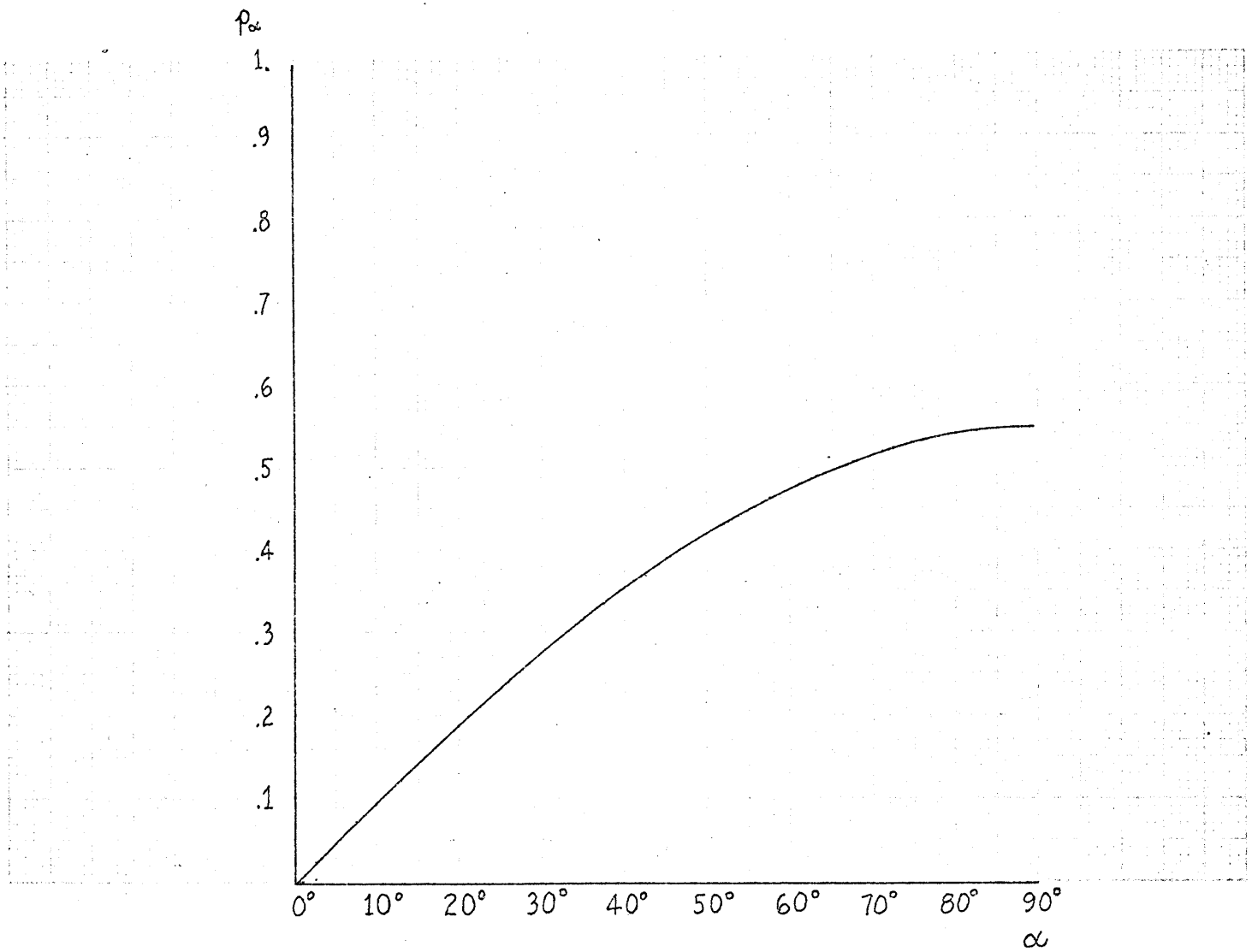

Figure 6.2 Weighting Function p_α for Averaging over Propagation Angles α, Assuming Isotropic Probability Distribution

6.3 Attenuation factor when the wave source is below the plasmapause

When we make the same assumptions about the incident waves as in the previous section, except that we locate the wave source below the plasmapause at R = 5.1 Re, and hence take into account damping by the lowest two of the three slabs considered in the previous section, we find the average attenuation factor δ to drop to 33.9. Figure 6.3 shows the variation of δ vs. propagation angle of the incident wave when the incident wave is below the plasmapause.

6.4 Attenuation factors for power spectra observed at the M.I.T. telluric station

Figure 6.4 shows the magnetic meridian plane through the M.I.T. midlatitude telluric station in New Hampshire from which the following power spectra of electric field fluctuations were taken. Figure 6.5 shows a representative spectrum and the exponential curves which may be fitted to it. Several combinations of n and δ can be found to fit it. However, n cannot be varied too much without producing large discrepancies at lower frequencies. We estimate an uncertainty in our values of δ such that $\delta/2 <$ true $\delta < \delta$.

We express power density in terms of power/octave because the power density then becomes directly related to the square of typical amplitudes. Santirocco and Parker (1963), in presenting their micropulsation spectra from Bermuda (see section 1.4), followed the common practice of giving power spectral density in terms of power/cps.

Figure 6.3 Power attenuation factor δ when source is below the plasmapause
Lat. = 0° (geomagnetic), Long. = 288°E, $K_p < 1^+$

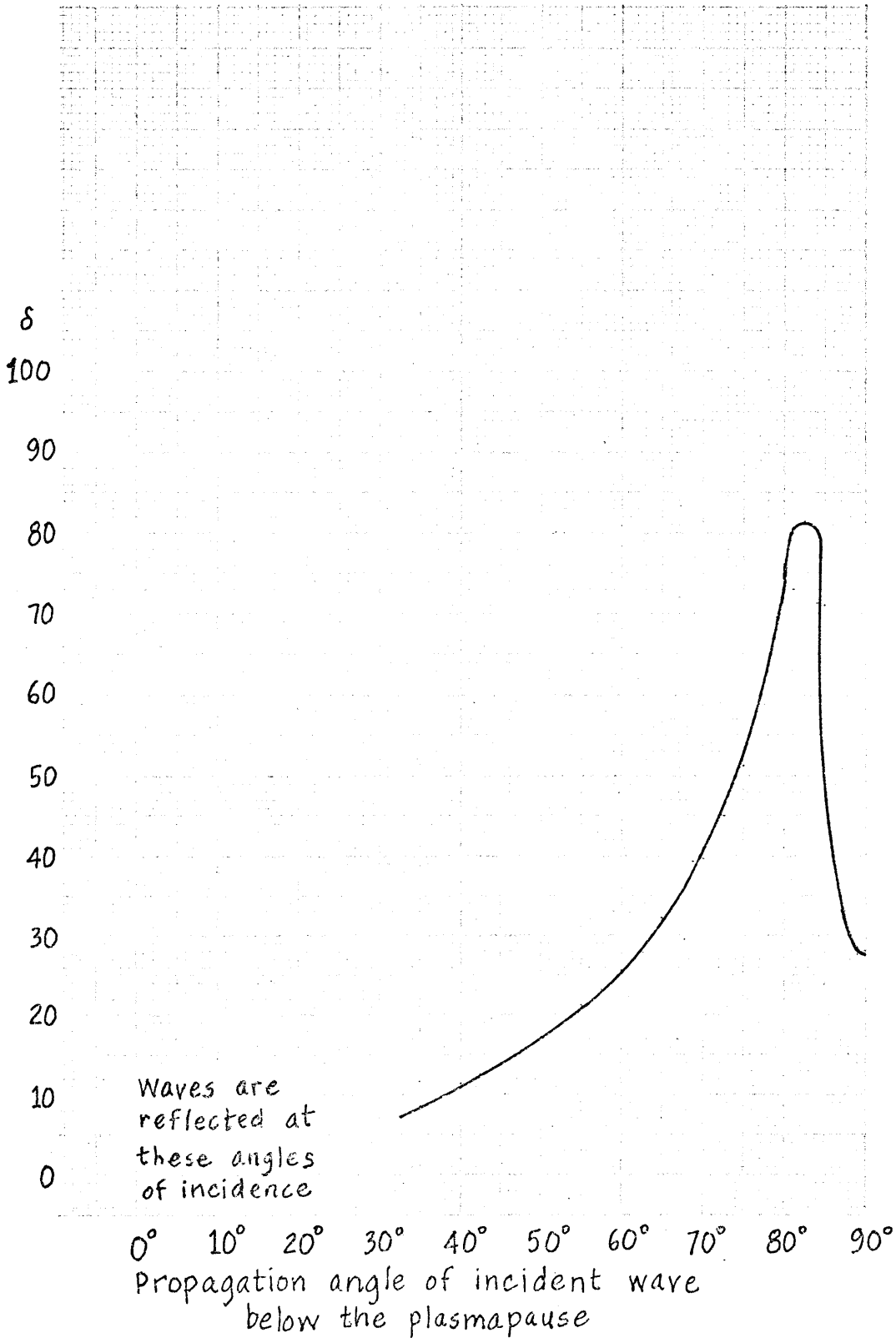

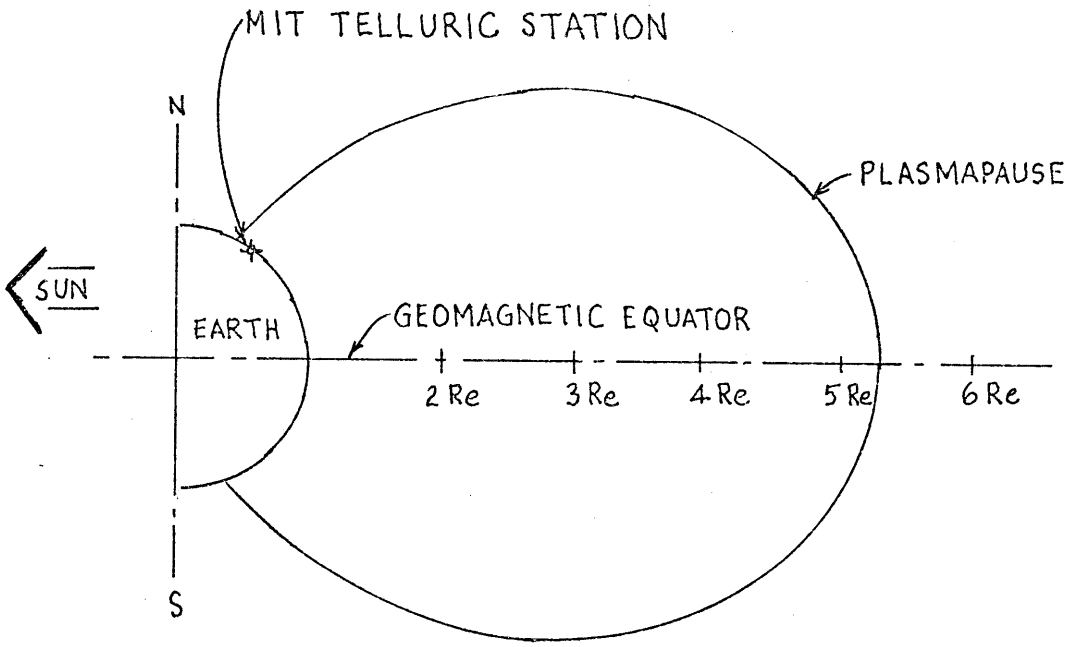

Figure 6.4 Magnetic meridian plane through the M.I.T. telluric station in New Hampshire

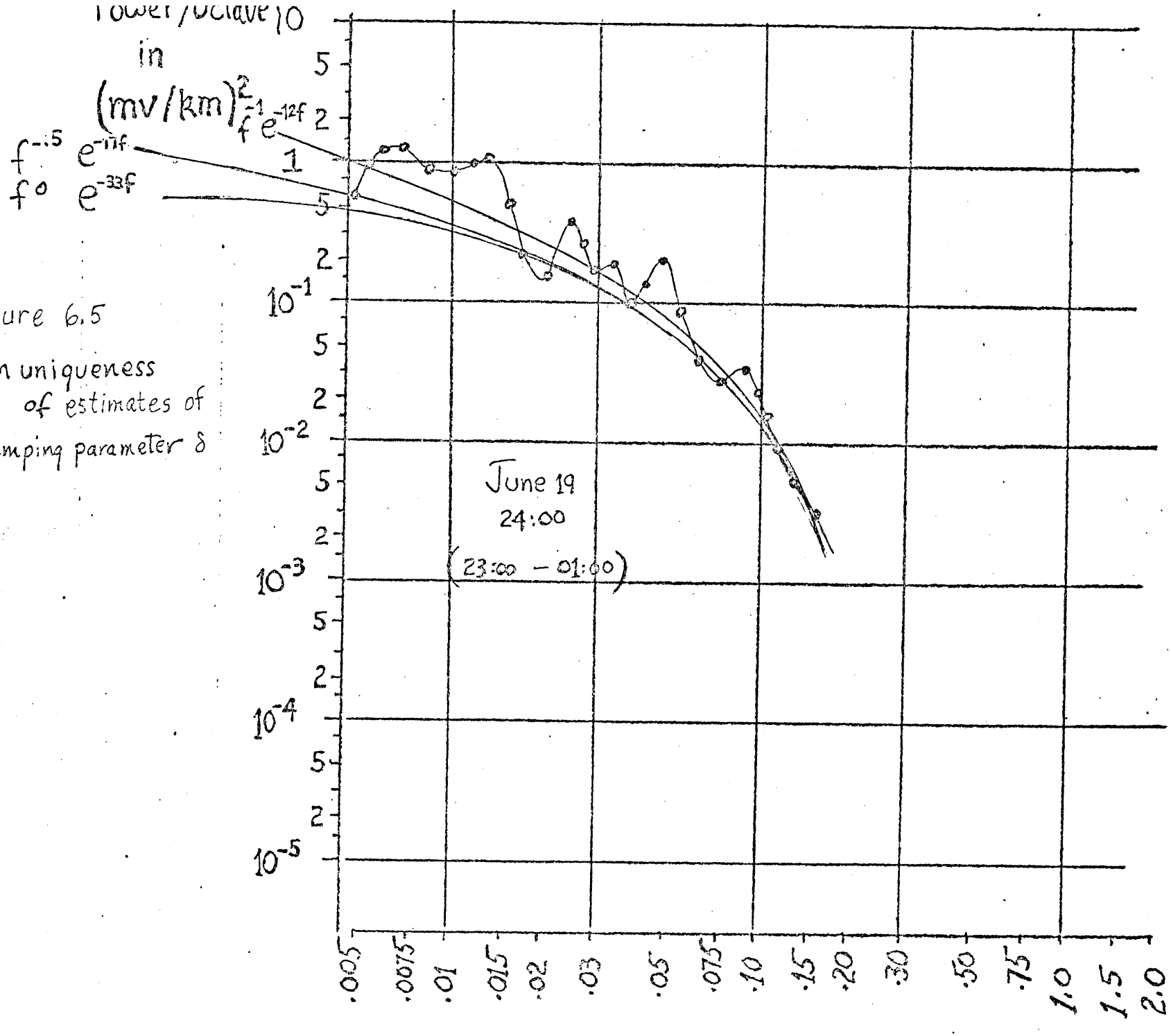

Figure 6.5
Non uniqueness of estimates of damping parameter δ

Figure 6.6 shows two spectra observed in the afternoon. The spectrum remained unchanged over several hours. Figure 6.7 shows a series of consecutive spectra observed around midnight. There was substantial change of power levels and damping rates. The three spectra in Figure 6.8 were taken on different days. They differ from the spectra in Figures 6.5 to 6.7 in that while the electronic filters used to obtain the spectra in Figures 6.5 to 6.7 had a pass band from 0.005 to 0.15 cps, the electronic filters used for Figure 6.8 had a pass band at a lower frequency range, from 0.001 to 0.03 cps. Furthermore, the spectra in Figures 6.5 to 6.7 were averages over $2\frac{1}{2}$ hours, while the spectra in Figure 6.8 were averages over 8 hours. Figure 6.9 shows another spectrum taken near midnight. This spectrum, and the others following in Figures 6.10 to 6.12 were taken using electronic filters which had pass bands from 0.005 to 2.0 cps. They were averages over the much shorter interval of 27.3 minutes. Because of those differences in pass bands, only the latter group of spectra, Figures 6.9 to 6.12, show the break in the spectra often found at about 0.1 cps.

Figure 6.13 shows a histogram of observed attenuation factors δ based on 112 spectra. An average value for δ is about 33.3, which means that a wave of frequency 0.021 will lose half its energy in traversing the plasmasphere. Occasionally much more severe damping is inferred.

When comparing Santirocco and Parker's (1963) spectra of magnetic field fluctuations from Bermuda with our spectra of electric field fluctuations from New Hampshire, we note that

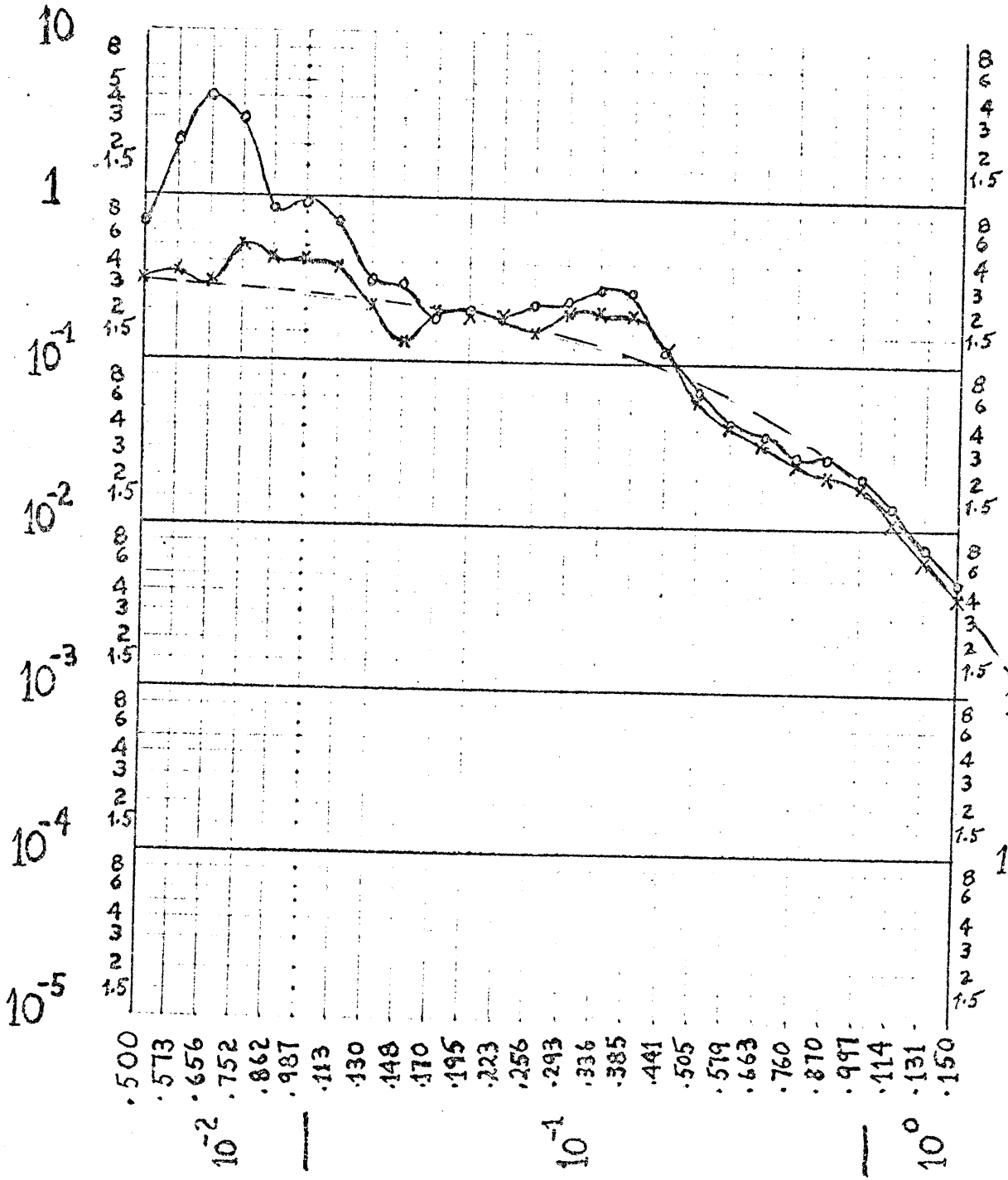

Figure 6.6
Estimate of attenuation factor δ from telluric spectrum from New Hampshire

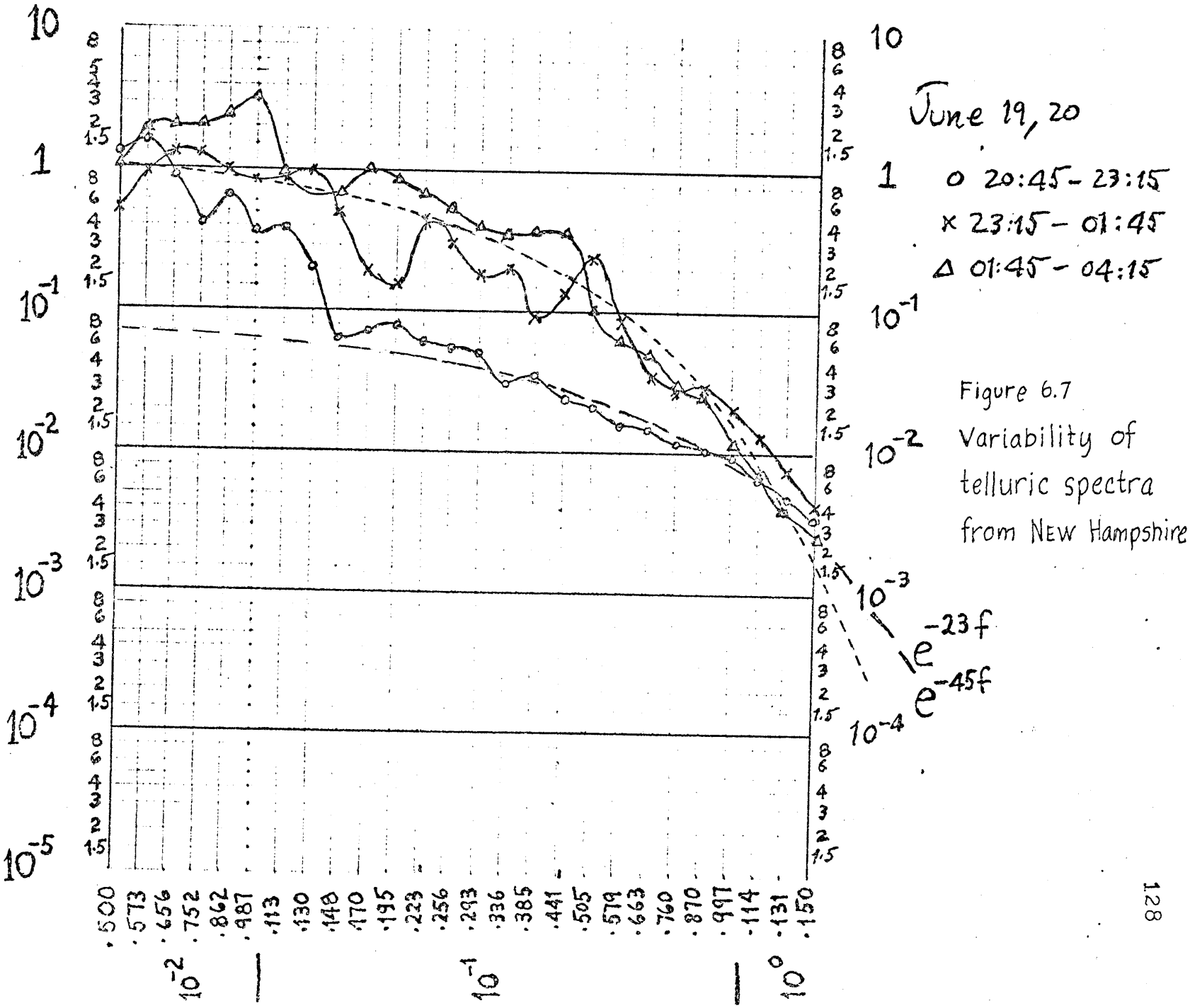

Figure 6.7
Variability of telluric spectra from New Hampshire

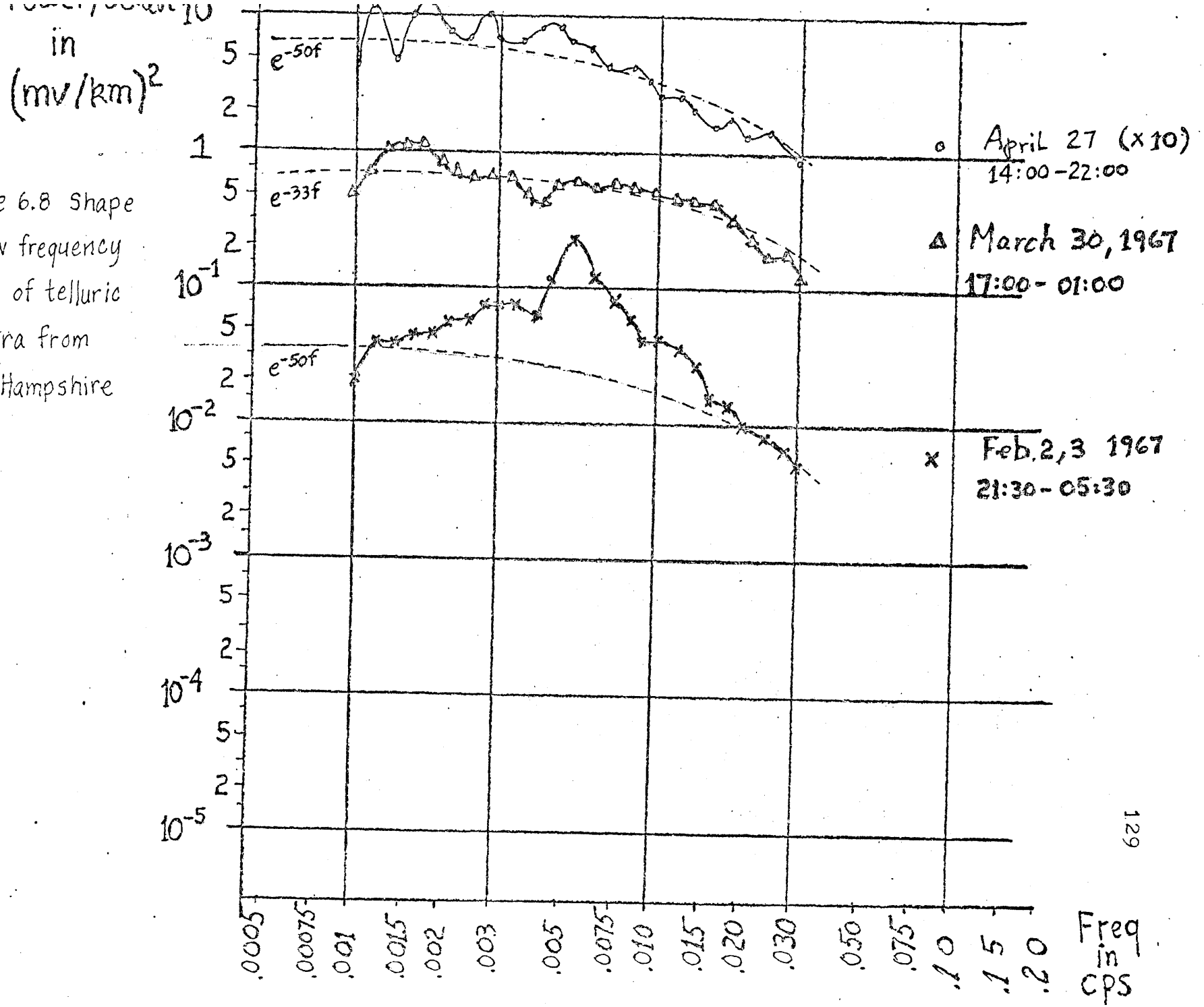

Figure 6.8 Shape of low frequency range of telluric spectra from New Hampshire

CONCORD-ETNA, N.H. TELLURIC FLUCTUATIONS, DEC. 30, 1971
C0:35 - 01:02 EST, 27.3 MINS DURATION
ELECT., NW. SAMPLING INTERVAL=0.20 SEC, FUND. FREQ=.0006 CPS.

FREQ, CPS. POWER/OCTAVE, ((MV/KM)**2)/OCTAVE

A=.1E-04, B=.1E-03, C=.1E-02, D=.1E-01, E=.100, F=1.00, G=10.0

	A
0.005	I
0.006	I
0.007	I
0.008	I
0.010	I
0.012	I
0.014	I
0.016	I
0.020	I
0.023	I
0.027	I
0.033	I
0.039	I
0.046	I
0.056	I
0.066	I
0.078	I
0.093	I
0.110	I
0.131	I
0.156	I
0.186	I
0.221	I
0.263	I
0.313	I
0.372	I
0.442	I
0.526	I
0.625	I
0.743	I
0.884	I
1.051	I
1.250	I
1.486	I
1.768	I
2.102	I
2.500	I

Figure 6.9 Strongly damped telluric fluctuations

Figure 6.10 Telluric spectrum during a "pearl" event

CONCORD-ETNA, N.H. "PEARL" FLUCTJATIONS, MAY 2, 1972
23:52 - 00:19 EST, 27.3 MINS. DURATION
ELECT., NW. SAMPLING INTERVAL=0.20 SEC, FUND. FREQ=.0006 CPS.

FREQ, CPS. POWER/OCTAVE, ((MV/KM)**2)/OCTAVE

A=.1E-04, B=.1E-03, C=.1E-02, D=.1E-01, E=.100, F=1.00, G=10.0

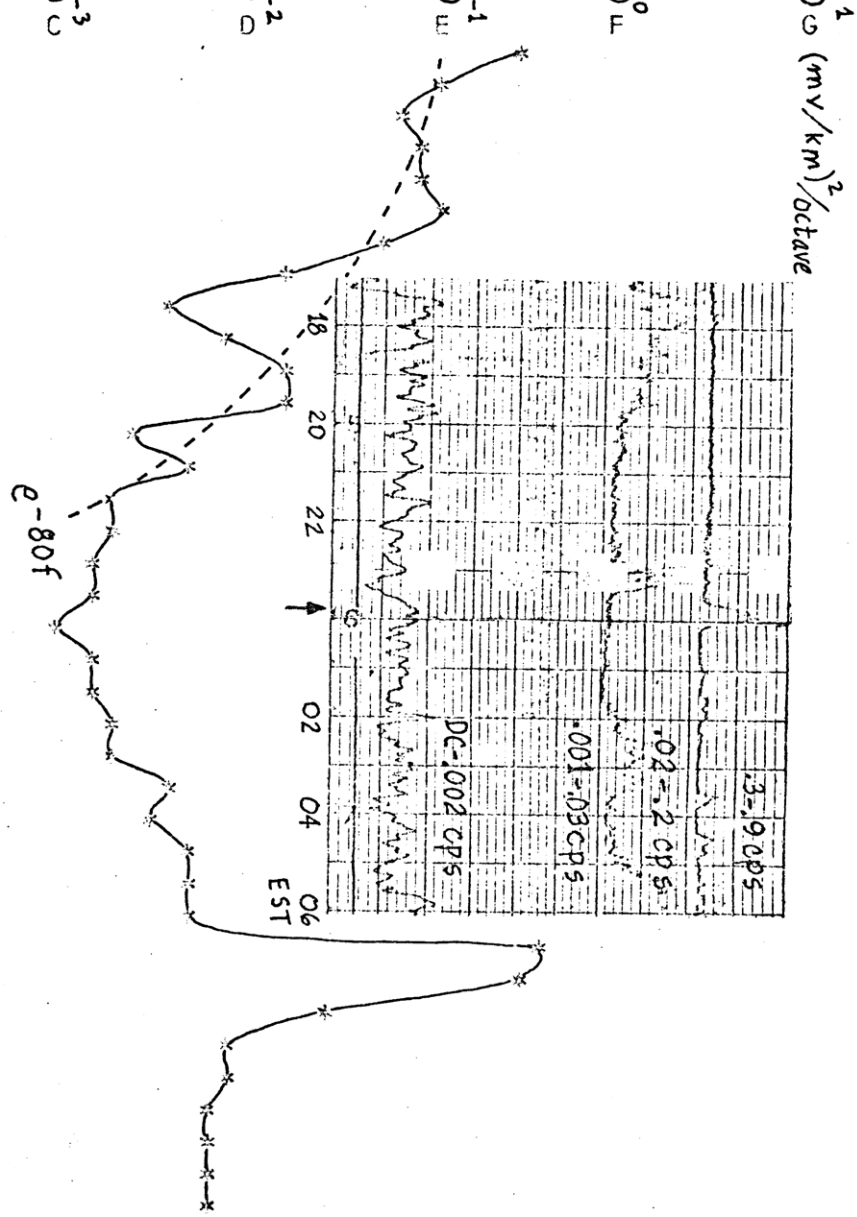

0.005	I
0.006	I
0.007	I
0.008	I
0.010	I
0.012	I
0.014	I
0.016	I
0.020	I
0.023	I
0.027	I
0.033	I
0.039	I
0.046	I
0.056	I
0.066	I
0.078	I
0.093	I
0.110	I
0.131	I
0.156	I
0.186	I
0.221	I
0.263	I
0.313	I
0.372	I
0.442	I
0.526	I
0.625	I
0.743	I
0.884	I
1.051	I
1.250	I
1.486	I
1.768	I
2.102	I
2.500	I

Figure 6.11 Strong damping during a "pearl" event

CONCORD-ETNA, N.H. PEARL FLUCTUATIONS, SEPTEMBER 22, 1971
01:51 - 02:18 EST, 27.3 MINS. SAMPLE LENGTH
ELECT., NW. SAMPLING INTERVAL=0.20 SEC, FUND. FREQ=.0006 CPS.

FREQ, CPS. POWER/OCTAVE, ((MV/KM)**2)/OCTAVE

A=.1E-04, B=.1E-03, C=.1E-02, D=.1E-01, E=.100, F=1.00, G=10.0

POINT AT FREQ= 0.5255 SHOULD BE ABOVE FIGURE.

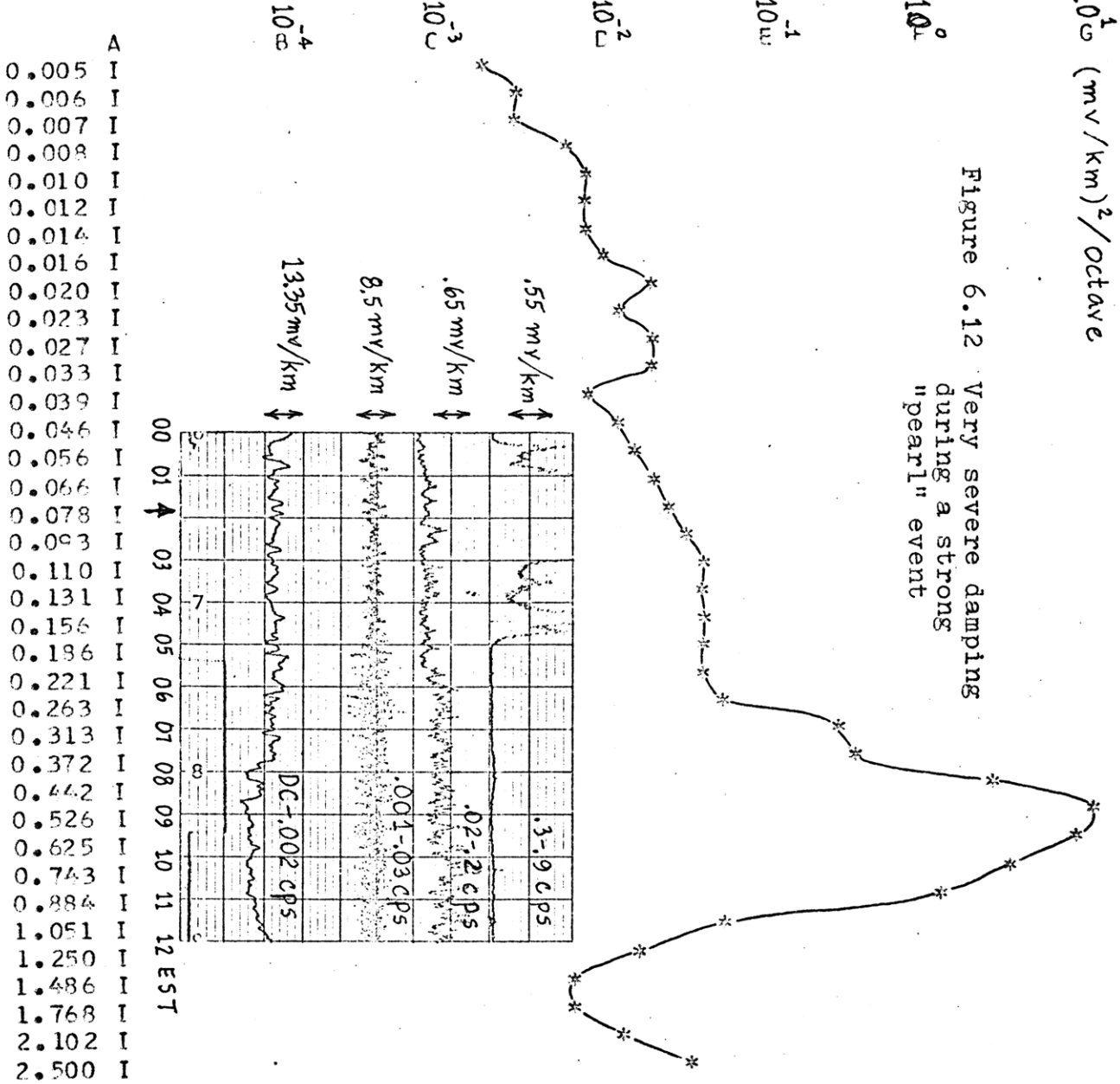

Figure 6.12 Very severe damping during a strong "pearl" event

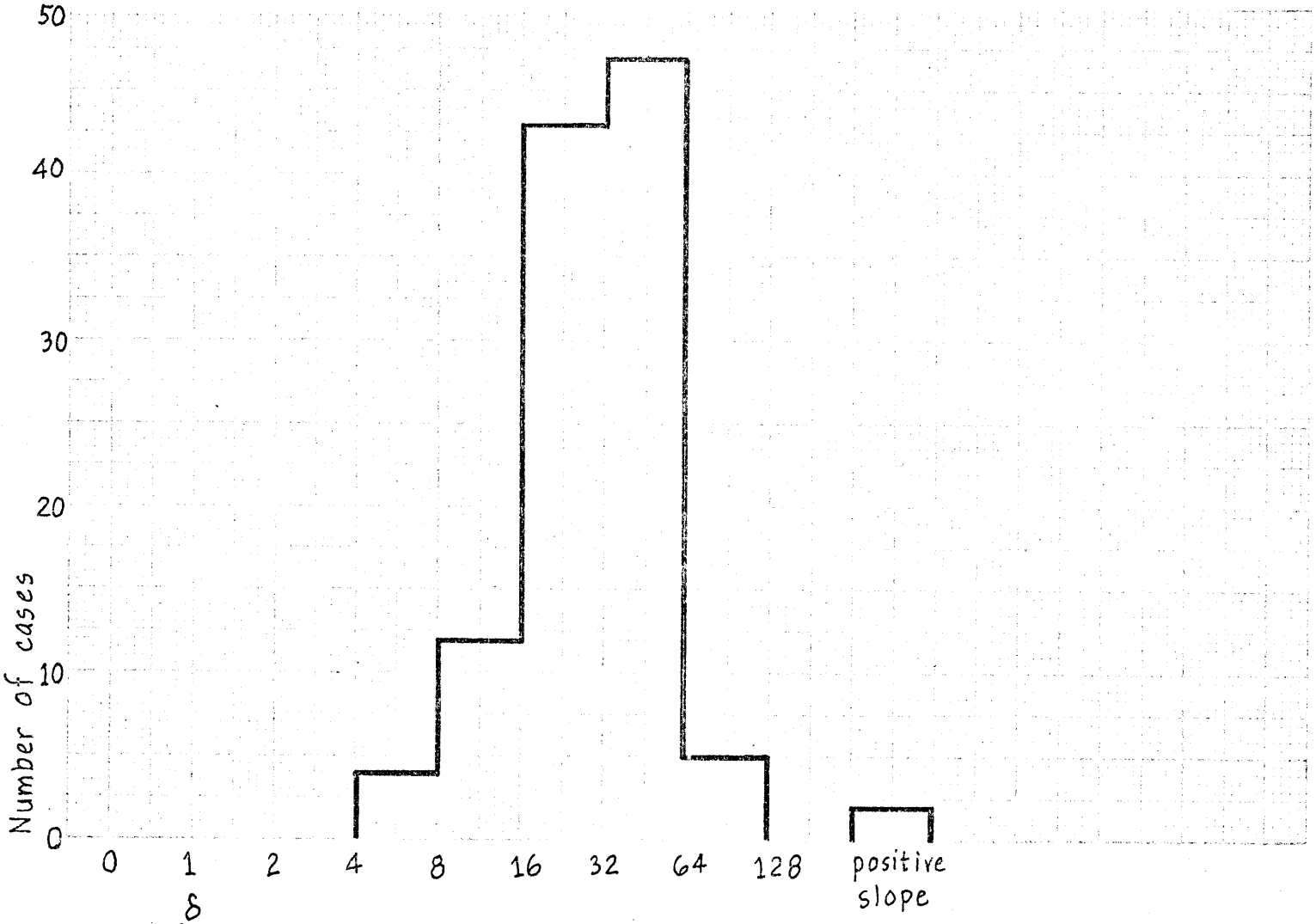

Figure 6.13 Histogram of attenuation factors δ from New Hampshire spectra

their value of -2.13 for the power-law index n would correspond to a value of -0.13 in our representation. First, in converting Santirocco and Parker's power density in terms of power/cps to our power/octave, the value of n is reduced by unity. Secondly, as is clear from equation (6.2) below, in converting power density of magnetic fluctuations to power density of electric fluctuations, the value of n is again reduced by unity.

For a semi-infinite uniformly conductive earth, the ratio of the magnetic flux density $\vec{B}$ (in gammas) to the electric field intensity $\vec{E}$ (in mv/km) of an electromagnetic wave which has penetrated just beneath the surface is given by

$$|\vec{B}|/|\vec{E}| = \sqrt{.2T/\rho} \qquad (6.2)$$

where T = wave period, in seconds
ρ = apparent resistivity of the earth, in ohm-meters

Our estimated value of δ of 16.4 for the Bermuda spectra is half of our average value of 33.3 for the New Hampshire spectra. Considering the large variation of the attenuation factor δ with angle of incidence, these values of δ for the observed spectra are in reasonable agreement with our computed values of 59 for wave sources above the plasmapause, and 34 for sources below the plasmapause.

6.5 Estimates of unguided Alfven wave amplitudes

Using the spectra of electric field fluctuations observed on the ground, and taking into account the effects of the earth's conductivity and hot plasma damping in the plasmasphere, we arrive at estimates of the unguided Alfven wave amplitudes

just below the plasmapause.

A typical idealized telluric spectrum may be represented by the following expression for the power density/octave, P:

$$P = Cf^{n}e^{-\delta f} \qquad (1.1)$$

with parameter values of $C = 0.7\ (mv/km)^2$/octave, $n = 0$, $\delta = 50$.

To estimate the effect on the wave spectra of the variation of earth conductivity in the vicinity of the M.I.T. telluric station, we used the results of a continuing study being made in New Hampshire of the $|\vec{B}|/|\vec{E}|$ ratios of long period micropulsations down to 50 second periods (Kasameyer, 1973). We extrapolated the slow trend that we found down to 6 second period fluctuations. The agreement between the power-law indices n for magnetic and electric spectra noted at the end of the preceding section strengthens our confidence in our extrapolation of the long period trends of the $|\vec{B}|/|\vec{E}|$ ratios down to 6 second periods.

The typical spectrum given above corresponds to waves with the following amplitudes:

Frequency, cps	$\vec{E}$ on ground, mv/km	$\vec{B}$ just below plasmapause, γ
0.005	0.738	0.232
0.02	0.508	0.121
0.08	0.113	0.0633

The last column gives the amplitude of micropulsation fluctuations when the telluric fluctuations on the ground are traced back to a point just below the plasmapause, taking into account partial reflection of waves at the earth's surface and hot plasma damping by the MMMFG wave-particle inter-

action. We note that the micropulsation amplitudes in the last column are below the 0.3 γ sensitivity threshold of recent satellite instrumentation (McPherron, Russell, and Coleman, 1972).

6.6 Damping effects on the magnetospheric plasma

Unguided Alfven waves with the power spectrum given in the preceding section, give up energy to resonant protons inside the plasmasphere at an average rate of 0.06 ev/cm^3-sec. Assuming that the hot proton population is that given for R = 4.6 Re in Table IA, the density of resonant (91 kev) protons is about 0.1 protons/cm^3. On the average, it will take about 12 hours for each resonant proton to gain 25 kev parallel energy from the wave. Ordinarily, then , the MMMFG interaction has a weak effect on the energies of plasma particles.

Since, however, telluric amplitudes during disturbed periods are often ten or more times larger than average (see Figure 6.14 for example), the rate of energy dissipation goes up to 6 ev/cm^3-sec. which adds 25 kev to the parallel energy of a resonant proton in about 7 minutes. Addition of 25 kev to the parallel energy of a 91 kev particle with a pitch angle of 45° lowers its pitch angle by 11°. Hence, during disturbed periods, the MMMFG interaction can have a significant effect on the hot plasma distribution in the plasmasphere.

6.7 Geophysical applications

In this section we will discuss some consequences of the MMMFG and ion cyclotron wave-particle interactions in the inner magnetosphere. These interactions, which affect both plasma and wave parameters, can result in growth or attenuation of a wave, in changes in the shape and power levels of the spectrum,

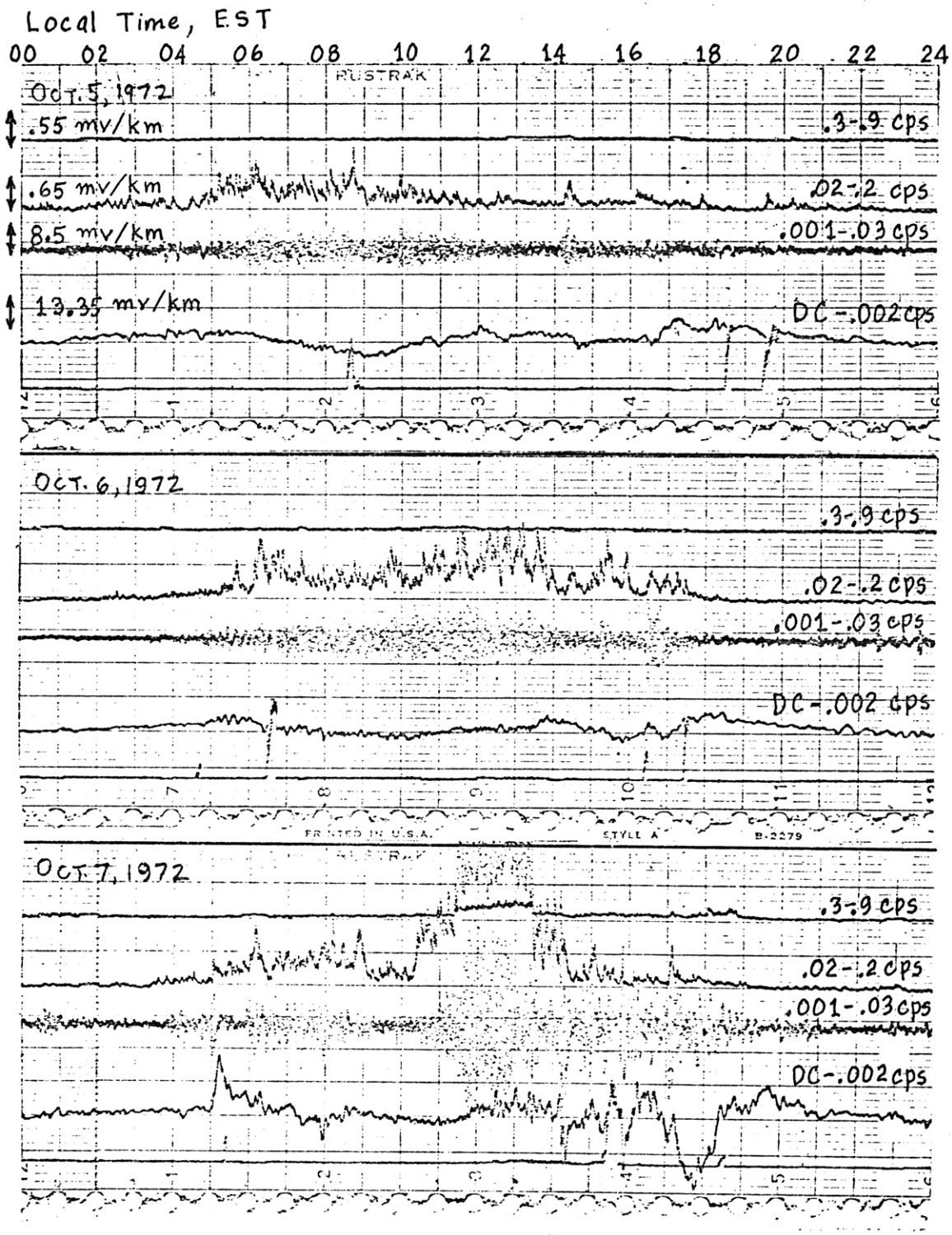

Figure 6.14 Continuous analogue records of telluric fluctuations at the M.I.T. telluric station in New Hampshire

and in changes in the sharpness of resonance peaks. The differences in effects of the plasma on various wave modes contain information on the plasma parameters. For example, the growth rate of the ion cyclotron instability in the guided Alfven mode gives information on the pitch angle anisotropy of the ion population, while the damping rate of the unguided Alfven mode gives information on the slopes of the energy spectrum. Both rates give information on the number densities of the plasma along the propagation path of the wave. Hence, if similar hot proton populations in one plasma cloud should be responsible for the simultaneous occurrence of the ion cyclotron instability in the Pc1 band and damping in the Pc2 and 3 band (possibly illustrated in Figure 1.2 and discussed in Chapter 4), a study of this phenomenon can be made to yield information on the magnetospheric plasma parameters by checking computed growth and damping rates from model plasma populations against observed rates. This procedure may yield valuable clues to various processes going on in the magnetosphere such as rapid transport of hot protons, and rapid heating or cooling of trapped protons.

Furthermore, MMMFG interaction computations can be combined with ion cyclotron interaction computations to study dumping into the atmosphere of particles with pitch angles close to 90°. Cyclotron interaction of charged particles with hydromagnetic waves causes strong pitch angle diffusion in particle populations with "loss-cone" distribution functions. Once the pitch angle has diffused down to the loss-cone angle, the particle is lost in the atmosphere. However, particles with

pitch angles closer to 90^{o} require higher frequency waves for cyclotron interaction than particles with smaller pitch angles. Since the power spectra of waves in the magnetosphere drop rapidly with increasing frequencies, above a certain pitch angle, diffusion by means of the cyclotron interaction virtually ceases. Since the MHMFG interaction transfers energy from the unguided Alfven wave to the parallel component of the resonant particle's kinetic energy, this interaction supersedes in importance cyclotron interaction for pitch angles close to 90^{o}.

CHAPTER 7

CONCLUSIONS

We have found that collisionless damping of the unguided Alfven wave by means of the magnetic moment-magnetic field gradient interaction with hot plasma is probably important in the inner magnetosphere. Damping is strong enough to produce observable effects on the wave spectrum as the wave propagates down through the plasmasphere. Damping rates estimated from observations of telluric and micropulsation spectra fall within values estimated for typical hot plasma populations in the inner magnetosphere.

Hot plasma damping is highly anisotropic. The shape of the attenuation factor vs. angle of propagation of the incident wave varies considerably depending on whether the incident wave is above or below the plasmapause. The anisotropy combined with the focusing effect of propagation across the plasmapause increases the difference in shape of these curves.

With the attenuation factor known, we are able to estimate amplitudes of the unguided Alfven wave just below the plasmapause in the vicinity of the geomagnetic equator. During average conditions, amplitudes are so low that these waves are not likely to be detected by instruments on recently launched satellites. The wave energy dissipation rates are small so that the magnetic moment-magnetic field gradient interaction exerts only a weak influence on the plasma particles.

On the other hand, during disturbed periods and during most daytime hours the wave amplitudes may rise enough to reach the

sensitivity thresholds of satellite instruments. During these active periods, the interaction may increase resonant protons' parallel energy enough to significantly affect the hot plasma distribution inside the plasmasphere, and to lower their pitch angles into the range where the cyclotron interaction can efficiently bring the pitch angles down to the loss-cone. The combined effects of the two interactions may explain how energetic particles with pitch angles originally close to 90° can enter the loss-cone.

Waves are attenuated much more just inside the plasmapause than outside, because the damping rates are higher just inside than just outside the plasmapause. Moreover, the shorter wavelengths inside the plasmapause cause the wave to go through more damping cycles inside than outside. Farther away outside the plasmapause, the magnetic field gets weaker, the wavelength gets shorter, more particles can resonate with the slower wave, and damping becomes stronger. We expect the unguided Alfven wave to be severely damped inside the plasma sheet, the neutral sheet, and the transition region just outside the sunward side of the magnetopause, because of the abundance of energetic particles to resonate with the wave, and the short wavelengths due to the low magnetic field strengths. Close to the earth, just outside the ionosphere, damping rates are expected to be low because the strong magnetic field results in high wave velocities.

Since unguided Alfven waves are strongly affected by the hot plasma, changes in the wave spectra are sensitive indicators of changes in the hot plasma parameters. This implies that

damping of the unguided Alfven wave could play an important role in ground-based diagnostics of the magnetosphere.

BIBLIOGRAPHY

Allis, William P., Solomon J. Buchsbaum, Abraham Bers, Waves in Anisotropic Plasmas, M.I.T. Press, Cambridge, Mass. (1963)

Aubry, M. P., "Diagnostics of the Magnetosphere from Ground based Measurements of Electromagnetic Waves," Ann. Geophysics, 26, 341 (1970)

Barnes, Aaron, "Collisionless Damping of Hydromagnetic Waves," Phys. of Fluids, 9, 1483 (1966)

Barnes, Aaron, "Stochastic Electron Heating and Hydromagnetic Wave Damping," Phys. of Fluids, 10, 2427 (1967)

Barnes, Aaron, "Quasilinear Theory of Hydromagnetic Waves in Collisionless Plasma," Phys. of Fluids, 11, 2644 (1968)

Cain, Joseph C., Shirley J. Hendricks, Robert A. Langel, and William V. Hudson, "A Proposed Model for the International Geomagnetic Reference Field - 1965," J. Geomagnetism and Geoelectricity, 19, 335 (1967)

Campbell, W. H., "Research on Geomagnetic Pulsations from January 1969 to July 1962 - A Review," J. Atm. & Terr. Phys., 35, 1147 (1973)

Chandrasekhar, S., R. N. Kaufman, and K. M. Watson, "Properties of an Ionized Gas of Low Density in a Magnetic Field. III.," Ann. Phys. (.Y.) 2, 435 (1957)

Chandrasekhar, S., A. N. Kaufman, and K. M. Watson, "Properties of an Ionized Gas of Low Density in a Magnetic Field. IV.," Ann. Phys. (N.Y.) 5, 1 (1958)

Chandrasekhar, S., A. N. Kaufman, and K. M. Watson, "The Stability of the Pinch," Proc. Roy. Soc. (London) A245, 435 (1958)

Chappell, C. R., K. K. Harris, and G. W. Sharp, "A Study of the Influence of Magnetic Activity on the Location of the Plasmapause as Measured by OGO 5," J. Geophys. Res., 75, 50 (1970)

Clemmow, P. C. and J. P. Dougherty, Electrodynamics of Particles and Plasmas, Addison-Wesley Publishing Company, Reading, Mass. (1969)

Cornwall, John M., F. V. Coroniti, and R. M. Thorne, "Unified Theory of SAR Arc Formation at the Plasmapause," J. Geophys. Res., 76, 4428 (1971)

Derfler, H., "Theory of R-F Probe Measurements in a Freely Ionized Plasma," Proceedings of the Fifth International Conference on Ionization Phenomena in Gases (Munich, 28 August to 1 September, 1961), edited by H. Maecker, 2; North Holland Publishing Company, Amsterdam (1962)

Dungey, J. W., "The Action of Vlason Waves on the Velocity Distribution in a Plasma," J. Fluid Mech. 10, 473 (1961)

Fried, B. D., and S. D. Conte, The Plasma Dispersion Function, Academic Press, New York (1961)

Hasegawa, Akira, "Drift Mirror Instability in the Magnetosphere," Phys. of Fluids 12, 2642 (1969)

Hasegawa, Akira, "Hydromagnetic Waves and Instabilities in the Magnetosphere," Particles and Fields in the Magnetosphere, edited by B. M. McCormac, D. Reidel, Dordrecht, Holland, 284 (1970)

Jackson, J. D., "Longitudinal Plasma Oscillations - Appendix 1-3," J. Nucl. Energy, Part C: Plasma Physics 1, 171 (1960)

Jacobs, J. A., Geomagnetic Micropulsations, Springer-Verlag, New York (1970)

Kaplan, Wilfred, Introduction to Analytic Functions, Addison-Wesley Publishing Company, Reading, Mass. (1966)

Kasameyer, Paul W., Private Communication (1973)

Kennel, C. F., and H. V. Wong, "Resonant Particle Instabilities in a Uniform Magnetic Field," J. Plasma Phys. 1, 75 (1967)

Kennel, C. F., and H. V. Wong, "Resonantly Unstable Off-angle Hydromagnetic Waves," J. Plasma Physics 1, 81 (1967)

King, J. H., Models of the Trapped Radiation Environment, Vol. IV: Low Energy Protons, NASA SP - 3024 (1967)

Kusse, Bruce R., "Plasma Dispersion Relations and the Stability Criteria," M.S. Thesis in Electrical Engineering, M.I.T., under Prof. L. D. Smullin (1964)

Kutsenko, A. B., and K. N. Stepanov, "Instability of Plasma with Anisotropic Distribution of Ion and Electron Velocities," Soviet Physics JETP 11, 1323 (1960)

Liemohn, Harold B., "Cyclotron-Resonance Amplification of VLF and ULF Whistlers," J. Geophys. Res. 72, 39 (1967)

Lorentz, H. A., The Theory of Electrons, Leipzig (1909), 2nd ed. reprinted by Dover, New York (1952)

Madden, Theodore R., Private Communication (1968)

McPherron, R. L., C. T. Russell, and P. J. Coleman, Jr., "Fluctuating Magnetic Fields in the Magnetosphere II. ULF Waves," Space Science Reviews 13, 411 (1972)

Navato, Alfredo R., "Hydromagnetic Wave Damping in the Magnetosphere" Research paper presented for the oral portion of the General Examination in Geophysics, Department of Earth and Planetary Sciences, M.I.T. (1970)

Navato, Alfredo R., "Hydromagnetic Wave Damping in the Inner Magnetosphere" (abstract), Paper given at the fifty-second annual meeting of the American Geophysical Union. EOS, Trans. Amer. Geophys. Union 52, 333 (1971)

Orr, D., "Magnetic Pulsations within the Magnetosphere: A Review," J. Atm. and Terrestr. Phys. 35, 1 (1973)

Parker, Eugene N., "Dynamical Properties of the Magnetosphere," Physics of the Magnetosphere, ed. by Robert L. Carovillano, John F. McClay, and Henry R. Radoski, D. Reidel Publishing Company, Dordrecht-Holland (1968)

Roberts, C. S., "Electron Loss from the Van Allen Zones due to Pitch Angle Scattering by Electromagnetic Disturbances," Radiation Trapped in the Earth's Magnetic Field, D. Reidel Publishing Company, Dordrecht-Holland (1966)

Saito, T.,"Statistical Studies of Three Types of Geomagnetic Continuous Pulsations. Part I. Type I Pc (5-40 sec)," Sci. Repts., Tohoku Univ., Ser. 5: Geophys. 14 (3), 81 (1962)

Santirocco, R. A., and D. G. Parker, "The Polarization and Power Spectrums of Pc Micropulsations in Bermuda," J. Geophys. Res. 68, 5545 (1963)

Stix, Thomas Howard, The Theory of Plasma Waves, McGraw-Hill Book Company, New York (1962)

Suguira, M., B. G. Ledley, T. L. Skillman, and J. P. Heppner, "Magnetospheric Field Distortions Observed by OGO's 3 and 5" Preprint (1972)

Tajiri, Masayoshi, "Propagation of Hydromagnetic Waves in Collisionless Plasma. II. Kinetic Approach," J. Physical Soc. of Japan, 22, 1482 (1967)

Titchmarsh, E. C., The Theory of Functions, Oxford University Press (1939)

Vette, James I., "Magnetospheric Particle Populations," Earth's Magnetospheric Processes, edited by Billy M. McCormac, D. Reidel Publishing Company, Dordrecht-Holland, 53 (1972)

Vette, J. I., A. B. Lucero, and J. A. Wright, Models of the Trapped Radiation Environment, Vol. II: Inner and Outer Zone Electrons, NASA SP - 3024 (1966)

Williams, D. J., and T. A. Fritz, "Energy Spectra and Pitch Angle Distributions of Storm-Time and Substorm Injected Protons," J. Geophys. Res. 78, 4739 (1973)

ACKNOWLEDGEMENTS

I gratefully acknowledge the invaluable help, guidance and encouragement given me by Professor Theodore R. Madden. I would like to acknowledge helpful discussions with Professors John Belcher, Reginald Newell, and George Siscoe; and with Dr. William R. Sill, Dr. Stanley J. Laster, Dr. William J. Burke, and Mr. Paul W. Kasameyer. For encouragement and helpful discussions I thank the Rev. James J. Hennessey, S.J., Rev. Victor L. Badillo, S.J., and Rev. Francisco N. Glover, S.J., all of the Manila Observatory. For helping with computer programming I thank Mrs. Leslie Mandl, Mr. Arthur Anger, and Mr. Norm Brenner. For help with data acquisition I thank Mr. and Mrs. William Miskoe, Mr. Sam Hendryx, and the staff of Weston Observatory. For help in typing and putting the thesis together I thank Miss Kate Crowley, Mrs. Ann Kasameyer, Miss Delia Macatangay, Mr. Marcelo Montaniel, and Mr. Joseph Ting. For their constant support and encouragement I thank the Very Rev. Benigno A. Mayo, S.J., Rev. James J. Meany, S.J., and Rev. Herbert J. Hezel, S.J., and the Community at St. Andrew Bobola House.

The American Chemical Society provided financial aid during my studies, and the Office of Naval Research provided funds for research (Contract NR-371-401, No. N0014-67-A-0204-0045).

BIOGRAPHICAL NOTE

The author was born in the Philippines and attended the P. Gomez Elementary School and Arellano High School in Manila. He received his B.S.M.E. degree (magna cum laude) from the University of the Philippines and his B.S.E.E. degree (magna cum laude) from the Manuel L. Quezon University. He worked for the National Power Corporation as a supervisor on the construction and operation of a chemical fertilizer plant. After three years he went to work for Colgate-Palmolive, Philippines, Inc. on the construction of an office building and a factory extension. At this time he also taught Engineering Thermodynamics at the Naval and Marine Engineering Institute in Manila.

On the completion of the Colgate-Palmolive project, he joined the Society of Jesus. He then studied philosophy at Berchmans College in Cebu City where he taught mathematics, and philosophy and science; received his A.B. degree; and set up and operated a geomagnetic station for the Manila Observatory. He helped teach a summer course in physics at the Ateneo de Manila University. He then went to the University of Saskatchewan, Canada, on a World University Service scholarship to study physics. After two years he entered M.I.T. where he completed studies leading to the degree of Ph.D. in Geophysics.